

**Climate variability over the last millennium as recorded in the
sediments of high-altitude Lake Silvaplana, Switzerland:
data, methods and limitations**

Inauguraldissertation
der Philosophisch-naturwissenschaftlichen Fakultät
der Universität Bern

vorgelegt von
Mathias Trachsel
von Lenk

Leiter der Arbeit:
Prof. Dr. M. Grosjean
Universität Bern

**Climate variability over the last millennium as recorded in the
sediments of high-altitude Lake Silvaplana, Switzerland:
data, methods and limitations**

Inauguraldissertation
der Philosophisch-naturwissenschaftlichen Fakultät
der Universität Bern

vorgelegt von
Mathias Trachsel
von Lenk

Leiter der Arbeit:
Prof. Dr. M. Grosjean
Universität Bern

Von der Philosophisch-naturwissenschaftlichen Fakultät angenommen.

Bern, 25.02.2010

Der Dekan:
Prof. Dr. U. Feller



Lake Silvaplana (foreground) and Lake Sils, Mathias Trachsel, 2009

Table of contents

Table of Contents	5
List of Figures	7
List of Tables	8
Abbreviations	9
Abstract	13
1. Introduction	19
1.1. General Introduction	19
1.2. The project frame-work and state of knowledge	22
1.3. General objectives and outline	23
2. Study area	31
2.1. Lake Silvaplana	31
2.2. The catchment	31
2.3. Climate	33
3. Data and Methods	41
3.1. Climate and paleoclimate data	41
3.2. Field and laboratory methods	41
3.3. Numerical methods	43
4. Scanning reflectance spectroscopy (380 – 730 nm): a novel method for quantitative high-resolution climate reconstructions from minerogenic lake sediments	51
4.1. Introduction	51
4.2. Study site	52
4.3. Materials and Methods	53
4.3.1. Material and analytical methods	53
4.3.2. Numerical methods	54
4.3.3. Calibration and climate reconstruction	55
4.4. Results	55
4.4.1. Reflectance-derived variables	55
4.4.2. Calibration and climate reconstruction	56
4.5. Discussion	59
4.5.1. Reflectance-derived variables	59
4.5.2. Calibration and climate reconstruction	59
4.6. Conclusions and outlook	61

5. Quantitative summer temperature reconstruction derived from a combined biogenic Si and chironomid record from varved sediments of Lake Silvaplana (south-eastern Swiss Alps) back to AD 1177	69
5.1. Introduction	69
5.2. Regional Setting	70
5.3. Materials and methods	72
5.3.1. Material and chronology, climate data	72
5.3.2. Statistical methods	72
5.3.3. Detrending methods	73
5.4. Results	74
5.4.1. Chronology	74
5.4.2. Biogenic silica as a temperature proxy: calibration, detrending and reconstruction	74
5.4.3. The combined temperature reconstruction	80
5.5. Discussion	80
5.5.1. Calibration (model choice)	80
5.5.2. Comparing the biogenic silica flux record with independent temperature reconstructions	81
5.6. Conclusions	83
6. Is interannual temperature variability related to the mean temperature? Evidence from instrumental, early instrumental and proxy data in Europe since 1600 AD.	91
6.1. Introduction	91
6.2. Data and Methods	92
6.3. Results	94
6.3.1. Instrumental data 1864-2007/2000	94
6.3.2. Comparison between instrumental and proxy data 1864 to 1940/2000	96
6.3.3. Temporal stability of correlations between 'mean' and 'variability'	97
6.3.3.1. Significant instrumental time series (1900 onwards)	97
6.3.3.2. Seasonal patterns in instrumental, early instrumental and proxy data	99
6.4. Discussion	100
6.4.1. Methods	100
6.4.2. Instrumental and early instrumental data	100
6.4.3. Comparison between instrumental data and proxy data	101
6.5. Conclusions	102
7. Concluding remarks and outlook	109
7.1. Quantitative climate reconstruction from Lake Silvaplana	109
7.1.1. Chronology	109
7.1.2. Lake Silvaplana as an archive for high-resolution quantitative climate reconstructions	109
7.2. The changes of mean and variance of seasonal temperatures over Europe in the last 250 years	110
7.3. Outlook	111
Acknowledgments	117
Appendix	121

List of Figures

Fig. 1.1. Mean annual temperature in North-Alpine Switzerland	19
Fig. 1.2. Projected surface temperature changes	20
Fig. 1.3. Records of Northern Hemisphere temperature variation	20
Fig. 1.4. Current limitations of European palaeoclimate reconstructions	21
Fig. 2.1. Overview map of the Lake Silvaplana catchment area	32
Fig. 2.2. Climate chart of Sils-Maria	33
Fig. 2.3. Spatial correlation	33
Fig. 2.4. Overview map of south-eastern Switzerland	34
Fig. 2.5. Annual precipitation cycle	34
Fig. 2.6. Annual temperature cycle	35
Fig. 3.1. Core correlation	41
Fig. 3.2. Comparison of biogenic silica measurements	42
Fig. 3.3. Example of a loess filter	43
Fig. 3.4. Ordinary least squares regression	43
Fig. 3.5. Total least squares regression	44
Fig. 3.6. Probability density function	45
Fig. 4.1. Reflectance spectra	57
Fig. 4.2. Principal component analysis on spectrum-derived variables	57
Fig. 4.3. Multivariate calibration of spectrum-derived variables	59
Fig. 4.4. Comparison of the reflectance inferred temperature reconstruction with independent temperature reconstructions	60
Fig. 5.1. Overview map of the Lake Silvaplana catchment area	71
Fig. 5.2. Age-depth model	74
Fig. 5.3. Comparison of biogenic silica flux with instrumental temperatures	75
Fig. 5.4. Calibration of biogenic silica flux	76
Fig. 5.5. Original data series	78
Fig. 5.6. Comparison of the bSi flux inferred temperature reconstruction with independent temperature reconstructions	79
Fig. 6.1. Spatial distribution of the meteorological data series	93
Fig. 6.2. Mean versus variability change plots of meteorological data series	95
Fig. 6.3. Mean versus variability change plots of proxy data series	97
Fig. 6.4. Running correlations between mean and variability	98

List of Tables

Table 4.1. Algorithms for the calculation of spectrum-derived variables	53
Table 4.2. Redundancy analysis between spectrum-derived variables and meteorological data	57
Table 4.3. Correlations between meteorological data and spectrum-derived variables	57
Table 4.4. Multivariate calibration of spectrum-derived variables	58
Table 5.1. Correlations between meteorological data and biogenic silica flux	75
Table 5.2. Calibration statistics	77
Table 6.1. List of the 16 investigated instrumental (or climate field) data sets	94
Table 6.2. Correlations between mean and variability of meteorological data series	96
Table 6.3. Correlations between mean (variability) of meteorological data series and proxy data series	96

Abbreviations

AD	Anno Domini
AR	Autoregressive
BC	Before Christ
bSi	Biogenic Silica
CE	Coefficient of Efficiency
DF	Degrees of Freedom
DJF	December, January, February
EAWAG	Swiss Federal Institute of Aquatic Science and Technology (former Eidgenössische Anstalt für Wasserversorgung, Abwasserreinigung und Gewässerschutz)
ENLARGE	ENvironmental changes in mountain regions; recorded in high-resolution archives of LAkes of the UppeR EnGadinE, Switzerland',
EOF	Empirical Orthogonal Function
EU-FP	European Union Framework Project
GAR	Greater Alpine Area
GLS	Generalised Least Squares
ICP-OES	Inductively Coupled Plasma Optical Emission Spectrometry
IP	Inverse Prediction
IR	Inverse Regression
JJA	June, July, August
JJAS	June, July, August, September
LIA	Little Ice Age
Loess	Locally Weighted Regression
LOO	Leave-One-Out
MA	Major Axis (regression)
MAM	March, April, May
MAR	Mass Accumulation Rate
MIN	Minimum
MJJAS	May, June, July, August, September
MLR	Multiple Linear Regression
MSEP	Mean Squared Error of Prediction
MVC	Mean versus Variability Change (plot)
MXD	Maximum Late-Wood Density
NAO	North Atlantic Oscillation

NCCR	National Centre of Competence in Research
OLS	Ordinary Least Squares (regression)
PCA	Principal Component Analysis
PC	Principal Component
PDF	Probability Density Function
PSI	Paul Scherrer Institut
RABD	Relative Absorption Band Depth
RDA	Redundancy Analysis
RE	Reduction of Error
RMA	Ranged Major Axis (regression)
RMSEP	Root Mean Squared Error of Prediction
SON	September, October, November
SMA	Standard Major Axis (regression)
SNF	Schweizerischer NationalFonds
SVP	SilVaPlana (not a political party)
TP	Total Phosphorus
TRW	Tree-Ting Width
TT	Temperature
T	Temperature
VITA	Varves, Ice cores, and Tree rings - Archives with Annual Resolution
VIVALDI	Variability in Ice, Vegetation, and Lake Deposits – Integrated
XRD	X-Ray Diffraction
XRF	X-Ray Fluorescence
USGS	United States Geological Survey

Abstract

To place the current warming into the context of long-term natural climate variability high-resolution quantitative temperature reconstructions are needed. Currently, a couple of temperature reconstructions are available for the last millennium. They show broad agreements on the existence of the Little Ice Age and the Medieval Warm Period. However the amplitudes of reconstructed temperatures differ substantially. Therefore, good proxy data and thoroughly validated calibrations are needed to reduce the uncertainty about past climate variability. Reducing the uncertainty about past climate will improve climate projections.

The aim of this thesis is to produce climate records covering large parts of the last millennium from sediments of annually laminated (varved) proglacial Lake Silvaplana, south-eastern Swiss Alps. Thereby, new methods are tested and the potential of data to address different questions in paleoclimatology is assessed. The main goals of this study are to:

i) Extend existing records of climate variability from sediments of Lake Silvaplana, south-eastern Swiss Alps back to approximately AD 1000 and compare these records with fully independent climate reconstructions.

(ii) Test the potential of new analytical methods on the sediments of Lake Silvaplana. Sediments of Lake Silvaplana are especially promising for this purpose because many studies have been carried out giving insight into sediment composition and sedimentary processes.

(iii) Assess the effects of different widely used univariate calibration methods on the reconstructed amplitude of past climate variability and thus to assess whether or not climate variability is related to the climatological mean.

(iv) Explore the potential of climate reconstructions derived from sediments of Lake Silvaplana to preserve interannual climate variability.

To achieve these goals sediment records of Lake Silvaplana were extended back to AD 1177. The chronology is based on varve counts which are corroborated with historical floods. Sediments were sampled varve by varve. The records of mass accumulation rate (MAR) and biogenic silica (bSi) concentration were extended back to AD 1177 at an annual resolution. Multiplication of these two records yields the biogenic silica flux ($\text{mgcm}^{-2}\text{yr}^{-1}$) the amount of bSi produced per year per unit area. Additionally, scanning (in-situ) reflectance spectroscopy (380 - 730 nm) was measured at a

resolution of 2 mm which gives a record at near-annual resolution.

Comparing reflectance measurements with meteorological data we find correlations up to $r = 0.84$ ($p < 0.05$, calibration period 1864-1950) between six reflectance-dependent variables and summer (JJAS) temperature. These reflectance-dependent variables mirror the mineralogical composition of the clastic sediments, which is known to be related to climate in the catchment of Lake Silvaplana.

Using multiple linear regression (MLR) we establish a calibration model that explains 84% of the variance of summer (JJAS) temperature during the calibration period 1864-1950.

Applying the calibration model downcore we develop a quantitative summer temperature reconstruction back to AD 1177. This temperature reconstruction is in good agreement with two fully independent temperature reconstructions based on documentary data (back to AD 1500) and tree-ring data (back to AD 1177).

This study confirms the great potential of scanning in-situ reflectance spectroscopy (380 – 730 nm) as a novel non-destructive technique to acquire very rapidly high-resolution quantitative paleoclimate information from minerogenic lake sediments.

The new bSi flux record and an existing chironomid-based summer temperature reconstruction allowed us to produce a summer temperature reconstruction with skill in all frequency domains back to AD 1177. For the calibration (period AD 1864 - 1949) we assess systematically the effects of six different regression methods (Type I regressions: Inverse Regression IR, Inverse Prediction IP, Generalised Least Squares GLS; Type II regressions: Major Axis MA, Ranged Major Axis RMA and Standard Major Axis SMA) with regard to the predicted amplitude and the calibration statistics such as root-mean square error of prediction (RMSEP), reduction of error (RE) and coefficient of efficiency (CE).

We found a trade-off in the regression model choice between a good representation of the amplitude (Type II regressions) and good calibration statistics (Type I regressions). Since the amplitude is the essence of climate variability, we recommend using a Type II regression which accounts for an error on the predictor and the predictand. Here, a combination between MA and SMA (Type II regressions) performed best ($r=0.67$, $p < 0.04$; $\text{RMSEP}=0.26^\circ\text{C}$, $\text{RE}=0.22$, $\Delta\text{Amplitude}(\text{predicted}$

- observed) = 0.03°C; RMSEP/Amplitude=0.197). The band-pass filtered (9 - 100 year) bSi flux record is in close agreement both in the structure and the amplitude with two fully independent reconstructions spanning back to AD 1500 and AD 1177, respectively. All known pulses of negative volcanic forcing are represented as cold anomalies in the bSi flux record. Volcanic pulses combined with low solar activity (Spörer and Maunder Minima) are seen as particularly cold episodes around AD 1460 and AD 1690. The combined chironomid and bSi flux temperature record is in good agreement with the glacier history of the Alps. The warmest (AD 1190) and coldest decades (17th century; 1680-1700) of our reconstruction coincide with the largest anomalies in the Alpine tree ring-based reconstruction; both records show in the decadal variability an amplitude of 2.6°C between AD 1180 and 1950, which is substantially higher than the amplitude of hemispheric reconstructions. Our record suggests that the current decade is slightly warmer than the warmest decade in the pre-industrial time of the past 800 years.

Climate models project an increase in the interannual variability of European summer temperatures as a consequence of warmer temperatures in the 21st century. This increase in variability has been attributed to an enhanced soil moisture-atmosphere feedback. An increase in variability would have significant impacts on climate extremes. Here, we assess whether a relationship between the 'mean' and 'variability' of temperatures in Europe has existed in the past. Using the non-parametric measure of the first two L-moments ('mean' and 'variability'), we investigate the climatology of interannual temperature variability in instrumental

(1864-2007) and early instrumental (1760-1864) data in Europe. This period covers the cooler 'Little Ice Age' and the warming of the 20th century. Only a few instrumental temperatures series show significant negative (mostly winter, sometimes autumn) or positive correlations between 'mean' and 'variability' since 1864 (referred to as 'Mean versus Variability Change' (MVC) of temperatures). Although these correlations are not stable in time, they are coherent in space over synoptic-scale regions of Europe. The spatio-temporal evolution of MVC behaviour is consistent with changes in the relative frequency of predominant circulation modes in Europe.

Exploring the potential to extend the record back to AD 1000, we investigate whether the MVC behaviour of temperatures can be assessed using annually resolved tree-ring and lake-sediment proxy data. Out of the six investigated data series, only one tree-ring series showed a similar MVC behaviour as local instrumental data. It appears that the proxy series used do not sufficiently well record (i) seasonal extremes ('variability') and/or (ii) centennial-scale trends ('mean').

We could confirm the high potential of sediments of Lake Silvaplana for climate reconstruction. This is valid for the application of conventional methods and for the application of the promising method scanning (in-situ) reflectance spectrometry. However, the potential to reconstruct interannual climate variability remains limited. Additionally, we could highlight the importance of a careful assessment of calibration methods when aiming to produce meaningful climate reconstructions. The amplitude of variability matters most.

Chapter 1



1. Introduction

1.1. General Introduction

In global temperature records a cluster of warm years is observed in the last two decades. Thirteen out of the seventeen warmest years (mean annual temperatures) between 1880 and 2006 (127 years) occurred after 1990 (17 years) (Zorita et al. 2008). In Northern Europe, nine out of the 17 warmest years since 1880 occurred between 1990 and 2006 and in the Mediterranean 11 out of the 17 warmest years were found post 1990. For the long temperature record of Genève-Cointrin in Switzerland spanning the last 253 years 14 out of the 17 warmest years were recorded since 1990. For the record of Bergen in Norway going back as far as 1816, six out of the 17 warmest years are recorded in the last 17 years. These clusters of warm years are not random since the probability of randomness is lower than 1% (Zorita et al. 2008).

For homogenised temperature series of North-Alpine Switzerland, 12 out of the 17 highest mean annual temperatures since 1864 (145 years) were recorded between 1990 and 2006 and 16 out of the 20 warmest years occurred between 1989 and 2008 (i.e. in the last 20 years, Fig. 1.1.). Moreover the warmest seasons on record were measured in the last decade: warmest summer in 2003. Warmest autumn, winter and spring occurred consecutively between September 2006 and May 2007 (Begert et al. 2005; Meteoschweiz).

In a long-term perspective the last IPCC (2007) assessment report states: **‘Current global temperatures are warmer than they have ever been**

during at least the past five centuries, probably even for more than a millennium.’ Recent climate change is regarded as exceptional because its cause is not natural. Warming in the last 50 years is mainly attributed to human induced CO₂-emissions. The concentration of CO₂ in the atmosphere **‘has reached a record high relative to more than the past half-million years, and has done so at an exceptionally fast rate’** (Jansen et al. 2007).

For the future the IPCC (2007) AR4 states: **‘Future changes in anthropogenic forcing will result not only in changes in the mean climate state but also in the variability of climate.** Addressing the inter-annual variability in monthly mean surface air temperature (...) Räisänen (2002) finds (...) **a slight increase in temperature variability (...) in warm season northern mid-latitudes.**’ (Meehl et al. 2007). Fig. 1.2. illustrates the projected increase in interannual variability going along with the increase in mean temperature.

Direct measurements of climate state variables (mainly temperature and precipitation) are available for the last 150 years. A few measurement series named early instrumental are going back another 100 years. Prior to this, our knowledge about past climate relies on proxy (approximation) data. Climate proxy data are typically based on documentary sources or on natural climate archives (e.g. trees and lake sediments). To give us quantitative information about past climate a statistical relation between a measured climate state variable and a climate proxy is developed.

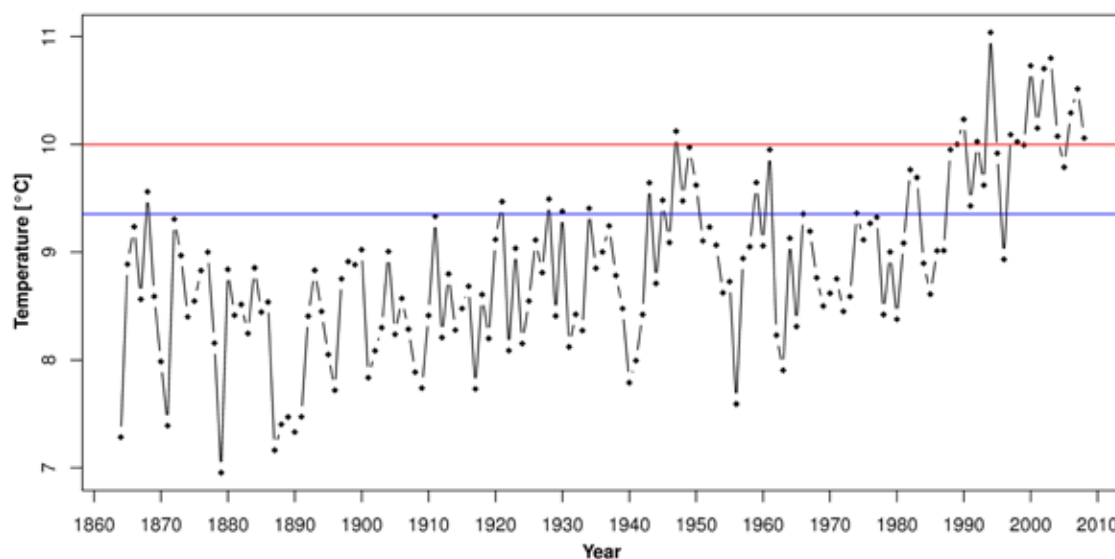


Fig. 1.1. Mean annual temperature in North-Alpine Switzerland (mean value of station data Basel, Bern, Genève and Zürich). The red line indicates the 90% quantile and the blue line indicates the 75% quantile. (Data: Begert et al. 2005; Meteoschweiz)

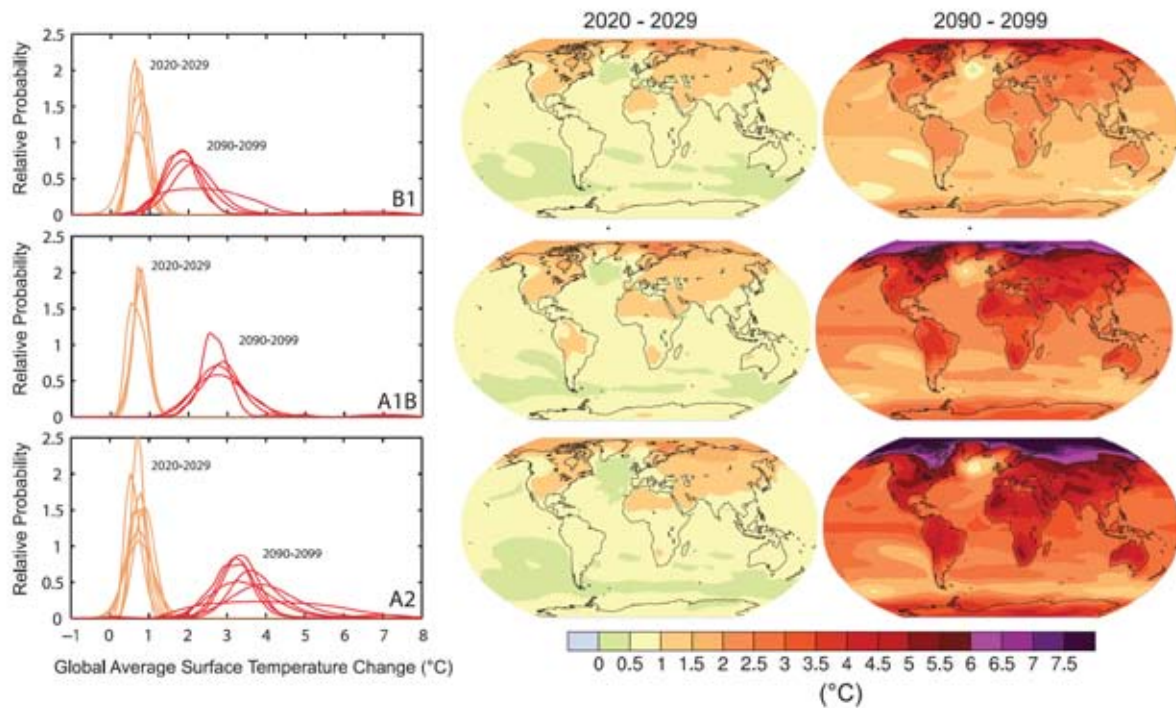


Fig. 1.2. Projected surface temperature changes for the early and late 21st century relative to the period 1980-1999. The central and right panels show the atmosphere ocean general circulation model (AOGCM) multi-model average projections for the B1 (top), A1B (middle) and A2 (bottom) emission scenarios (SRES) averaged over the decades 2020-2029 (centre) and 2090-2099 (right). The left panels show corresponding uncertainties as the relative probabilities of estimated global average warming from several AOGCM and earth system models of intermediate complexity studies for the same periods. (Taken from IPCC (2007), SPM.6.)

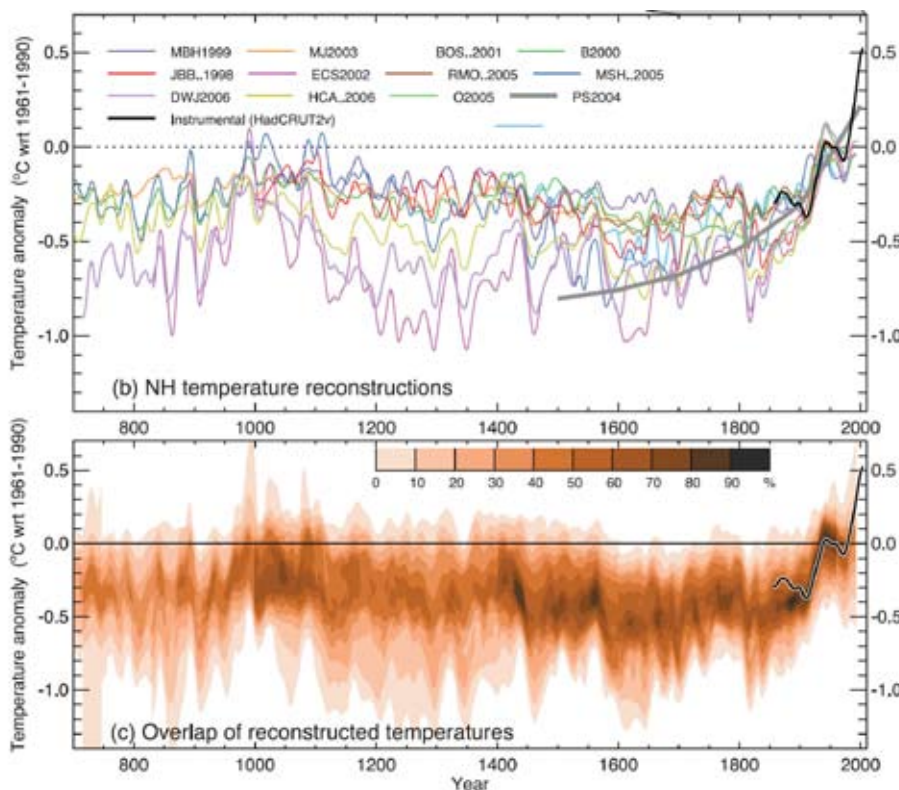


Fig. 1.3. Records of Northern Hemisphere temperature variation during the last 1,300 years. All temperatures represent anomalies (°C) from the 1961 to 1990 mean. Upper panel: Reconstructions using multiple climate proxy records and the Had- CRUT2v instrumental temperature record in black. Lower Panel: Overlap of the published multi-decadal time scale uncertainty ranges of all temperature reconstructions with temperatures within 1 standard error (SE). The HadCRUT2v instrumental temperature record is shown in black. All series have been smoothed with a Gaussian-weighted filter to remove fluctuations on time scales less than 30 years (Jansen et al. 2007). For additional information regarding the reconstructions see Jansen et al. (2007).

This can be done for a single proxy (univariate calibration) or several proxies can be combined (multivariate calibration). For univariate and multivariate calibration different statistical methods can be applied. This results in changes of structure and amplitude of the reconstructed climate (Fig. 1.3; e.g. Zorita et al. 2003; von Storch et al. 2004; Esper et al. 2005; Bürger et al. 2006; Hegerl et al. 2007; Riedwyl et al. 2008). At present we are therefore not able to answer with certainty the very fundamental question: how unusual and possibly unprecedented is the current climate change?

Stated in a more specific way a fundamental question in paleoclimatology covering the last millennium is:

Does the magnitude and rate of 20th Century climate change exceed the natural variability of European climate over the last millennium?

Given the current knowledge about past climate variability it is still an enormous challenge to answer this question. Fig. 1.4. shows some challenges we are currently facing, when trying to answer this question (upper panel). The lower panel shows the advancements current research aims to provide improving the knowledge about European climate variability in the last 1000 years:

(i) currently there are only a few quantitative temperature reconstructions spanning the last 1000 years (e.g. Grudd et al. 2002; Büntgen et al. 2005; Büntgen et al. 2006; Glaser and Riemann, 2009).

(ii) Most of these proxies are tree-ring and documentary based. The debate whether tree-ring based reconstructions capture centennial to multi-centennial climate variability (e.g. Esper et al. 2004) is still ongoing. The same applies to documentary data (e.g. Glaser and Riemann, 2009; Moberg et al. 2009).

(iii) Different calibration approaches result in different structures and amplitudes of climate reconstructions (e.g. von Storch et al. 2004; Esper et al. 2005).

(iv) The uncertainties about amplitudes of past climates are in turn affecting the sensitivity of climate to different forcings (e.g. solar and volcanic forcing).

Solving these challenges will improve our knowledge about the climate system and about the complex and non-linear ways it is responding to forcings (e.g. solar and volcanic forcing; von Storch et al. 2004). This increasing knowledge will help improving models and thus reduce the uncertainty in climate projections.

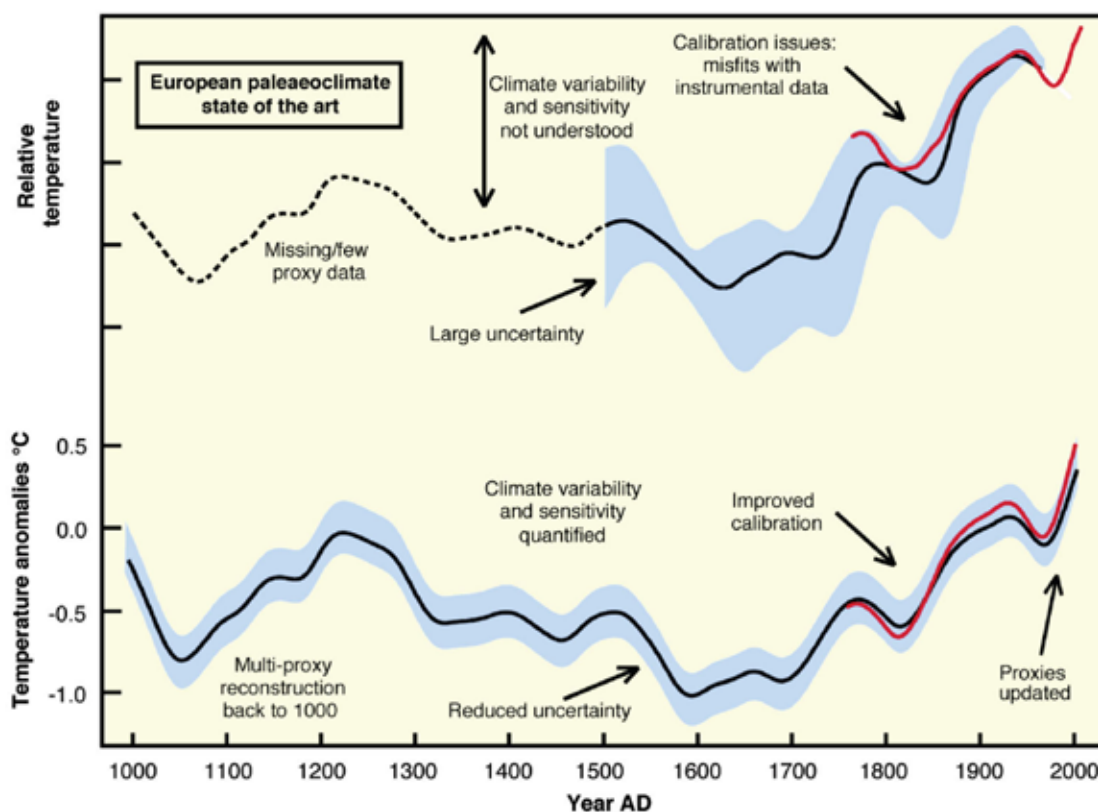


Fig. 1.4. Schematic diagram showing the current limitations of European palaeoclimate reconstructions and the advancements in the detection and quantitative understanding of European climate variability that the EU-FP 6 project 'Millennium' aims to make possible (www.geography.swansea.ac.uk/millennium/index.htm).

1.2. The project frame-work and state of knowledge

To solve these challenges large climate reconstruction campaigns are ongoing.

This PhD study was carried out in the frame of several European and Swiss projects focusing on paleoclimatology.

The thesis was funded by the EU-FP 6 project 'Millennium' (duration from 2006 to 2010). „The Millennium project is a multidisciplinary consortium of more than 38 partners from 16 European countries bringing together historians, chemists, physicists, biologists, geographers, climate modellers and geologists in a multi-disciplinary effort to reconstruct the climate of Europe over the last 1000 years using historical documents ranging from ships logs, church annals and harvest records, and natural archives such as tree rings, insect and plant remains from lakes and peat bogs, ice cores and sea shells” (Millennium web page 2009).

In a long-term perspective this PhD thesis is as well associated with the Swiss National Center of Competence in Research (NCCR)-climate projects VITA (**V**arves, **I**ce cores, and **T**ree rings - **A**rchives with Annual Resolution, duration 2001 - 2005) and VIVALDI (**V**ariability in **I**ce, **V**egetation, and **L**ake **D**eposits – **I**ntegrated, duration 2005 - 2009) and - the SNF funded project ENLARGE, (**E**Nvironmental changes in mountain regions; recorded in high-resolution archives of **L**Akes of the **U**pper **E**ngadine, Switzerland', duration 2004-2006).

The goal of the projects mentioned is to put the current warming in a wider perspective and to reconstruct climate forcings such as total solar irradiance. Thereby, the sensitivity of climate to different forcings is constrained. To achieve these goals a large number of new proxy records were generated.

In the frame of the NCCR-Climature projects VITA and subsequently VIVALDI ice cores, tree rings, peat bogs and varved lake sediments from the Swiss Alps were analysed. This research was carried out applying a multitude of methods by researchers from different scientific fields. The most important study area within the frame of the NCCR-Climature projects was the Upper Engadine Valley in the south-eastern Swiss Alps. An ice core was drilled at Piz Zupo (Jenk, 2001), tree-ring chronologies were developed for four sites in the Upper Engadine Valley (Esper et al. 2008). These tree-ring chronologies are partly included in the tree-ring width and late-wood density based Alpine summer temperature reconstructions of Büntgen et al. (2005) and Büntgen et al. (2006).

In addition, the isotopic composition of a core from the peat bog Mauntschas close to Lake St. Moritz was measured (Schreier, 2005). Regarding lake sediments Lake St. Moritz, Lake Silvaplana and Lake Tscheppa were analysed. For these three lakes diatom assemblages were studied and linked to environmental conditions (von Gunten, 2004; von Gunten et al. 2008; Bigler et al. 2007). In Lake St. Moritz human induced eutrophication starts around 1910. In Lake Silvaplana eutrophication is recorded in the 1950ies whereas in high-altitude Lake Tscheppa no signs of eutrophication were detected (Bigler et al. 2007).

In the frame of the Projects VITA and VIVALDI and in the frame of the SNF-funded project ENLARGE geochemical analyses of sediments of Lake Sils (Blass et al. 2005) and of high-altitude Lakes Tscheppa, Lunghin, Nair (all Margreth, 2006) and Pisch (Schmid, 2007) were carried out.

Finally, the varved sediments of Lake Silvaplana were analysed (Blass, 2006; Trachsel, 2006).

In the frame of the EU-FP 6 project 'Millennium' climate related research in the Upper Engadine Valley was intensified.

For the peat bog Mauntschas a pollen-based climate calibration was developed (Kamenik et al. 2009). In the frame of this study effects of several multivariate calibration methods on the predicted temperatures were tested. For the same peat bog a depth to water-table (dwt) reconstruction using testate amoebae was presented (Lamentowicz et al. in press).

In Lake Silvaplana diatom assemblages were analysed and were used to reconstruct total phosphorus (TP) in the lake (Bigler et al. 2007, see above). This diatom record was extended back to AD 1050 (Westover and Bigler, 2009). In addition the annual cycle of diatoms as reflected in sediment trap data was analysed (Westover and Bigler, 2009). The same study was carried out for chrysophyte stomatocysts (Gisler, 2008). In a further study, chrysophytes were shown to reflect cold-season temperatures for at least the last 70 years although the nutrient input changed considerably in the 1950ies (Baumann, 2009). The chrysophyte record is currently available back to 1870 and is in good agreement with cold-season temperatures during this time period (de Jong and Kamenik personal communication, 2009). Larocque et al. (2009a) showed the high potential of chironomid assemblages in Lake Silvaplana for July temperature reconstruction. These studies were first extended back to AD 1580 (Larocque-Tobler et al. 2009b) and then to AD 1050 (Larocque-Tobler et

al. in review). This July temperature reconstruction is in good accordance with records of Alpine glacier history (Holzhauser et al. 2005).

Beside this work on biotic proxies, geochemical and sedimentological analyses of the sediments of Lake Silvaplana have been carried out for more than twenty years. In a first study Leemann (1993) analysed cores covering the entire Holocene. Four different sediment facies were described. One indicative for the human induced eutrophication (1950ies - 1990), in a second facies varves with low contents of organic matter were formed (1500 BC to 1950 AD). In a third facies varves are absent and grain size median and organic matter content are increased (8700 BC to 1500 BC). In a fourth facies varves are again present and the amount of organic matter is low (0.2%). This different sediment facies were interpreted as indicators for Holocene glacial activity. Varve formation was interpreted as indicative for glacial activity in the catchment (Leemann and Niessen, 1994). This record is still regarded as one of the most important lacustrine records of Holocene glacial activity in the Alps (Ivy-Ochs et al. 2009).

In the next study Ohlendorf (1998) changed the temporal focus and focused on the last 200 to 400 years. The main focus of this thesis was to describe the parameters influencing mass accumulation rate (MAR). On multidecadal time scales changes in MAR are linked to changes in glacier extent (Ohlendorf et al. 1997). On annual to decadal basis changes in MAR are related to summer temperatures. Summer precipitation and snow days have a minor contribution. All these relations are highly non-linear (Ohlendorf, 1998). Additionally, the potential of trace elements and mineralogy to yield MAR-related information was assessed. Thereby, mineralogy was found to be indicative for source regions of the sediments (Ohlendorf, 1998).

In 2001 sediment traps were installed in the lake to get an improved knowledge about sedimentation processes. On the sediment trap material several studies have been carried out. Bluszcz (2003) focused on grain size and mineralogy. Grain size has an annual cycle with maximum grain size occurring in summer. Mineralogy is connected to meteorological conditions mainly to heavy precipitation events.

Troxler (2005) compared the amount of sediment transported to the lake with meteorological and hydrological parameters. On daily to weekly basis no accordance between 'weather' and sedimentation could be detected. On longer time scales

the connections are very complex and highly non-linear.

Between 2003 and 2006 Blass (2006) assessed and highlighted the potential of annually laminated (varved) sediments of Lake Silvaplana for high-resolution quantitative temperature reconstruction. In Blass et al. (2007a) the potential of the sub-centennial component of mass accumulation rate (MAR) for summer temperature reconstruction was demonstrated. Interestingly, the sedimentary system differs from the Little Ice Age (LIA) conditions in the 20th century. In Blass et al. (2007b) bSi flux was shown to give valuable warm season temperature reconstructions. This reconstruction is in good accordance with fully independent warm season temperature reconstructions. In another study (Trachsel 2006, Trachsel et al. 2008), the connection between mineralogy and climate conditions established by Bluszcz (2003) was found as well for the sediment.

1.3. General objectives and outline

Starting from this information about Lake Silvaplana and known challenges in paleoclimatology, the focus of this thesis was four-fold:

- (i) Extend existing records of climate variability in Lake Silvaplana back to approximately AD 1000. Compare these records with fully independent climate reconstructions and compare the recent warming with the climate of the last millennium.
- (ii) Test the potential of new analytical methods on the sediments of Lake Silvaplana. Sediments of Lake Silvaplana are especially promising for this purpose because many studies have been carried out giving insight into sedimentary processes.
- (iii) Assess the effects of different widely used univariate calibration methods on the reconstructed amplitude of past climate variability.
- (iv) Explore the potential of climate reconstructions derived from sediments of Lake Silvaplana to preserve interannual climate variability.

These main questions of this thesis are addressed in chapters four to six.

Preceding the main part, in chapter two Lake Silvaplana, its catchment and the climate of the Engadine Valley is described. In chapter three meteorological data and climate reconstructions mentioned in this thesis are described. Field methods, analytical methods and numerical methods used in this thesis are introduced.

In chapter 4, the potential of a relatively new, non-destructive sediment scanning technique for climate reconstruction is tested. This article presents

results from one of the first times that scanning in-situ reflectance spectroscopy is applied on minerogenic sediments. Therefore, we systematically test the method and the significance of the data produced. We further describe a possible way of how to get step-by-step from the raw reflectance measurement to a climate reconstruction.

We first look for published algorithms that describe the reflectance characteristics of minerals that are known to be present in the sediments (from XRD data). In addition, we define further algorithms that describe the remaining (yet unexplained) distinct characteristics of the measured reflectance spectra of the sediment of Lake Silvaplana. Each of these algorithms is then used to produce a spectrum-derived variable. To gain further insight into the known and unknown variables extracted, we apply a principal component analysis (PCA) on the extracted variables to detect similarities. Subsequently we perform and discuss the transformation of the raw reflectance data into a climate reconstruction, which involves several steps: (i) Testing the effects of climate and sediment parameters on the spectrum-derived variables (using redundancy analysis RDA), (ii) establish univariate and multivariate calibration models for climate and sediment parameters (iii) apply the optimal calibration model downcore, and (iv) verify the reconstruction back in time (here back to AD 1177) with fully independent data sets. (The study presented in this chapter will be submitted the Journal of Paleolimnology with the title '*Scanning reflectance spectroscopy (380 – 730 nm): a novel method for quantitative high-resolution climate reconstructions from minerogenic lake sediments*').

In Chapter 5, a summer to summer-autumn temperature reconstruction back to AD 1177 is presented. This reconstruction, based on biogenic silica (bSi) flux, is in good accordance with fully independent temperature reconstructions and has skill on decadal to centennial time scales. We therefore propose a method to combine the bSi flux based summer temperature with another, chironomid based, summer temperature reconstruction which has skill on centennial to multi-centennial time-scales. We further show the high sensitivity of the amplitude of reconstructions to calibration methods used. We therefore tested the effects of six different univariate calibration methods (Inverse Regression, Inverse Prediction, Generalised Least Squares, Major Axis regres-

sion, Ranged Major Axis regression and Standard Major Axis regression) on predicted amplitudes. We also test the accuracy of different measures for the quality of a calibration such as measures reduction of error (RE), coefficient of efficiency (CE), root mean square error of prediction (RMSEP) divided by the predicted amplitude and the correct representation of the amplitude of the instrumental target. Thereby, weaknesses of the widely used calibration measures RE and CE are found. (This study is in review with Quaternary Science Reviews with the title '*Quantitative summer temperature reconstruction derived from a combined biogenic Si and chironomid record from varved sediments of Lake Silvaplana (south-eastern Swiss Alps) back to AD 1177*').

In chapter 6 a statistical analysis was carried out on the reconstructions derived from sediments of Lake Silvaplana. As mentioned in chapter 1.1. climate models project changes in interannual variability of summer temperatures going along with projected increases in mean temperatures. In this chapter, we assess past climates for such changes using long instrumental temperature series (from 1659, 1760 and 1864 onwards) distributed across Central Europe. These records extend back to the Little Ice Age, thus covering a broad temperature range. We ask the following questions: (i) how does the interannual summer temperature variability during the Little Ice Age compare to the variability during the 20th century and the associated strong warming trend? (ii) How were the other seasons different? (iii) Are the observed changes in the interannual temperature variability of the different seasons related to the climatology and occurrence of synoptic scale circulation types? (iv) Can natural proxies such as tree rings and annually laminated lakes sediments provide adequate information to address these questions? If yes, this would allow us to test the model projections for the end of the 21st century with proxy data extending back to the best warm analogues during the Medieval Warm Period or even the Roman Time. (This study is in revision with Climate Dynamics with the title '*Is inter-annual temperature variability related to the mean temperature? Evidence from instrumental, early instrumental and proxy data in Europe since 1600 AD*').

Finally, in chapter 7 general conclusions emerging from this thesis are drawn and a few challenges climatologists are facing are mentioned.

References

- Baumann, E., 2009. Effects of human impact and climate change on sedimentary chrysophyte stomatocyst assemblages in Lake Silvaplana. MSc thesis. University of Bern, Bern.
- Begert, M., Schlegel, T., Kirchhofer, W., 2005. Homogeneous temperature and precipitation series of Switzerland from 1864 to 2000. *International Journal of Climatology* 25, 65 - 80.
- Bigler, C., von Gunten, L., Lotter, A.F., Hausmann, S., Blass, A., Ohlendorf, C., Sturm, M., 2007. Quantifying human-induced eutrophication in Swiss mountain lakes since AD 1800 using diatoms. *Holocene* 17, 1141 - 1154.
- Blass, A., 2006. Sediments of two high-altitude Swiss lakes as high-resolution late Holocene paleoclimate archives. PhD thesis. University of Bern, Bern.
- Blass, A., Grosjean, M., Troxler, A., Sturm, M., 2007a. How stable are twentieth-century calibration models? A high-resolution summer temperature reconstruction for the eastern Swiss Alps back to AD 1580 derived from proglacial varved sediments. *The Holocene* 17, 51 - 63.
- Blass, A., Bigler, C., Grosjean, M., Sturm, M., 2007b. Decadal-scale autumn temperature reconstruction back to AD 1580 inferred from the varved sediments of Lake Silvaplana (southeastern Swiss Alps). *Quaternary Research* 68, 184 - 195.
- Bluszcz, P. 2003. Prozessstudien zur Kalibration sedimentärer Tracer. Partikeldynamik im Silvaplanner See (Südost-Schweiz). MSc thesis. University of Bremen, Bremen.
- Büntgen, U., Esper, J., Frank, D.C., Nicolussi, K., Schmidhalter, M., 2005. A 1052-year tree-ring proxy for Alpine summer temperatures. *Climate Dynamics* 25, 141 - 153.
- Büntgen, U., Frank, D.C., Nievergelt, D., Esper, J., 2006. Summer temperature variations in the European Alps, AD 755-2004. *Journal of Climate* 19, 5606 - 5623.
- Bürger, G., Fast, I., Cubasch, U., 2006. Climate reconstruction by regression - 32 variations on a theme. *Tellus Series A-Dynamic Meteorology and Oceanography* 58, 227 - 235.
- Crowley, T.J., 2000. Causes of climate change over the past 1000 years. *Science* 289, 270 - 277.
- Esper, J., Frank, D.C., Wilson R., 2004. Climate Reconstructions: Low-Frequency Ambition and High-Frequency Ratification. *Eos* 85, 113.
- Esper, J., Frank, D., Wilson, R., Briffa, K., 2005. Effect of scaling and regression on reconstructed temperature amplitude for the past millennium. *Geophysical Research Letters* 32.
- Gisler, P., 2008. Die Sedimentation der Stomatozysten von Chrysophyten im Silvaplana-See - Bedeutung für die Rekonstruktion des saisonalen Klimas. MSc thesis. University of Bern, Bern.
- Glaser, R. and Riemann, D., 2009. A thousand-year record of temperature variations for Germany and Central Europe based on documentary data. *Journal of Quaternary Science* 24, 437 - 449.
- Grubb, H., Briffa, K.R., Karlen, W., Bartholin, T.S., Jones, P.D., Kromer, B., 2002. A 7400-year tree-ring chronology in northern Swedish Lapland: natural climatic variability expressed on annual to millennial timescales. *Holocene* 12, 657 - 665.
- Hegerl, G.C., Crowley, T.J., Allen, M., Hyde, W.T., Pollack, H.N., Smerdon, J., Zorita, E., 2007. Detection of human influence on a new, validated 1500-year temperature reconstruction. *Journal of Climate* 20, 650 - 666.
- Holzhauser, H., Magny, M., Zumbühl, H.J., 2005. Glacier and lake-level variations in west-central Europe over the last 3500 years. *Holocene* 15, 789 - 801.
- IPCC (2007). *Climate Change 2007: the Physical Science Basis. Contribution of Working Group I to the Fourth Assessment Report of the Intergovernmental Panel on Climate Change.* Cambridge University Press, Cambridge.
- Ivy-Ochs, S., Kerschner, H., Maisch, M., Christl, M., Kubik, P.W., Schlüchter, C., 2009. Latest Pleistocene and Holocene glacier variations in the European Alps. *Quaternary Science Reviews* 28, 2137 - 2149.
- Jansen E. et al. 2007. Paleoclimate. In: Solomon, S., et al. (eds.). *Climate Change 2007: The Physical Science Basis. Contribution of Working Group I to the Fourth Assessment Report of the Intergovernmental Panel on Climate Change.* Cambridge University Press, Cambridge, pp. 434 - 498.
- Jenk, T., 2001. Suche nach einem als Klimaarchiv geeigneten Gletscher im Bernina-Gebiet. MSc thesis. University of Bern, Bern.

- Kamenik, C., van der Knaap, W.O., van Leeuwen, J.F.N., Goslar, T., 2009. Pollen/climate calibration based on a near-annual peat sequence from the Swiss Alps. *Journal of Quaternary Science* 24, 529 - 546.
- Lamentowicz, M., van der Knapp, W.O., Lamentowicz, L., van Leeuwen, J.F.N., Mitchell, E.A.D., Goslar, T., Kamenik, C., (in press). A near-annual palaeohydrological study based on testate amoebae from a sub-alpine mire: surface wetness and the role of climate during the instrumental period. *Journal of Quaternary Science*.
- Lamoureux S., 2001. Varve chronology techniques. In: Last, W.M., and Smol, J.P., (eds.) *Tracking environmental change using lake sediments*. Kluwer, Dordrecht, pp. 247 – 259.
- Larocque, I., Grosjean, M., Heiri, O., Bigler, C., Blass, A., 2009a. Comparison between chironomid-inferred July temperatures and meteorological data AD 1850-2001 from varved Lake Silvaplana, Switzerland. *Journal of Paleolimnology* 41, 329 - 342.
- Larocque-Tobler, I., Grosjean, M., Heiri O., Trachsel, M., 2009b. High-resolution chironomid-inferred temperature history since AD 1580 from varved Lake Silvaplana, Switzerland: comparison with local and regional reconstructions. *The Holocene* 19, 1201–1212.
- Larocque-Tobler I., Grosjean, M., Heiri, O., Trachsel, M., Kamenik, C., (in review) 1000 years of climate change reconstructed from chironomid subfossils preserved in varved-lake Silvaplana, Engadine, Switzerland. *Quaternary Science Reviews*.
- Leemann, A., 1993. Rhythmite in alpinen Vorgletscherseen – Warvenstratigraphie und Aufzeichnung von Klimaveränderungen. PhD thesis. ETH Zürich. Zürich.
- Leemann, A., and Niessen, F., 1994. Holocene glacial activity and climatic variations in the Swiss Alps: reconstructing a continuous record from proglacial lake sediments. *The Holocene* 4, 259-268.
- Margreth, S., 2006. Partikelfluss und Sedimentbildung in Oberengadiner Seen. MSc thesis. University of Zürich, Zürich.
- Meehl G. et al. 2007. Global Climate Projections. In: Solomon, S., et al. (eds.). *Climate Change 2007: The Physical Science Basis. Contribution of Working Group I to the Fourth Assessment Report of the Intergovernmental Panel on Climate Change*. Cambridge University Press, Cambridge, pp. 747 - 846.
- Meteoschweiz. Swiss Federal Office of Meteorology and Climatology. www.meteoschweiz.ch.
- Moberg A., Dobrovolny, P., Wilson, R., Brazdil, R., Pfister, C., Glaser, R., Leijonhufvud, L., Zorita E., 2009. Quantifying uncertainty in documentary-data based climate reconstructions? EGU general assembly, CL50, Uncertainties in climate estimates and their time-scales: past, present and future.
- Ohlendorf, C., Niessen, F., Weissert, H., 1997. Glacial varve thickness and 127 years of instrumental climate data: a comparison. *Climatic Change* 36, 391 - 411.
- Ohlendorf, C., 1998. High Alpine Lake Sediments as Chronicles for Regional Glacier and Climate History in the Upper Engadine, Southeastern Switzerland. PhD thesis. ETH Zürich, Zürich.
- Räisänen, J., 2002. CO₂-induced changes in interannual temperature and precipitation variability in 19 CMIP2 experiments. *Journal of Climate* 15, 2395 - 2411.
- Riedwyl, N., Luterbacher, J., Wanner, H., 2008. An ensemble of European summer and winter temperature reconstructions back to 1500. *Geophysical Research Letters* 35.
- Schreier, R., 2005. Studies on past climatic and environmental changes by chemical investigations of peat cores from the Upper Engadine (Swiss alpine area). PhD thesis. University of Bern, Bern.
- Trachsel, M., 2006. Mineralogie der Varven des Silvaplannersees (Engadin) als quantitativer Proxy für eine hochaufgelöste Klimarekonstruktion 1580 - 1950 AD. MSc thesis. University of Bern, Bern.
- Trachsel, M., Eggenberger, U., Grosjean, M., Blass, A., Sturm, M., 2008. Mineralogy-based quantitative precipitation and temperature reconstructions from annually laminated lake sediments (Swiss Alps) since AD 1580. *Geophysical Research Letters* 35.
- Troxler, A., 2005. Sedimentationsraten im Silvaplannersee und deren Abhängigkeit von hydro-meteorologischen Parametern. MSc thesis. University of Bern, Bern.
- von Gunten, L., 2004. Diatomeen eines Hochgebirgssees (Lej da la Tscheppa, Oberengadin) als Umweltindikatoren der letzten 400 Jahre. MSc

thesis. University of Bern, Bern.

von Gunten, L., Heiri, O., Bigler, C., van Leeuwen, J., Casty, C., Lotter, A.F., Sturm, M., 2008. Seasonal temperatures for the past similar to 400 years reconstructed from diatom and chironomid assemblages in a high-altitude lake (Lej da la Tscheppa, Switzerland). *Journal of Paleolimnology* 39, 283 - 299.

von Storch, H., Zorita, E., Jones, J.M., Dimitriev, Y., Gonzalez-Rouco, F., Tett, S.F.B., 2004. Reconstructing past climate from noisy data. *Science* 306, 679 - 682.

Westover, K., and Bigler C., 2009. High-resolution diatom-inferred temperature reconstruction from the southeastern Swiss alps, AD 1350 to present. *Millennium Abstract Volume*.

Zorita, E., Gonzalez-Rouco, F., Legutke, S., 2003. Testing the Mann et al. (1998) approach to paleoclimate reconstructions in the context of a 1000-yr control simulation with the ECHO-G coupled climate model. *Journal of Climate* 16, 1378 - 1390.

Zorita, E., Stocker, T.F., von Storch, H., 2008. How unusual is the recent series of warm years? *Geophysical Research Letters* 35.

Chapter 2



2. Study area

2.1. Lake Silvaplana

Lake Silvaplana is located in the Upper Engadine Valley (south-eastern Swiss Alps) at an altitude of 1791 m asl. (Fig. 2.1). Clastic sedimentation is dominant until 1950 when human induced eutrophication started (Bigler et al. 2007; Blass et al. 2007b). Average depth of Lake Silvaplana is 47 m, maximum depth amounts to 77 m. The volume is of $127 \cdot 10^6 \text{ m}^3$ and the mean water residence time is eight month (LIMNEX, 1994). The lake water pH is 7.8. Lake Silvaplana is a dimictic lake with a rather short spring mixis after the ice break-up, followed by the summer stratification from June through November (Bosli-Pavoni, 1971). The second overturn of the year usually occurs in December. The ice-cover usually lasts from January to May. In the exceptional warm winter 2006/2007 the lake did not entirely freeze up. The sediment formed clastic varves during the last 3300 years (Leemann and Niessen, 1994). A detailed description of hydrography, hydrochemistry and limnology of Lake Silvaplana is found in Ohlendorf (1998).

2.2. The catchment

The catchment of Lake Silvaplana covers 175 km² including the catchment of Lake Sils with about 9.7 km² (6 %) glaciated area (Fig. 2.1). Lake Sils retains most of the sediments of its catchment and does not contribute to the sediment budget of Lake Silvaplana (Blass et al. 2007a). The catchment of Lake Silvaplana contributing to sedimentation (i.e. without the catchment of Lake Sils) amounts to 129 km² with about 6 km² (5 %, status 1998) of area covered by glacier. The catchment of Lake Silvaplana is characterized by steep slopes to the northwest and by rather smooth slopes rising up in the south-east. Most glaciers are located south of the lake in the Fex Valley. The outflow of Lake Sils, the Inn River, is discharging $2 \text{ m}^3 \text{ s}^{-1}$ on average into Lake Silvaplana. The second important tributary of Lake Silvaplana is the Fedacla River ($1.5 \text{ m}^3 \text{ s}^{-1}$) which carries a lot of suspended particles. The Fedacla river is draining the glaciated

Fex Valley. The Rivers Vallun and Surlej (Vallun; $0.7 \text{ m}^3 \text{ s}^{-1}$ and Surlej; $0.3 \text{ m}^3 \text{ s}^{-1}$) which formed the alluvial fans of Silvaplana and Surlej are particularly active during spring snowmelt and thunderstorms in summer.

The north-east dipping main valley follows the Engadine line, a major geologic fault system. This discontinuity dissects a pile of east dipping Austro-Alpine and Pennine nappes. Three of them are found in the catchment. The Pennine Margna nappe (orthogneisses and schists) crops out in the glaciated Fex Valley to the south. The Pennine Platta nappe (ophiolites including serpentinite, gabbro and greenschists) covers the south-eastern part of the catchment. The Austro-Alpine Err-Bernina nappe (gneiss and granite) covers the north-western area (Staub, 1946; Spillmann, 1993). Highest elevations in the catchment are Piz Corvatsch (3451 m asl.) to the east and Piz Güglia (3380 m asl.) to the north. Both are situated in the Err-Bernina nappe.

The lakes developed in depressions where probably large dead-ice bodies melted in Late Glacial times (Suter, 1981).

Human impact on vegetation (increase in grazing and cerealia pollen) is recorded since 2000 BC with strongest impacts in the last millennium (Gobet, 2004). In the 19th century the forested area increased due to afforestation programs and prohibition of grazing of goats (Caviezel, 2007). Throughout the entire Engadine Valley field terraces are found on the slopes. Up to the connection with the railway in 1903 crops were grown on these field terraces (Mathieu, 1992).

In the 1950ies tourism experienced a boom resulting in human induced eutrophication of Lake Silvaplana.

Pre quaternary and quaternary geology are widely described in Ohlendorf (1998) and information about Holocene vegetation history is found in Gobet (2004). Environmental history since 1750 is presented in Caviezel (2007) and population, economic and agricultural history is reviewed in Mathieu (1992) and Mathieu (1998).

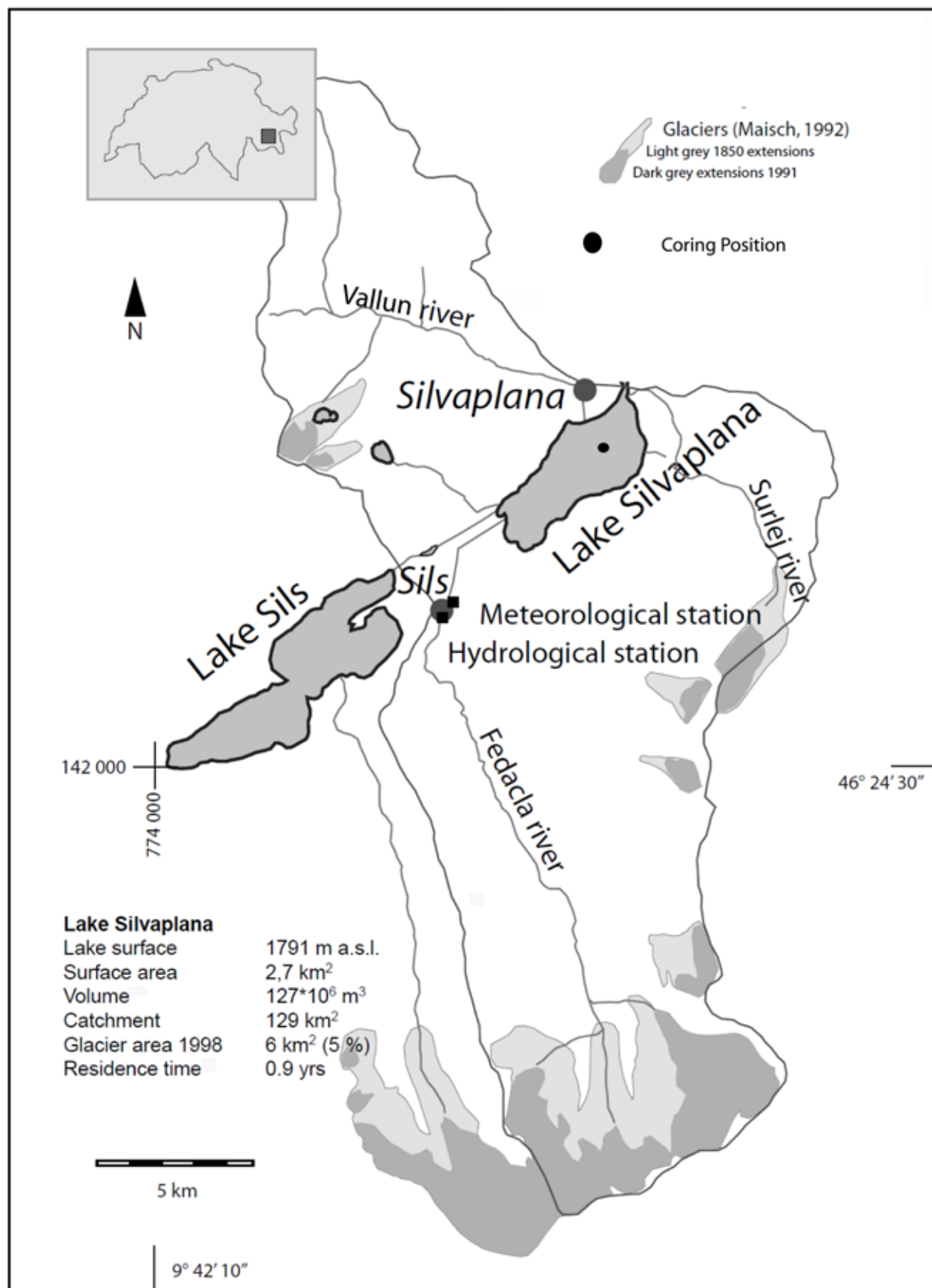


Fig. 2.1. Overview map of the Lake Silvaplana catchment area, including the coring position, meteorological station and the glacier extent during the Little Ice Age and in 1991 (redrawn from Blass et al. 2007a).

2.3. Climate

The Engadine Valley is a typical inner-alpine dry valley (Gensler and Schüepf, 1991). In Sils-Maria mean annual precipitation amounts to 978 mm (climatological standard period 1961 – 1990). A precipitation maximum occurs in August (121 mm) and a minimum is found in February (42 mm). Maximum temperature is measured in July (10.5°C) and minimum temperature occurs in January (-7.3°C) resulting in an annual temperature cycle of 17.8°C (Fig. 2.2 and 2.6.).

The spatial representativity of summer temperatures of the Engadine Valley is high (Fig. 2.3): the grid box (9°–10°E, 46°–47°N) representing the Engadine shows a correlation higher than $r > 0.9$ for entire Switzerland and a correlation higher than $r > 0.7$ for large parts of Central Europe. The spatial homogeneity of summer precipitation is considerably lower than for temperature, hence correlations higher than $r > 0.7$ are only found for adjacent regions.

Brunetti et al. (2006) classified the precipitation in the Alps based on EOF-analysis (empirical orthogonal function, same as principal component analysis). In this analysis the Upper Engadine is

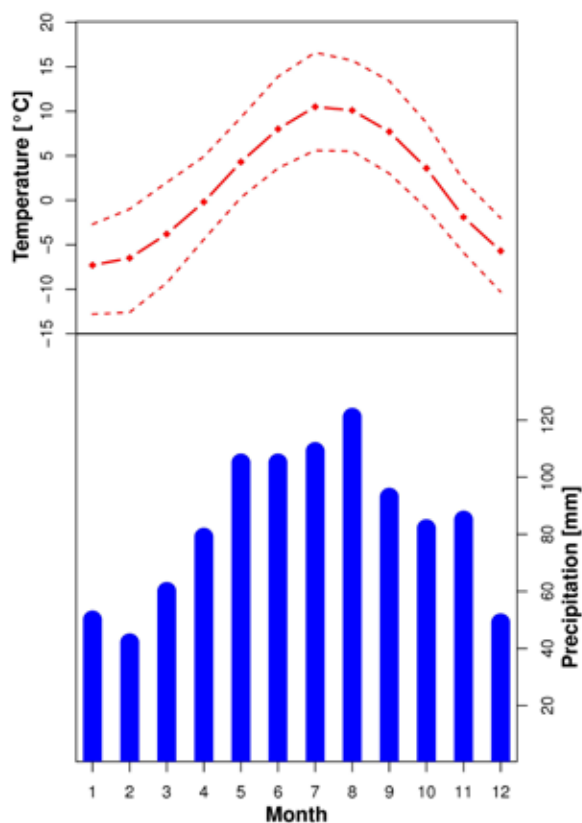


Fig. 2.2. Monthly mean temperatures and precipitation of the meteorological station in Sils-Maria between 1961 - 1990 according to Meteoschweiz.

situated at the border of the EOFs generating high loadings for the south-west or for the north-east of the Alps. However, the Engadine does not experience summer drought the most typical feature of precipitation in the south-west of the Alps (Brunetti et al. 2006).

A cluster analysis by Begert (2008) further revealed the complexity of the spatial distribution of precipitation in Switzerland. Overall 32 precipitation areas are generated. The Engadine Valley is divided into three precipitation regions: the Upper Engadine (Sils-Maria and Samedan, for the exact location see Fig. 2.4.), the upper part of the Lower Engadine (Zernez and Susch) and the lower part of the Lower Engadine (Scuol and Martina). The two latter regions form own clusters, whereas the Upper Engadine is in the same cluster as the stations Poschiavo and Santa Maria located in inner-alpine valleys to the south and to the south-east. (Begert, 2008). From the Upper Engadine there is a sharp border to the north and to the south-west. Station Soglio in Val Bregaglia to the south-west of Sils Maria is clustered together with the stations in the Tessin Valley (Southern Switzerland) whereas Bivio to the north is clustered with the stations in

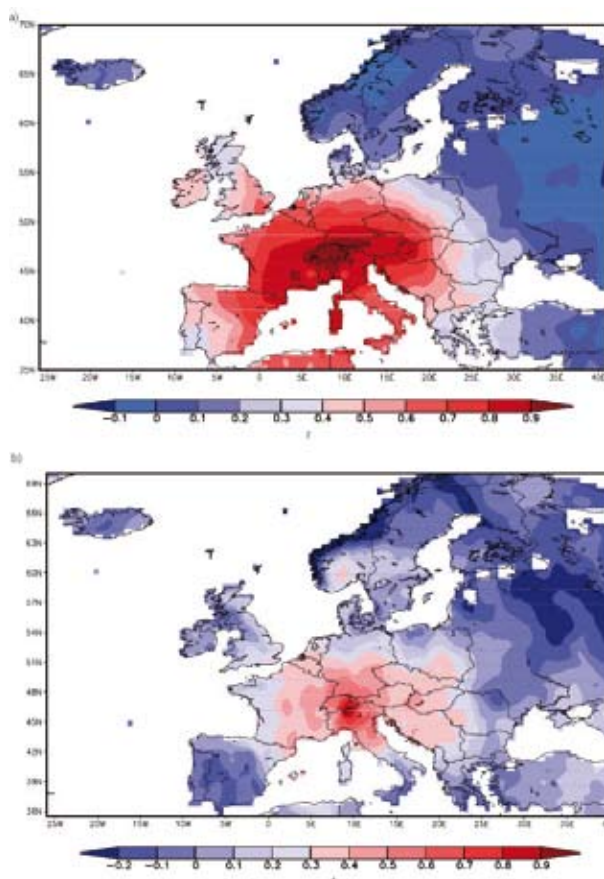


Fig. 2.3. Spatial correlation between the Engadine grid box (9°–10°E, 46°–47°N) and Europe for JJA temperatures (a) and precipitation (b) for the period 1900–2000. (Trachsel et al. 2008)



Fig. 2.4. Overview map of south-eastern Switzerland including all meteorological stations mentioned.

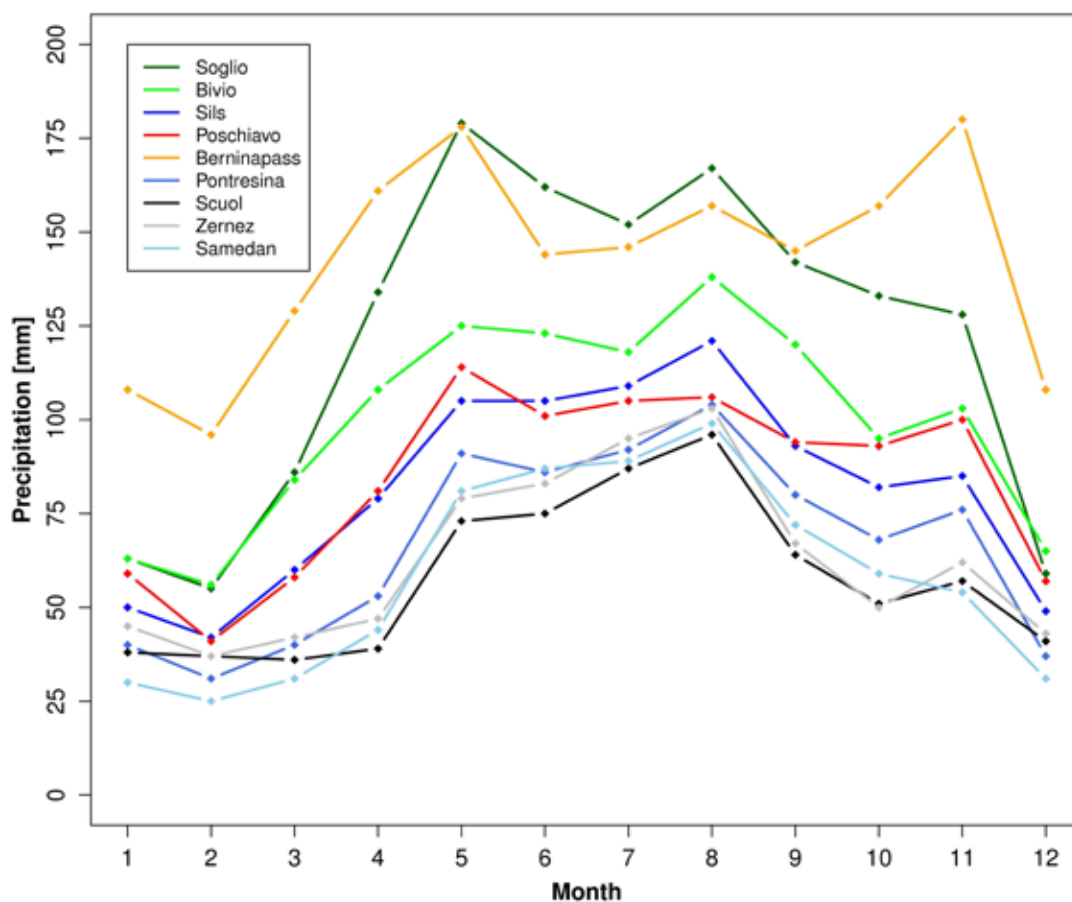


Fig. 2.5. Annual precipitation cycle recorded at meteorological stations Berninapass, Bivio, Pontresina, Poschiavo, Samedan, Scuol, Sils, Soglio and Zernez. For the exact location see Fig. 2.4. (Data Meteoschweiz).

Central Graubünden (Begert, 2008). The amount of precipitation in these three stations is differing massively. In Bivio (9 km distance to Sils-Maria) precipitation amounts to 1198 mm per year with constant values between May and September. In Soglio (19 km distance to Sils-Maria) 1459 mm of precipitation fall on annual average. The maximum is found in May, and precipitation is only low from December to March (Fig. 2.5).

In the Upper Engadine Valley large precipitation gradients are found as well: in Sils-Maria 978 mm precipitation are registered, whereas in the station Samedan situated 15 km down-valley the precipitation only amounts to 700 mm and in station Pontresina 5 km from Samedan 799 mm of precipitation are measured on annual average (Fig. 2.5). Interestingly, relative precipitation maxima occur in May and November in Pontresina. These relative maxima are neither found in Sils-Maria nor in Samedan but in station Poschiavo situated in the Valley south of the Engadine and at Berninapass

connecting the two valleys (Fig. 2.4). These heterogeneities of precipitation in the small area described by the three stations Sils-Maria, Samedan and Pontresina give an impression of the complex processes controlling precipitation formation in the Upper Engadine Valley.

Compared to other valley-bottom stations in the Engadine the climate is humid in Sils-Maria. Two stations in the Lower Engadine (Zernez 753 mm, Scuol 694 mm) are as well experiencing dry conditions.

For temperature the situation is less complicated. Begert (2008) found 13 clusters to give an appropriate overview of Swiss temperature regions. The entire Engadine valley is in one cluster. However, temperature in the Engadine Valley is as well affected by local effects. The annual temperature amplitude of Samedan (1702 m) is 2.8°C higher than in Sils-Maria (1798 m). In winter temperature is up to 2.5°C lower in Samedan than in Sils-Maria (Fig. 2.6). This is mainly because Samedan is

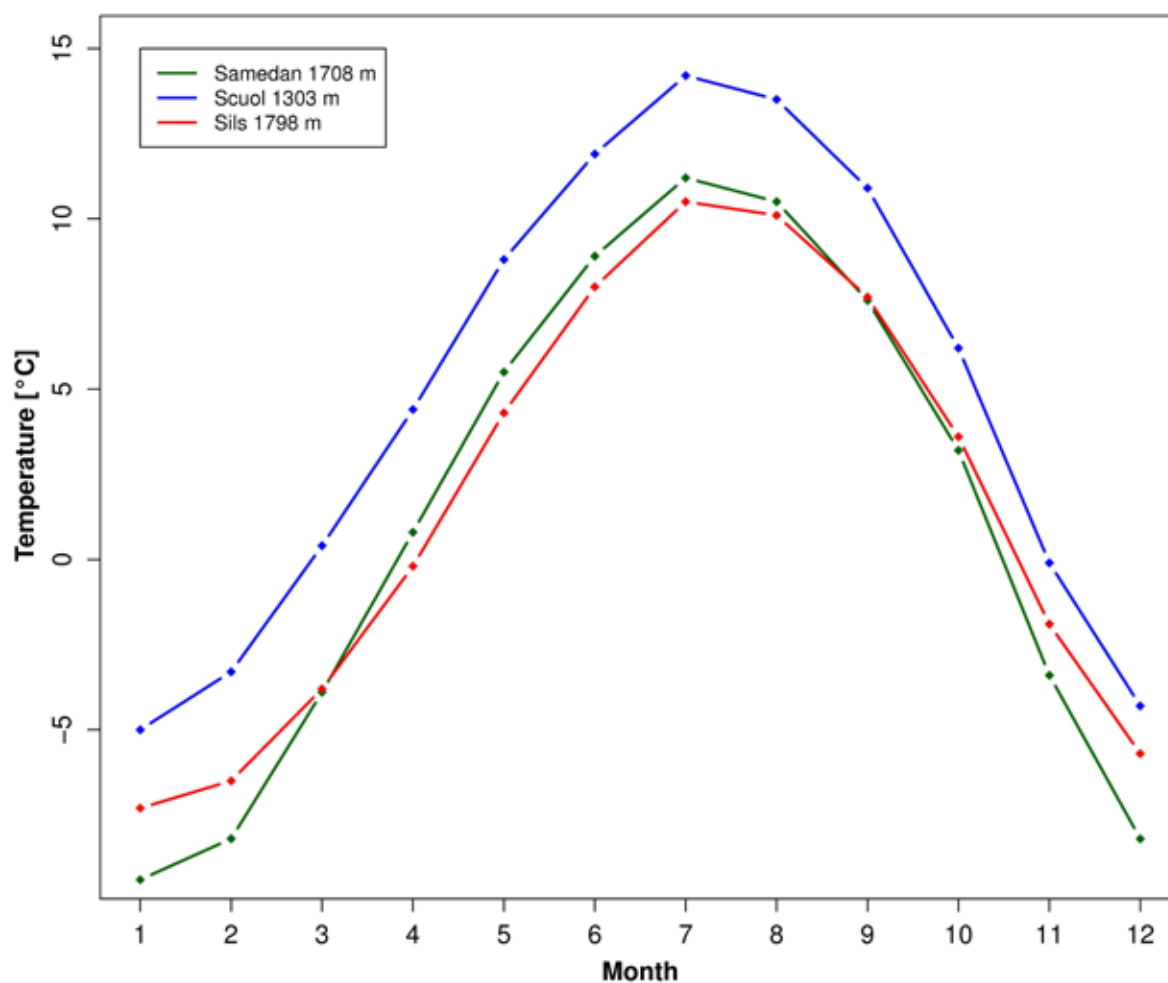


Fig. 2.6. Annual temperature cycle of the meteorological stations Samedan, Scuol and Sils. For the exact location see Fig. 2.4. (Data Meteoscheiz).

situated in a topographic depression where cold air masses remain and form an inversion (Gensler and Schüepp, 1991). In summer the temperature difference between Sils-Maria and Samedan expected from the altitudinal difference based on the usual lapse rate (0.7°C) is only found for July. The difference is lower in August (0.4°C) and higher in June (0.9°C) (all data Meteoschweiz).

Typically, the annual temperature amplitude of the Engadine is expected to be larger than on the Swiss plateau (Ohlendorf, 1998). This is clearly the case for Samedan with an annual temperature range of 20.6°C and for Scuol (19.2°C). Nevertheless, the annual temperature amplitude of Sils Maria (17.8°C) is lower than the temperature amplitude on the Swiss plateau [e.g. Bern (18.5°C); Zürich (18.4°C); Payerne (18.5°C)]. Further, the positive trends in seasonal and annual temperatures are less pronounced in the Engadine Valley (station Sils-Maria) than in North-Alpine Switzerland (period 1864 – 2000; Begert et al. 2005).

References

- Begert, M., Schlegel, T., Kirchhofer, W., 2005. Homogeneous temperature and precipitation series of Switzerland from 1864 to 2000. *International Journal of Climatology* 25, 65 - 80.
- Begert, M., 2008. Die Repräsentativität der Stationen im Swiss National Basic Climatological Network (Swiss NBCN). *Arbeitsbericht MeteoSchweiz* Nr. 217.
- Bigler, C., von Gunten, L., Lotter, A.F., Hausmann, S., Blass, A., Ohlendorf, C., Sturm, M., 2007. Quantifying human-induced eutrophication in Swiss mountain lakes since AD 1800 using diatoms. *Holocene* 17, 1141 - 1154.
- Blass, A., Grosjean, M., Troxler, A., Sturm, M., 2007a. How stable are twentieth-century calibration models? A high-resolution summer temperature reconstruction for the eastern Swiss Alps back to AD 1580 derived from proglacial varved sediments. *Holocene* 17, 51 - 63.
- Blass, A., Bigler, C., Grosjean, M., Sturm, M., 2007b. Decadal-scale autumn temperature reconstruction back to AD 1580 inferred from the varved sediments of Lake Silvaplana (southeastern Swiss Alps). *Quaternary Research* 68, 184 - 195.
- Bosli-Pavoni, M., 1971. Ergebnisse der limnologischen Untersuchungen der Oberengadiner Seen. *Schweizerische Zeitschrift für Hydrologie* 33, 386 - 409.
- Brunetti, M., Maugeri, M., Nanni, T., Auer, I., Böhm, R., Schöner, W., 2006. Precipitation variability and changes in the greater Alpine region over the 1800-2003 period. *Journal of Geophysical Research* 111.
- Caviezol, G., 2007. Hochwasser und ihre Bewältigung anhand des Beispiels Oberengadin 1750 – 1900. MSc thesis. University of Bern, Bern.
- Gensler, G. and Schüepp, M. 1991. Witterungsklimatologie von Graubünden. *Beiträge zur Geographie Graubündens*, 7 - 17.
- Gobet, E., 2004. Landschafts und Vegetationsdynamik der letzten 12000 Jahre im Oberengadin. PhD thesis. University of Bern, Bern.
- Leemann, A., and Niessen, F., 1994. Holocene glacial activity and climatic variations in the Swiss Alps: reconstructing a continuous record from proglacial lake sediments. *Holocene* 4, 259 - 268.
- LIMNEX. 1994: Gewässerzustand und Gewässerschutzmassnahmen im Oberengadin. Bericht zuhanden des Amtes für Umweltschutz, Kanton Graubünden.
- Mathieu, J., 1992. Eine Agrargeschichte der inneren Alpen. Chronos, Zürich.
- Mathieu, J., 1998. Geschichte der Alpen 1500-1900. Böhlau, Wien.
- Meteoschweiz. Swiss Federal Office of Meteorology and Climatology. www.meteoschweiz.ch
- Ohlendorf, C., 1998. High Alpine Lake Sediments as Chronicles for Regional Glacier and Climate History in the Upper Engadine, Southeastern Switzerland. PhD thesis. ETH Zürich, Zürich.
- Spillmann, P., 1993. Die Geologie des penninisch-ostalpinen Grenzbereichs im südlichen Berninagebirge. PhD thesis. ETH Zürich, Zürich.
- Staub, R., 1946. Geologische Karte der Bernina Gruppe und Umgebung. *Geologische Spezialkarte der Schweiz*. Blatt 118.
- Suter, J., 1981. Gletschergeschichte des Oberengadins: Untersuchungen von Gletscherschwankungen in der Err-Julier-Gruppe. PhD thesis. University of Zürich, Zürich.
- Trachsel, M., Eggenberger, U., Grosjean, M., Blass, A., Sturm, M., 2008. Mineralogy-based quantitative precipitation and temperature reconstructions from annually laminated lake sediments (Swiss Alps) since AD 1580. *Geophysical Research Letters* 35.

Chapter 3



3. Data and methods

In this chapter climate data, field methods and laboratory methods used in this thesis are described. Then, special emphasis is given to numerical methods. In contrast to sedimentological methods these latter methods are not yet widely used in the field of geochemical and sedimentological analyses.

3.1. Climate and paleoclimate data

Homogenised monthly temperature and precipitation data from the meteorological station Sils-Maria close (3 km) to Lake Silvaplana are available back to 1864 (Beger et al. 2005). These data were used for calibration-in-time. Further back in time early instrumental data are available back to 1760 (e.g. Böhm et al. 2001; Auer et al. 2007). These early instrumental data are included in the gridded temperature reconstruction for the Alpine area of Casty et al. (2005). This reconstruction as well includes documentary data and spans back to 1500. Two tree-ring based summer temperature reconstructions (Büntgen et al. 2005; Büntgen et al. 2006) cover the last millennium. These two reconstructions rely on tree ring-width (Büntgen et al. 2005) and maximum late-wood density (Büntgen et al. 2006) measurements. In this thesis the sediment-derived reconstructions were compared to the mean value of the temperature field reconstruction of Casty et al. (2005) and to the late-wood density based reconstruction of Büntgen et

al. (2006).

3.2. Field and laboratory methods

One short core of 130 cm length (SVP 06-1) and three Niederreiter piston cores of nine meter length (SVP 06-2, SVP 06-3, SVP 06-4) were recovered from Lake Silvaplana on 21. and 22. 3. 2006.

In this thesis the uppermost three metres of cores SVP 06-2 and SVP 06-3 were analysed. These three meter long cores were divided into three approximately 1 m long cores named SVP 06-2 I, SVP 06-2 II, SVP 06-2 III, SVP 06-3 I, SVP 06-3 II and SVP 06-3 III (Fig. 3.1).

Prior to sampling on varve basis the cores SVP 06-2 and SVP 06-3 were shock-frozen with liquid nitrogen. Core pictures were taken on which layers were provided with numbers. This allowed the correlation between the photographs and the core during the sampling procedure in the freeze laboratory. Sampling was carried out as described by Blass (2006): Sub-samples of the individual annual layers were scratched off the frozen sediment slab in the freeze laboratory. The core temperature was constantly kept below - 8 °C.

Sediments were sub-sampled for thin-sections by cutting 19 cm long and 2 cm wide, overlapping slabs. Samples were freeze dried and subsequently impregnated with a four component mixture (NSA, VCD, DER and DMAE, Polysciences Europe GmbH) and processed to 30 µm thin-sections at the MK-Factory, Potsdam (M. Köhler).

The chronology of cores SVP 04–11 and SVP 05–1 (Blass et al. 2007a) was refined according to a flood history based on historical records (Caviezel, 2007). In the process of refinement a section prior dated to 1779 -1794 where varve counts were inconclusive (Blass et al. 2007a) was removed from the chronology. This inconclusive section was most probably caused by a major flood recorded in 1793. After removing this inconclusive section major flood deposits downcore got in line with historical floods. Additionally, two major floods recorded in 1834 and 1868 (Caviezel, 2007) prior dated to 1831 and 1866 were adjusted to the year in which the flood was recorded.

The chronology of cores SVP 06-2 and SVP 06-3 extending the record back in time was established by varve counting. Counting of varves was carried out on high-resolution digital core photographs and verified on thin-sections throughout the cores.

Varve counts were corroborated by two major floods recorded in 1566 (Caviezel, 2007; Pfister, 1999) and 1177 (Christian Pfister, personal communication, 2008). The latter was dated to 1170

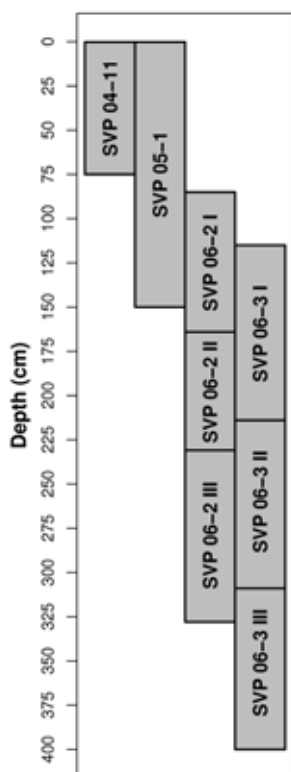


Fig. 3.1. Core correlation of the cores analysed by Blass (2006) (SVP 04-11 and SVP 05-1) and the cores analysed in this thesis (SVP 06-2 and SVP 06-3). In total cores cover a sediment depth of 4 meters. The horizontal black lines in cores SVP 06-2 and SVP 06-3 indicate the length of core subsections I, II and III.

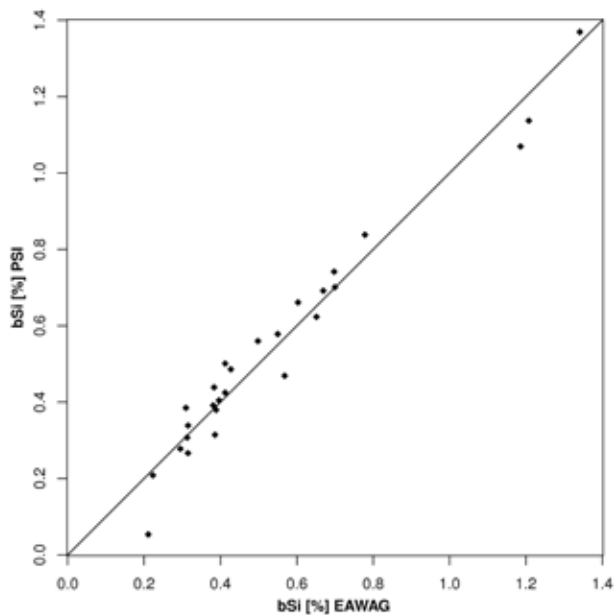


Fig. 3.2. Comparison of biogenic silica measurements at EAWAG and PSI. In total 27 samples were compared $r=0.96$.

by varve counts. The flood 1177 caused a mass flow deposit of more than 30 cm thickness. Since the erosive power of this deposit is not known records presented in this thesis are currently constrained to the time after 1177.

Major floods not used for constraining the chronology gave the opportunity to test the accuracy of varve counts. Major floods recorded in 1342 and 1479 (e.g. Röthlisberger, 1991) were dated to 1344 and 1480 by varve counts.

Since the records presented in this thesis are only going back to AD 1177 and the chronology is based on varve counts, all years mentioned are years AD.

Varve thicknesses were measured on thin sections and when possible on digital photographs along three scan-lines. Then mean values were calculated. The annual mass accumulation rate (MAR) was calculated using the algorithms of Berner (1971) and Niessen et al. (1992). These algorithms transfer thickness measurements into mass flux rates accounting for both water content and organic carbon. Layers that were interpreted as mass-flow deposits were excluded from the record.

Biogenic silica (bSi) was leached from organic free (30% H_2O_2) sediments with 1M NaOH at 90°C for three hours (wet alkaline leaching) following Mortlock and Froehlich (1989) and measured by means of ICP-OES (inductively coupled plasma optical emission spectrometry) at Paul Scherrer

Institut (PSI) in Villigen (S. Köchli). Silica concentrations were corrected for inorganic silica derived from clay minerals (probably chlorite, according to X-ray analysis) using the concentration of Al in the leachate. The Al:Si ratio was analytically determined to be 2:1 (Ohlendorf and Sturm, 2007).

Since Blass et al. (2007b) had measured bSi at EAWAG (Dübendorf) we compared the measurements of EAWAG and PSI in order to produce homogenous data series. Therefore 27 samples previously measured at EAWAG were measured as well at PSI. Thereby, the entire sample preparation was repeated. The correlation among the samples amounted to $r = 0.96$ (Fig. 3.2.). The bSi concentration of the test samples was between 0.2 % and 1.4 %. This is the range of bSi concentration in the sediments of Lake Silvaplana prior to human induced eutrophication (Blass et al. 2007b).

For correction of minerogenic Si the correction factor is assumed to be stable for every sample (Ohlendorf and Sturm, 2007; Blass et al. 2007b). This assumption can not be verified analytically. Changes in the 'real' correction factor through time could considerably affect the estimation of bSi concentration. Assuming a Si concentration of 4 ppm and an Al concentration of 1.6 ppm an Al:Si correction factor of 2 results in 0.8 ppm bSi. An Al:Si correction factor of 1.9 results in a bSi concentration of 0.96 ppm. This is 120% of the value obtained for an Al:Si correction factor of 2.

Scanning in-situ reflectance spectroscopy was carried out as described by Rein and Sirocko (2002): "A Gretag Spectrolino (GretagMacbeth, Switzerland) was used which allows measurement down to millimetre resolution. The sensor's field of view is 2.5 mm. The spectral coverage ranges from 380 to 730 nm, with a spectral resolution of 3-nm band pass filter width which is resampled to 10 nm. Wavelength-dependent illumination and transparency effects were corrected by dividing each radiance spectrum acquired from the sediment by that of the transparency-covered white standard. The photospectrometre uses a ceramic plate (BCA – GretagMacbeth) as white standard." The split cores were cleaned and covered with a transparency. The transparency avoids contamination of the sensor head, protects the sediment from the atmosphere (oxidation), and minimises porosity effects. Finally, in-situ reflectance spectroscopy was measured at 2 mm intervals on split sediment cores.

3.3. Numerical methods

In this section numerical methods used in chapters four and five are described first. Then methods applied in chapter six are introduced.

In chapters four and five we had to detrend our data. In our studies we applied loess (locally weighted regression; Cleveland and Devlin, 1988) filters to detrend data. We choose loess for two reasons: it is based on non-parametric regression and on a local fitting algorithm. This makes loess superior to polynomials (Cleveland and Devlin, 1988). Fig 3.3. illustrates the function of a loess filter. In loess data points in a time window are weighted according to their distance to the centre of the time window. These data points are used to define a first or second order polynomial ($y = a + bx$; $y = a + bx + cx^2$). With this polynomial the value of y is predicted for a given x -value. This procedure is repeated for every x -value.

Due to dating uncertainties and sampling errors we further applied a 9-year running mean to the

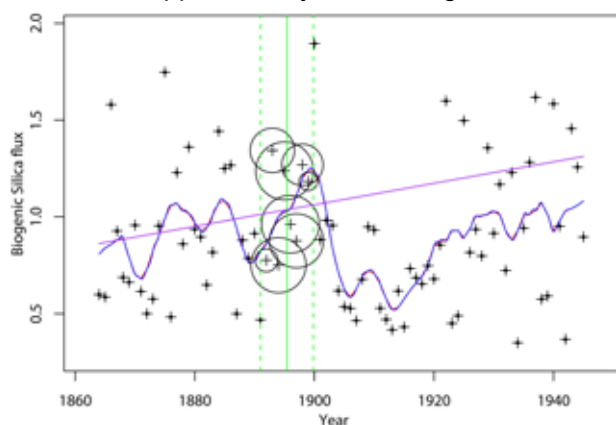


Fig. 3.3. BSi flux data (chapter 5) smoothed with a first order polynomial loess filter (blue and red line). The dashed green lines delimit the window of points included in the fitting. The solid green is the center of the window considered and the circle diameter is proportional to the weight of that specific point in the linear fit. Purple line: linear fit used to predict at the selected point.

data. This results in band-pass filtering.

With filtering autocorrelation is introduced in time series and the number of independent samples (degrees of freedom) is reduced. Therefore in any statistical test applied to filtered data degrees of freedom (DF) have to be adjusted (Trenberth, 1984). In our studies we corrected degrees of freedom for correlation coefficients according to Dawdy and Matalas (1964).

Degrees of freedom are calculated with the equation

$$DF_{adj} = (n - 2) \cdot \frac{(1 - a_i \cdot a_j)}{(1 + a_i \cdot a_j)}$$

n is the initial sample size and a_i and a_j are the lag-1 autocorrelations of the two time series compared. Since adjusted degrees of freedom are always lower than 20 we applied t-tests to assess significances of correlation coefficients.

Another method to test significances of correlations between autocorrelated time series was proposed by Mudelsee (2003). This method is based on detrending and bootstrap resampling (e.g. Davison and Hinkley, 1997).

The regression method used for the calibration of two data series affects the predicted amplitude. (Esper et al. 2005). In chapter 5 we test the effects of three type I regressions (inverse regression, inverse prediction and generalised least squares, all ordinary least squares regressions) and of three type II regressions (major axis regression, ranged major axis regression and standard major axis regression) on predicted amplitudes.

In type I regressions the sum of vertical or horizontal squared deviations to the regression line is minimised (Fig. 3.4.). In type II regressions the sum of squared Euclidean distances (orthogonal distances) to the regression line is minimised (Fig. 3.5.). Hence in type I regressions the slope of the regression line is depending on the assignment of dependent and independent variable. Further predictors are assumed to be error free. For type II regressions, the regression line does not depend on the assignment of dependent and independent variable and an error is attributed to both variables.

The six tested regression methods are based on the equation: $y = a + bx + \varepsilon$ (e.g. Bahrenberg et al. 1999) where a is the intercept and b the slope parameter. The slope parameter b determines the

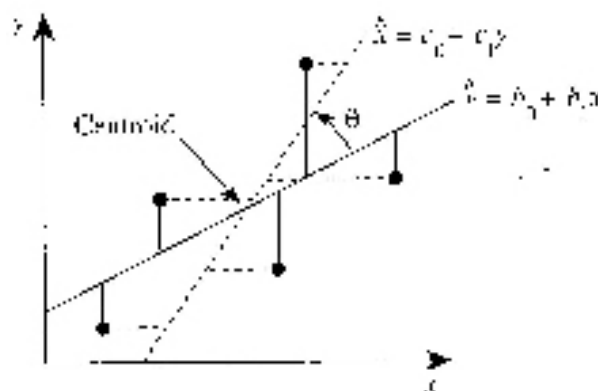


Fig. 3.4. For ordinary least squares regression (type I regression) two regression equations are possible. When regressing x on y (y on x) the sum of vertical (horizontal) squared deviations is minimised (Legendre and Legendre, 1998).

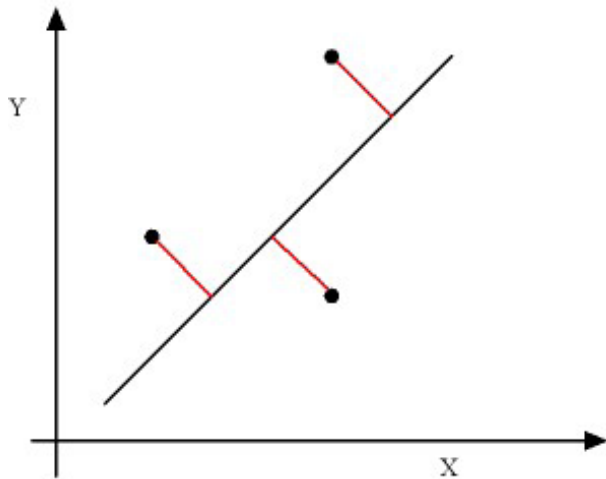


Fig. 3.5. In major axis regression (type II regression, total least squares) the sum of the squared Euclidean distances is minimised (Legendre and Legendre, 1998).

amplitude of prediction.

Inverse regression is the most commonly used type I regression. The proxy is the independent variable and the instrumental target is the dependent variable. i.e. $T = a + \text{Proxy} \cdot b + \varepsilon$.

In generalised least squares regression the assignment of proxy and target is similar to inverse regression but residuals are allowed to be autocorrelated (Venables and Ripley, 2002). In inverse prediction the instrumental target is the independent variable and the proxy is the dependent variable (Sokal and Rohlf, 2001). This makes more sense from a process based point of view. The equation is: $\text{Proxy} = a + T \cdot b + \varepsilon$. This equation is solved for T and results in:

$$T = \frac{(\text{Proxy} - a)}{b}$$

As shown above the assignment of dependent and independent variable does not affect results of type II regressions. The difference between the three type II regressions major axis regression, ranged major axis regression and standard major axis regression is the data treatment prior to regression. For major axis regression untransformed data is used, for standard major axis regression data is standardised prior to regression, and for ranged major axis regression data is ranged (brought to values between 0 and 1) prior to regression.

Ranging is based on following equations:

$$y'_i = \frac{y_i}{y_{\max}}$$

for relative scale variables and

$$y'_i = \frac{y_i - y_{\min}}{y_{\max} - y_{\min}}$$

for absolute scale variables Legendre and Legendre, 1998).

The application of different regression methods changes the amplitude of prediction. Every regression is characterised by the equation:

$$y = a + bx + \varepsilon.$$

In inverse regression the slope parameter b is estimated as follows:

$$b_{ir} = \frac{s_{xy}}{s_x^2}$$

where s_{xy} is the covariance of x and y and s_x^2 is the variance of x. Standard major axis regression is as well referred to as scaling. Scaling is based on the equation:

$$y = \left[\left(\frac{(x - \bar{x})}{s_x} \right) \cdot s_y \right] + \bar{y} \quad \text{where } s_x \text{ and } s_y \text{ are the}$$

standard deviations of the data series.

This equation includes an additive and a multiplicative term. Hence we can change the equation to

$y = a + bx$, where a and b are

$$a = (\bar{y} - \bar{x})$$

$$b = \frac{s_y}{s_x}$$

Given $s_{xy} = r \cdot s_x \cdot s_y$ (e.g. Bahrenberg et al. 1999)

$$b_{ir} = r \cdot \frac{s_y}{s_x} \quad \text{hence } b_{ir} = r \cdot b_{sc}$$

Thus the amplitude predicted by inverse regression is the correlation coefficient between the two variables multiplied with the amplitude predicted by standard major axis regression (e.g. Esper et al. 2005). In theory the amplitude predicted by standard major axis regression is the mean value between the amplitude predicted by inverse regression and inverse prediction (Legendre and Legendre, 1998).

For further descriptions of regression methods see Sokal and Rohlf (2001), Legendre and Legendre (1998) and Venables and Ripley (2002).

To validate climate reconstructions we followed split period calibration approaches (e.g. Cook et

al. 1994) and calculated calibration statistics RE (reduction of error) and CE (coefficient of efficiency). These two measures are based on lowest mean squared error of prediction (MSEP).

We further calculated the ratio of root mean squared error of prediction (RMSEP) and predicted amplitude (e.g. Birks, 1998). RMSEP was calculated using leave-one-out (LOO) or k-fold cross-validation (e.g. Legendre and Legendre, 1998).

Principal component analysis (PCA) was first described by Hotelling (1933). PCA is an ordination technique and is mainly used to extract 'relevant' information from multivariate datasets. Therefore new variables (principal components) that are linear combinations of the initial variables are generated. Thereby, a multivariate (multidimensional) dataset is reduced to a few important variables (principal components).

In multiple linear regression (MLR) several independent variables are regressed to a single dependent variable simultaneously. The regression coefficients are calculated simultaneously using the equation

$B = ([X^T \cdot X])^{-1} \cdot (X^T \cdot Y)$ (e.g. Legendre and Legendre, 1998).

Colinearities among independent variables complicate the correct estimation of slope parameters. (e.g. Legendre and Legendre, 1998). For univariate calibration (i.e. X as a vector) the slope parameter b is covariance divided by variance of x (see above).

In the univariate case the equation

$$([X^T \cdot X]) = \sum_{i=1}^n x_i^2 \text{ and } (X^T \cdot Y) = \sum_{i=1}^n x_i \cdot y_i$$

Covariance is defined as

$$s_{xy} = \frac{1}{n-1} \cdot \sum_{i=1}^n (x_i - \bar{x}) \cdot (y_i - \bar{y}) \text{ and variance is}$$

$$s^2_x = \frac{1}{n-1} \cdot \sum_{i=1}^n (x_i - \bar{x})^2 \text{ (e.g. Bahrenberg et al. 1999).}$$

Considering standardised data (i.e. mean = 0) we see that covariance/variance is similar to

$B = ([X^T \cdot X])^{-1} \cdot (X^T \cdot Y)$ i.e.

$$B = \frac{\sum_{i=1}^n x_i \cdot y_i}{\sum_{i=1}^n x_i^2} = \frac{\frac{1}{n-1} \sum_{i=1}^n (x_i - 0) \cdot (y_i - 0)}{\frac{1}{n-1} \sum_{i=1}^n (x_i - 0)^2}$$

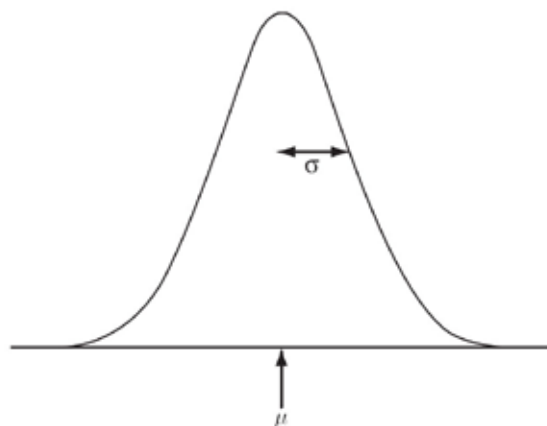


Fig. 3.6. Probability density function for the Gaussian distribution. The mean, μ , locates the center of this symmetrical distribution, and the standard deviation, σ , controls the degree to which the distribution spreads out (Wilks, 2006).

In redundancy analysis (RDA) the sensitivity of a multivariate dataset (Y) to one or more explanatory (independent) variable(s) (X) is assessed.

RDA is a combination of ordination and regression techniques. In RDA the variables in Y are ordinated. The ordination vectors of Y are constrained to be linear combinations of the variables in X (MLR).

The variance of Y explained by the ordination vectors is the variance explained by the dataset of explanatory variables X. (e.g. Legendre and Legendre, 1998).

In chapter six probability density functions (PDF) of 30-year time windows of meteorological data series are calculated. In our study we describe a PDF with two measures: a measure for location and a measure for spread (Fig. 3.6).

The most often used first moment (location, further referred to as mean) and second moment (spread further referred to as variability) of a PDF are the product-moments mean (first moment) and variance (second moment). Product-moments are based on the assumption of normality and are therefore not resistant to outliers. A number of more robust estimators for the first and second moment exist (see Wilks, 2006). Product-moments are more efficient in detecting changes of PDFs but are not resistant to outliers (Scherrer et al. 2005).

A series of shapiro-wilk tests (e.g. Wilks, 2006) revealed non-normality of the data assessed (see chapter 6). We therefore assessed the location and spread of PDFs calculating L-moments (Hosking, 1990). L-Moments are non-parametric estimators for moments of a PDF.

Variance is defined as $s^2_x = \frac{1}{n-1} \cdot \sum_{i=1}^n (x_i - \bar{x})^2$.

A trend in a data set is increasing the difference between x_i and the mean. Thereby the variance is increased. To remove trend induced variance and to only calculate intrinsic variance (the real year to year variability) the data series have to be detrended (Räisänen, 2002; Schär et al. 2004; Scherrer et al. 2005). Effects of trends on the estimation of mean and variance are described in Scherrer et al. (2005). For detrending Scherrer et al. (2005) and Della Marta et al. (2007) propose to remove a linear trend. We follow this method although a linear trend can not account for increasing and decreasing trends in the same time window (Trachsel et al. in review, *Clim Dyn.*).

To compare the behaviour of mean and variability Scherrer et al. (2005) developed MSC (mean versus standard deviation change) plots.

In MSC-plots standardised mean ($\frac{(x - \bar{x})}{s_0}$) values

of the running windows are plotted on the abscis-

sa and the standardised variabilities ($\frac{s_0}{s}$) are

plotted on the ordinate. Since we are not calculating product-moments we renamed the plots to MVC (mean versus variability change) plot.

References

Auer, I., Böhm, R., Jurkovic, A., Lipa, W., Orlik, A., Potzmann, R., Schöner, W., Ungersböck, M., Matulla, C., Briffa, K., Jones, P., Efthymiadis, D., Brunetti, M., Nanni, T., Maugeri, M., Mercalli, L., Mestre, O., Moisselin, J.M., Begert, M., Muller-Westermeier, G., Kveton, V., Bochnicek, O., Stastny, P., Lapin, M., Szalai, S., Szentimrey, T., Cegnar, T., Dolinar, M., Gajic-Capka, M., Zaninovic, K., Majstorovic, Z., Niepova, E., 2007. HISTALP - historical instrumental climatological surface time series of the Greater Alpine Region. *International Journal of Climatology* 27, 17 - 46.

Bahrenberg G., Giese, E., Nipper, J., 1999. *Statistische Methoden in der Geographie*. Borntraeger, Berlin.

Begert, M., Schlegel, T., Kirchhofer, W., 2005. Homogeneous temperature and precipitation series of Switzerland from 1864 to 2000. *International Journal of Climatology* 25, 65 - 80.

Berner R.A., 1971. *Principles of chemical sedimentology*, McGraw-Hill Book Company, New York.

Birks, H.J.B., 1998. Numerical tools in palaeolimnology - Progress, potentialities, and problems. *Journal of Paleolimnology* 20, 307 - 332.

Blass, A., 2006. *Sediments of two high-altitude Swiss lakes as high-resolution late Holocene paleoclimate archives*. PhD thesis. University of Bern, Bern.

Blass, A., Grosjean, M., Troxler, A., Sturm, M., 2007a. How stable are twentieth-century calibration models? A high-resolution summer temperature reconstruction for the eastern Swiss Alps back to AD 1580 derived from proglacial varved sediments. *Holocene* 17, 51 - 63.

Blass, A., Bigler, C., Grosjean, M., Sturm, M., 2007b. Decadal-scale autumn temperature reconstruction back to AD 1580 inferred from the varved sediments of Lake Silvaplana (southeastern Swiss Alps). *Quaternary Research* 68, 184 - 195.

Böhm, R., Auer, I., Brunetti, M., Maugeri, M., Nanni, T., Schöner, W., 2001. Regional temperature variability in the European Alps: 1760-1998 from homogenized instrumental time series. *International Journal of Climatology* 21, 1779 - 1801.

Büntgen, U., Esper, J., Frank, D.C., Nicolussi, K., Schmidhalter, M., 2005. A 1052-year tree-ring proxy for Alpine summer temperatures. *Climate Dynamics* 25, 141 - 153.

Büntgen, U., Frank, D.C., Nievergelt, D., Esper, J., 2006. Summer temperature variations in the European Alps, AD 755-2004. *Journal of Climate* 19, 5606 - 5623.

Casty, C., Wanner, H., Luterbacher, J., Esper, J., Böhm, R., 2005. Temperature and precipitation variability in the European Alps since 1500. *International Journal of Climatology* 25, 1855 - 1880.

Caviezel, G., 2007. *Hochwasser und ihre Bewältigung anhand des Beispiels Oberengadin 1750 - 1900*. MSc thesis. University of Bern, Bern.

Cleveland, W.S. and Devlin, S.J., 1988. Locally Weighted Regression - An Approach to Regression-Analysis by Local Fitting. *Journal of the*

- American Statistical Association 83, 596 - 610.
- Cook, E.R., Briffa, K.R., Jones, P.D., 1994. Spatial Regression Methods in Dendroclimatology - A Review and Comparison of 2 Techniques. *International Journal of Climatology* 14, 379 - 402.
- Davison, A.C., and Hinkley D.V., 1997. *Bootstrap methods and their application*. Cambridge University Press, Cambridge.
- Dawdy, D. R., and Matalas N.C., 1964. Statistical and probability analysis of hydrologic data, part III: Analysis of variance, covariance and time series, In: Chow, V.T., (Ed.), *Handbook of Applied Hydrology, a Compendium of Water-Resources Technology*. McGraw-Hill, New York, pp. 8.68-8.90.
- Della-Marta, P., Haylock, M., Luterbacher, J., Wanner, H., 2007. Doubled length of western European summer heat waves since 1880. *Journal of Geophysical Research-Part D-Atmospheres* 1 - 11.
- Esper, J., Frank, D., Wilson, R., Briffa, K., 2005. Effect of scaling and regression on reconstructed temperature amplitude for the past millennium. *Geophysical Research Letters* 32.
- Hosking, J.R.M., 1990. L-Moment - Analysis and Estimation of Distributions Using Linear-Combinations of Order-Statistics. *Journal of the Royal Statistical Society Series B-Methodological* 52, 105 - 124.
- Hotelling, H., 1933. Analysis of a complex of statistical variables into principal components. *Journal of Educational Psychology* 24, 417 - 441.
- Legendre, P., and Legendre, L., 1998. *Numerical ecology*, second ed. Elsevier, Amsterdam.
- Mortlock, R., and Froelich, P., 1989. A simple method for the rapid determination of biogenic opal in pelagic marine sediments. *Deep-Sea Research* 36, 1415-1426.
- Mudelsee, M., 2003. Estimating Pearson's correlation coefficient with bootstrap confidence interval from serially dependent time series. *Mathematical Geology* 35, 651 - 665.
- Niessen, F., Wick, L., Bonani, G., Chondrogianni, C., Siegenthaler, C., 1992. Aquatic system response to climatic and human changes— Productivity, bottom water oxygen status, and sapropel formation in Lake Lugano over the last 10,000 years. *Aquatic Sciences* 54, 257-276.
- Ohlendorf, C., and Sturm, M., 2007. A modified method for biogenic silica determination. *Journal of Paleolimnology* 39, 137-142.
- Pfister, C., 1999. *Wetternachhersage*. Haupt, Bern.
- Räisänen, J., 2002. CO₂-induced changes in interannual temperature and precipitation variability in 19 CMIP2 experiments. *Journal of Climate* 15, 2395 - 2411.
- Rein, B. and Sirocko, F., 2002. In-situ reflectance spectroscopy - analysing techniques for high-resolution pigment logging in sediment cores. *International Journal of Earth Sciences* 91, 950 - 954.
- Röthlisberger, G., 1991. *Chronik der Unweterschäden in der Schweiz*. WSL, Birmensdorf.
- Schär, C., Vidale, P.L., Lüthi, D., Frei, C., Häberli, C., Liniger, M.A., Appenzeller, C., 2004. The role of increasing temperature variability in European summer heatwaves. *Nature* 427, 332 - 336.
- Scherrer, S.C., Appenzeller, C., Liniger, M.A., Schär, C., 2005. European temperature distribution changes in observations and climate change scenarios. *Geophysical Research Letters* 32.
- Sokal, R.R., and Rohlf F.J., 2001. *Biometry the Principles and Practice of Statistics in Biological Research*, third ed. W. H. Freeman, New York.
- Trachsel, M., Hänggi, P., Grosjean, M., (in review)b. Is inter-annual temperature variability related to the mean temperature? Evidence from instrumental, early instrumental and proxy data in Europe since 1600 AD. *Climate Dynamics*.
- Trenberth, K.E., 1984. Some Effects of Finite-Sample Size and Persistence on Meteorological Statistics .1. Autocorrelations. *Monthly Weather Review* 112, 2359 - 2368.
- Venables, W.N., and Ripley, B.D, 2002. *Modern Applied Statistics with S*, fourth ed. Springer, New York.
- Wilks, D.S., 2006. *Statistical Methods in the Atmospheric Sciences*. Elsevier, Amsterdam.

Chapter 4



4. Scanning reflectance spectroscopy (380 – 730 nm): a novel method for quantitative high-resolution climate reconstructions from minerogenic lake sediments

M. Trachsel^{1,2}, M. Grosjean^{1,2}, D. Schnyder¹, C. Kamenik^{1,2}, and B. Rein³.

(1) Department of Geography, University of Bern, Erlachstrasse 9a, 3012 Bern, Switzerland.

(2) Oeschger Center for Climate Change Research, University of Bern, Zähringerstrasse 25, 3012 Bern, Switzerland.

(3) University of Mainz, Institute for Geosciences, Becherweg 21, Mainz, 55099 and GeoConsult Rein, Katharinenblick 5, Oppenheim, 55276 Germany

To be submitted to Journal of Paleolimnology

Abstract

To place current climate change into the context of long-term natural variability, high-resolution (annual to sub-decadal) quantitative reconstructions of climate state variables are needed from a variety of archives across the world. In order to produce such high-resolution records from lake sediments, methodological development and assessment of rapid, high-resolution and non-destructive scanning techniques is fundamental. In this study we explore the potential of scanning reflectance spectroscopy (380 – 730 nm) to produce quantitative summer temperature reconstructions from minerogenic sediments of proglacial, annually laminated Lake Silvaplana (south-eastern Swiss Alps). The scanning resolution is 2 mm which corresponds to between one and two years of sediment deposition.

We find correlations up to $r = 0.84$ ($p < 0.05$, calibration period 1864-1950) between six reflectance-dependent variables and summer (JJAS) temperature. These reflectance-dependent variables (e.g. slope of the reflectance 570nm/630nm, indicative for illite, biotite and chlorite; minimum reflectance at 690 nm indicative for chlorite) mirror the mineralogical composition of the clastic sediments, which is known to be related to climate in the catchment of this particular proglacial lake.

Using multiple linear regression (MLR) we establish a calibration model that explains 84% of the variance of summer (JJAS) temperature during the calibration period 1864-1950.

Applying the calibration model downcore we develop a quantitative summer temperature reconstruction back to AD 1177. This temperature reconstruction is in good agreement with two fully independent temperature reconstructions based on documentary data (back to AD 1500) and tree ring data (back to AD 1177).

This study confirms the great potential of scanning in-situ reflectance spectroscopy (380 – 730 nm) as a novel non-destructive technique to acquire very

rapidly high-resolution quantitative paleoclimate information from minerogenic lake sediments.

4.1. Introduction

High-resolution, well calibrated temperature reconstructions are fundamental to put the current warming into a wider perspective. To improve the knowledge about past climate and to further constrain uncertainties in climate reconstructions, new high-quality time series of proxy data are required. These proxy series need to fulfil several criteria that are fundamental for quantitative reconstructions: the proxy data have to be highly correlated with climate variables; very high temporal resolution (annual to multi-annual) is required, and the proxy time series has to rely on a high-precision chronology.

In the past decade, considerable advancements have been made to reconstruct past climate from geochemical proxies in lake sediments. These reconstructions are based on sedimentological or geochemical analysis of thin sections (Francus et al., 2002; Kalugin et al., 2006) or sediment subsamples (McKay et al., 2008; Kaufman et al., 2009) and are, thereby, destructive and rather time-consuming in the sample preparation. Major developments have also taken place to explore methods for direct measurements on sediment cores using non-destructive scanning techniques such as XRF (e.g., Zolitschka et al. 2001).

In this study we present results from scanning in situ reflectance spectroscopy in the visible spectrum (380 – 730 nm), another non-destructive rapid scanning method (Rein and Sirocko, 2002). One of the great advantages of that method is that data acquisition is very rapid and inexpensive: several meters of sediment can be processed at a 2 mm measuring interval in a day (i.e. > 1000 data points can be generated), and the same sediment material can be used for further analysis. More difficult is the data analysis, interpretation and the transformation of the raw reflectance spectroscopy

py data into quantitative variables describing sediment compounds and properties and, ultimately climate or environmental change. Reflectance spectroscopy in the visible and infrared range is widely used to detect organic components in subsamples of lake sediments (Rosen et al. 2000; Rein and Sirocko, 2002; Wolfe et al. 2006, Michelutti et al. 2009). But non-destructive scanning (in-situ) reflectance spectroscopy with direct measurements on sediment half cores is poorly known in the literature. This method has been used so far to detect organic and clastic components in marine sediments off Peru (Rein and Sirocko 2002, Rein et al. 2005). In a recent study, von Gunten et al. (2009) showed that this scanning technique can also be used for biogenic freshwater sediments in eutrophic Laguna Aculeo (central Chile) to determine photopigments and to produce high-resolution quantitative reconstructions of austral summer DJF temperatures.

In this study we show the potential of this method for minerogenic freshwater sediments in a proglacial lake environment. We have chosen Lake Silvaplana (eastern Swiss Alps) for this methodological case study because the mineralogical and geochemical composition of the sediment is very well known from established analytical techniques (X-ray diffraction, biogenic Si, grain size and Mass Accumulation Rate; Blass et al. 2007a, b and references therein), and the mineralogical composition of individual varves has been shown to be controlled by climate (Trachsel et al. 2008). These sediments contain less than 1% of organic material. The rest is composed of mineroclastic fine silt particles that are transported as suspended load from glacial meltwater and rainfall runoff (Blass et al. 2007a).

This article presents results from one of the first times that scanning in-situ reflectance spectroscopy is applied on minerogenic sediments. Therefore, we systematically test the method and the significance of the data produced. We further describe a possible way of how to get step-by-step from the raw reflectance measurement to a climate reconstruction.

We first look for published algorithms that describe the reflectance characteristics of minerals that are known to be present in the sediments (from XRD data). In addition, we define further algorithms that describe the remaining (yet unexplained) distinct characteristics of the measured reflectance spectra of the sediment of Lake Silvaplana.

Each of these algorithms is then used to produce a spectrum-derived variable. To gain further insight into the known and unknown variables extracted, we apply a principal component analysis (PCA) on the extracted variables to detect similarities. Subsequently we perform and discuss the transformation of the raw reflectance data into a climate reconstruction, which involves several steps: (i) Testing the effects of climate and sediment parameters on the spectrum-derived variables (using redundancy analysis RDA), (ii) establish univariate and multivariate calibration models for climate and sediment parameters (iii) apply the optimal calibration model downcore, and (iv) verify the reconstruction back in time (here back to AD 1177) with fully independent data sets.

4.2. Study site

Lake Silvaplana (46°27'N, 9°48'E) is a postglacial, high elevation (1800 m), 2.7 km² large (water volume 127*106 m³), 77 m deep, dimictic lake of glacio-tectonic origin (Figure see e.g. Blass et al., 2007a). Typically, the lake is ice-covered between January and May. The catchment stretches over 129 km² and ranges up to 3441 m. About 6 km² (5% of the catchment) are glaciated (status 1998). The Fedacla River (average runoff 1.5 m³s⁻¹) is the only glacial river in the catchment and, therefore, the principle conveyor of sediments to the lake. The Inn River, connecting Lake Sils with Lake Silvaplana is larger (discharge 2 m³s⁻¹) but is almost devoid of sediments. Two small rivers (Vallun; 0.7 m³s⁻¹ and Surlej; 0.3 m³s⁻¹) are particularly active during spring snowmelt and summer rainstorms. The specific geological setting of the basin is fundamental to our study: Lake Silvaplana is located on the tectonic Engadine Line which separates the Lower Austroalpine basement (granites with high amounts of feldspar) in the NW from the Penninic basement (orthogneiss and gabbro, with high amounts of mica) in the S (Spillmann, 1993). This difference is reflected in the mineral spectra of sediments around the shore of the lake (Ohlen-dorf, 1998).

The Engadine exhibits climate typical for an inner-Alpine dry valley. Maximum monthly precipitation occurs in August (121 mm) whereas a minimum is observed in February (42 mm). Annual precipitation amounts to 978 mm (1961–1990, data from MeteoSwiss). Mean monthly temperature ranges from -7.2°C (January) to 10.4°C (July).

4.3. Materials and Methods

4.3.1. Material and analytical methods

A gravity core (SVP 06-1) and two piston cores (06-2 and 06-3) were recovered from Lake Silvaplana in March 2006. The chronology of the top section (SVP 06-1; AD 1620 onwards) was established by optical correlation of 16 diagnostic sediment strata (nine flood layers for the calibration period 1864 – 1950; seven flood layers 1620 – 1864) with the master chronology developed for freeze cores in previous work (Blass et al. 2007a, Trachsel et al. in review; varve counting and documented flood layer events) and interpolated with a mixed-effect regression model (Heegaard et al. 2005). The maximum error of the chronology amounted to ± 7 years. The chronology of the cores SVP 06-2 and SVP 06-3 (AD 1177-1620) was established using varve counts and historically documented flood layer events (Caviezal, 2007), extending the record back to AD 1177 (Trachsel et al. in review).

For the numerical calibration analysis we used the data set of the time period 1864 to 1950 where monthly temperature and precipitation data are available from nearby meteorological station Sils-Maria (Begert et al. 2005). From 1950 onwards, anthropogenic eutrophication (Blass et al. 2007b; Bigler et al. 2007) is strongly affecting the sediment composition, which in turn affects the reflectance characteristics of a sediment (Rein and Sirocko 2002; Wolfe et al. 2006). The climate signal is masked.

The reflectance data were acquired by high-resolution photospectrometric logging of split cores with a Gretag Spectrolino (GretagMacbeth, Switzerland). The aperture of the sensor is 2.5 mm and the spectral coverage ranges from 380 to 730 nm with a spectral resolution of 3 nm integrated to intervals of 10 nm bands. The photo-spectrometer uses a ceramic plate (BCA – GretagMacbeth)

as white standard. Prior to analysis the split cores were covered with a polyethylene transparent foil to minimise oxidation and to avoid contamination of the sensor head. Wavelength-dependent illumination and transparency effects were corrected by dividing each spectrum acquired from the sediment by that of the transparency-covered standard (Rein and Sirocko, 2002). The measurement interval on the core was of 2 mm.

After the data acquisition, diagnostic reflectance characteristics (further referred to as 'variables') have to be extracted from the overall reflectance spectra applying specific algorithms (Rein and Sirocko 2002, Wolfe et al. 2006). In Lake Silvaplana the reflectance spectra are combinations of the reflectance spectra of the main minerals present in the sediment i.e. quartz, mica (muscovite, biotite, illite), chlorite, plagioclase and amphibole (Ohlendorf 1998; Trachsel et al. 2008).

For this study (minerogenic sediments from Lake Silvaplana), we used a series of four algorithms that are well established and documented in the literature and indicative of illite, biotite and chlorite (Rein 2003, USGS 2007), and two algorithms that describe further characteristics of the spectra but are presently 'unknown' (Table 4.1). In general, either slopes of reflectance spectra in defined windows (Rein and Sirocko 2002, Wolfe et al. 2006), relative absorption band depths (Rein and Sirocko, 2002), or absorption band areas (Rein and Sirocko 2002; Wolfe et al. 2006) are used to describe the spectra. Furthermore, a comprehensive collection of reflectance spectra for different minerals can be found in the spectral library of the US Geological Survey (USGS 2007). Rein and Sirocko (2002) have assigned the slope of the reflectance spectra of sediments between 570 nm and 630 nm to the amount of clastic material, more precisely to the amount of illite or chlorite in the sediment (Rein 2003). In Lake Silvaplana, the

Algorithm		
R_{590} / dR_{690}	R_{590} / R_{690}	Biotite, Illite, Chlorite (USGS, 2007)
R_{570} / dR_{630}	R_{570} / R_{630}	Biotite, Illite, Chlorite (Rein, 2003)
Min ₆₉₀	$[(4 * R_{590} + 10 * R_{730}) / 14] / R_{690}$	Chlorite (USGS, 2007)
Trough ₅₉₀₋₇₃₀	$141 * R_{730} + [141 * (R_{590} - R_{730}) / 2] - (6 * R_{590} + 5 * R_{730}) - 10 * \sum R_{600-720}$	Chlorite (USGS, 2007)
Min _{690 or 700}	$[(R_{660} + 3 * R_{710}) / 4] / R_{690 or 700}$	Unknown
Min ₄₈₀	$[(R_{460} + 2 * R_{490}) / 3] / R_{480}$	Unknown

Table 4.1. Algorithms for the calculation of spectrum-derived variables.

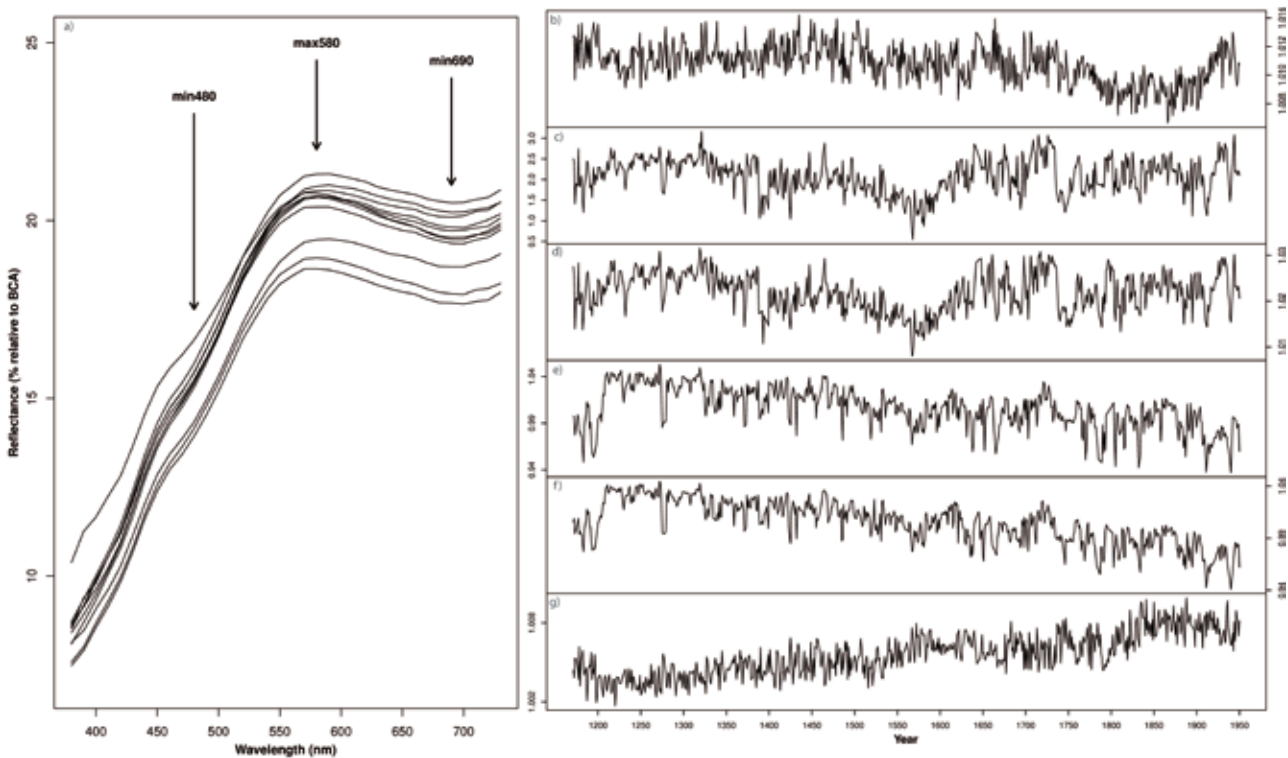


Fig. 4.1. (a) Selected reflectance spectra of the clastic sediment (prior to 1950) of Lake Silvaplana. (b) – (g) raw time series. (b) min690 or 700 (c) min690 (d) trough590-730 (e) R590d630 (f) R570d630 (g) min480.

spectra have a maximum at 580–590 nm and a minimum at 690 nm to 700 nm (Fig. 4.1). The maximum at 590 nm can be assigned to the amount of illite, biotite (both mica) and chlorite, the minimum at 690 nm can be attributed to the amount of chlorite (USGS 2007). The presence and relative abundance of these minerals in the sediments of lake Silvaplana has been experimentally documented by XRD analysis of more than 400 individual varves (Trachsel et al. 2008).

To link the amount of different minerals and the mineral composition in the sediments of lake Silvaplana to local climate variables, we follow the model presented by Trachsel et al. (2008): three different geological formations with diagnostic bedrock composition crop out in the catchment, which results in a different mineralogical composition of the sediment from different tributaries (Ohlendorf, 1998). Since the bedrock geology of the glaciated part in the catchment is relatively enriched in mica (biotite, illite) and chlorite, the sediment transported by glacial meltwater during warm summers carries that signature. The relative proportion of these minerals (mainly chlorite and mica) can be detected by XRD or by specific characteristics of the reflectance spectra.

Prior to numerical analysis, all turbidities were removed from the sediment record, and the raw reflectance data (2 mm increments, resolution of

1–2 years) were converted into a time series with homogenous (annual) intervals using resampling and linear interpolation procedures. To account for the minimum instrumental sampling resolution and for dating uncertainties we applied finally 5 and 9-year running means to the time series (referred to as 5 or 9-year smoothed).

4.3.2. Numerical methods

In this section we describe the numerical methods applied in this study. First we test the independence of the reflectance-derived variables and assess the amount of redundancy in the multivariate data set. In a second step we assess the potential and suitability of reflectance-derived variables for climate reconstructions and calibrate the variables against local meteorological data. We compare univariate and multivariate calibration approaches since it is not a priori known whether one individual reflectance variable or a combination of them reveals better calibration statistics.

The technical resolution (aperture of the sensor) of the Spectrolino instrument is 2.5 mm. However it is not known if the technical resolution is equal to the area measured on the sediment core. To evaluate the effective measurement resolution and to assess the independence of the individual measurements (at 2 mm increments) we calculate autocorrelations of the reflectance derived varia-

bles for the calibration period 1864–1950. The significance of the lag-1 autocorrelations were tested with a z-test (Venables and Ripley, 2002). We then applied a principal component analysis (PCA, Hotelling, 1933) to our data to detect similarities among the six reflectance-dependent variables (Table 4.1; two variables for illite, biotite and chlorite, two for chlorite and two ‘unknown’) and tested the significance of the PC-axes with the broken stick model (Frontier 1976, Legendre and Legendre 1998).

4.3.3. Calibration and climate reconstruction

Blass et al. (2007a) and Trachsel et al. (2008) have shown that the amount of clastic material (i.e. the mass accumulation rate MAR) and the mineralogical composition of the sediment reflect summer temperature and summer precipitation. Therefore, we used redundancy analysis (RDA, van der Wollenberg, 1977) to assess the sensitivity of the reflectance spectrum-derived variables to all possible combinations of the three parameters ‘mass accumulation rate’ (MAR), ‘temperature’ and ‘precipitation’ for 5 and 9-year smoothed data (Table 4.2). MAR shows a low-frequency trend related to glacier lengths fluctuations and is mainly influenced by summer temperatures on shorter (inter-annual, decadal to multi-decadal) time-scales (Blass et al. 2007a). Therefore, in all cases where RDA reveals an influence of MAR on the reflectance derived variables, we detrended our data set to remove effects that are related to the low-frequent trend in the MAR. We used locally weighted regression (loess, Cleveland and Devlin, 1988) to detrend our data. The span of the filter was set to represent 100 years.

To detect the relations between reflectance-derived variables, and climate parameters individually, we correlated unsmoothed, 5 and 9-year smoothed data with temperature and precipitation (both raw data and loess detrended data). The degrees of freedom (DF) were corrected for autocorrelated time series according to Dawdy and Matalas (1964); multiple testing was taken into account following Benjamini and Hochberg (1995). P-values adjusted for autocorrelation are referred to as p_c and p-values adjusted for autocorrelation and multiple testing are referred to as p_{ca} .

To produce a summer temperature reconstruction we used inverse regression to calibrate those variables individually that are significantly ($p_{ca} < 0.05$) correlated with detrended summer temperatures. We then tested whether multiple linear

regression (MLR) yields better calibration models than univariate calibration. Leave-one out (LOO) cross-validated RMSEP was used to choose the best model (e.g. Kamenik et al. 2009). For MLR model, we included an additional variable only if the RMSEP of the new model (with the additional variable) decreased by more than 5% (Birks, 1998). Since the focus of this paper is put on the reflectance spectroscopy method, we did not compare the performance of MLR compared to other multivariate calibration approaches.

To assess the performance of our 800-years reflectance-spectra-based summer temperature reconstruction, we compared our data with two fully independent reconstructions based on documentary data (Casty et al. 2005) and tree ring late-wood density data (Büntgen et al. 2006).

4.4. Results

4.4.1. Reflectance-derived variables

The reflectance spectra (Fig. 4.1a) of the sediments from Lake Silvaplana show distinct characteristics: a reflectance maximum at 580 nm to 590 nm is followed by decreasing reflectance with a minimum at 690 nm to 700 nm. The reflectance increases again towards 730 nm. A further local reflectance minimum is found at 480 nm. The six variables derived from the reflectance spectra and used in this study (Table 4.1) describe distinct characteristics of the spectra.

The time series of these six variables are shown in Fig. 4.1.(b-g). Three of them (Ratio R590dR690, Ratio R570dR630 and min480) exhibit a long-term trend, whereas no trend is detected for the other variables.

The lag-1 autocorrelation of the spectrum-derived time series during the calibration period (is significant ($p < 0.05$) for all unsmoothed not-detrended data series as well as for unsmoothed detrended time series except for min480. After 5 and 9-year smoothing the lag-1 autocorrelation is higher than 0.9 for all variables. When smoothing with filters higher than 9-year, smoothing does no longer increase the lag-1 autocorrelation.

The results for the PCA are shown in Fig. 4.2. For raw unsmoothed data, we find two significant PC-Axes which explain 47% and 30% of the variance (Fig. 4.2a). The four variables R590dR690, R570dR630 (both indicative of illite, biotite (mica) and chlorite), the trough590-730 and min690 (both indicative of chlorite) have high positive loadings in the first principal component PC1 (Fig.

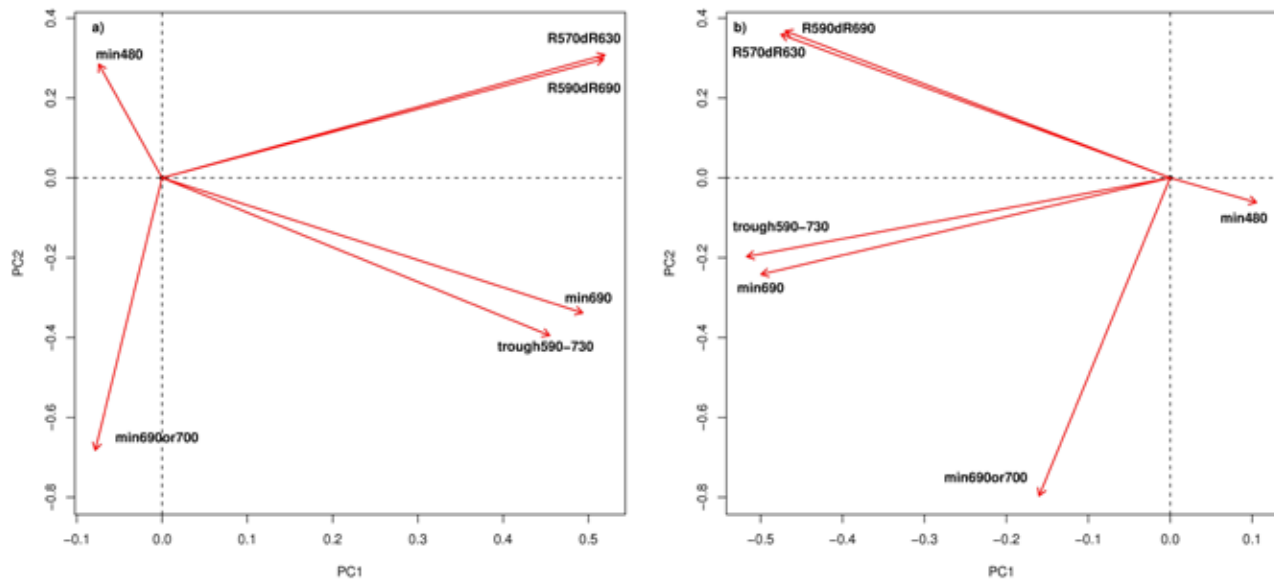


Fig. 4.2. Plot of the loadings of the principal component analysis applied to the spectrum-derived variables (a) raw variables (b) detrended variables.

4.2a). PC2 loadings are positive for R590dR690 and R570dR630 (illite, biotite) but negative for trough590-730 and min690 (chlorite). Min690or700 and min480 have moderate negative loadings in PC1. Min690or700 has a high negative loading in PC2 whereas the loading of min480 is moderately positive in PC2. The loading of min480 is high in PC3 which is, however, not significant.

For the PCA of detrended spectrum-derived variables (Fig. 4.2b) we find one significant PC which explains 54% of the variance. The second, non-significant PC-axis explains 22% of the variance, and the third PC explains 16% of the variance. The picture of the variables R590dR690, R570dR630, the trough590-730 and min690 is similar to the PCA for raw, not detrended data (Fig. 4.2a). Min690or700 has again a high loading in the second PC and the loading of min480 is high in the third principal component. Although R570dR630 and min480 are opposite in the biplot of the loadings of the first two PC-axes, the correlation between the two variables amounts only to $r = -0.14$.

4.4.2. Calibration and climate reconstruction

After having described the data by PCA we used RDA to look for environmental parameters that might influence the reflectance data. Here we limit the comparison with temperature to the summer season JJAS (precipitation MJJAS). This season explains the highest proportion of variance in the reflectance-derived variables.

For the raw reflectance data, T JJAS and MAR ex-

plain the highest proportion of variance ($> 27\%$ for 5-year as well as for 9-year smoothed data; Table 4.2). The proportion of variance explained by P MJJAS is considerably lower and amounts to 9% for 5-year smoothed variables and to 20% for 9-year smoothed variables. Combined T JJAS and MAR explain more than 50% of the variance for 5-year as well as for 9-year smoothed data. Adding precipitation to T JJAS and MAR does not increase the proportion of explained variance; hence, the third RDA axis is not significant.

For the detrended reflectance data sets, the variance explained by T JJAS is higher (compared with the raw data) whereas the variance explained by MAR and by P MJJAS is low. For the 5-year smoothed data set all of the three constraining data sets (temperature, precipitation and MAR) are significant ($p < 0.05$); the same is valid for the 9-year smoothed data. When combining explanatory variables, only the first RDA-axis is significant ($p < 0.05$). The second and third RDA axis do not reach the significance level ($p < 0.05$) when the explanatory variables are combined.

Table 4.3 summarises the relationship between individual reflectance variables and climate variables (June to September temperatures and May to September precipitation). For raw (not detrended) reflectance data, the highest correlations are found between summer temperatures and the variables min690 and trough590-730 (unsmoothed, 5-years and 9-years). While the correlation of trough590-730 with summer temperature fulfils

		T JJAS	MAR	P MJJAS	T JJAS + MAR	T JJAS + P MJJAS	P MJJAS + MAR	T MJJAS + P MJJAS + MAR
Raw data								
5-year Spetrolino	1 RDA	29.5%*	27.1%*	8.4%*	30.7%*	31.2%*	28%*	32.2%*
	2 RDA				24%*	4.3%	0.01%	23.9%*
	3 RDA							0.2%
9-year Spetrolino	1 RDA	32.8%*	33.4%*	19.25%*	35%*	33.7%*	36.1%*	35.5%*
	2 RDA				21%*	12.9%*	3.5%	31.5%*
	3 RDA							0.4%
Loess detrended data								
5-year Spetrolino	1 RDA	34.9%*	6%*	6%*	35%*	38.5%*	8.79%	38.5%*
	2 RDA				2%	0.2%	1.9%	2.3%
	3 RDA							0.2%
9-year Spetrolino	1 RDA	46.9%*	9%*	12.9%*	47%*	48.4%*	17%*	48.4%*
	2 RDA				1.6%	1.1%	1%	1.6%
	3 RDA							0.9%

Table 4.2. Amount of variation (%) explained by T JJAS, P MJJAS or MAR and their combinations among six spectrum-derived variables. Significant RDA-axes ($p < 0.05$) are denoted with an asterisk.

	T JJAS unsmoothed	5-year	9-year	P MJJAS Unsmoothed	5-year	9-year
min480	-0.34**	-0.50	-0.58*	0.19	0.08	-0.04
R590dR630	0.23	0.60*	0.61	0.08	0.44	0.66*
min690	0.31*	0.70*	0.75*	-0.07	0.12	0.08
min690or700	0.05	0.00	0.07	-0.20	-0.25	-0.46
R570dR630	0.23	0.61*	0.60	0.09	0.39	0.56*
trough590-730	0.31*	0.73**	0.81*	-0.01	0.16	0.13
detrended data						
	T JJAS unsmoothed	5-year	9-year	P MJJAS Unsmoothed	5-year	9-year
min480	-0.31*	-0.51**	-0.63	0.13	-0.12	-0.36
R590dR630	0.26	0.72**	0.83**	0.04	0.38	0.50*
Min690	0.26	0.66**	0.74	-0.07	0.21	0.26
Min690or700	0.06	-0.01	0.00	-0.18	-0.08	-0.17
R570dR630	0.24	0.71**	0.84**	0.05	0.35	0.41
trough590-730	0.27	0.72**	0.82**	-0.07	0.20	0.32

* $p < 0.05$ taking into account autocorrelation

** $p < 0.05$ taking into account autocorrelation and multiple testing

Table 4.3. Correlations between T JJAS and P MJJAS and spectrum-derived variables for (a) unsmoothed, 5- and 9-year smoothed data and (b) loess-detrended unsmoothed, 5- and 9-year smoothed spectrum-derived variables.

the rigorous significance level ($p_{ca} < 0.05$ corrected for autocorrelation and multiple testing; marked with ** in Table 4.3) for 5-year smoothed data, all other correlations are only significant for $p_c < 0.05$ (marked with * in Table 4.3).

Reflectance variables are generally not significantly correlated ($p_c < 0.05$) with summer precipitation except 9-year smoothed R590d630 and

R570d630 (significant at $p_c < 0.05$; marked with * in Table 4.3).

For detrended data, highest correlations with summer temperature are found for R590d690, R570d630 and trough590–730. These correlations are significant ($p_{ca} < 0.05$; serial correlation and multiple testing) for 5-year and 9-year smoothed data series. For detrended precipitation only

one significant ($p_c < 0.05$) correlation is found after 9-year smoothing (R590d690).

In summary, the variables trough590–730, and to some extent R590d690 and R570d630 have the potential to serve as robust predictors for summer temperature. While the variable trough590–730 is also robust for raw (not detrended) data, loess-detrending enhances the significance of the correlations with R590d690 and R570d630. As a result of the RDA and correlation analysis, a calibration for and reconstruction of ‘precipitation’ is no longer pursued.

Table 4.4 shows the quality of the calibration (criterion: leave-one-out RMSEP) between detrended reflectance data and summer temperatures for univariate and multivariate (2 – 6 variables) models. The multivariate calibration approaches yield consistently better results (smaller RMSEP)

than those models that are based on one single reflectance variable. Calibrations including two variables (trough590-730, min690or700) resulted in a decrease of RMSEP by 15% compared to the best univariate calibration (smallest RMSEP). Including three variables in MLR (trough590-730, min690or700, min480) resulted in a further decrease of RMSEP by 8%. When including more than three variables, the improvement of the calibration (decrease in RMSEP) was always lower than 5%. Thus the MLR model including three variables was found to be optimal and was used in the following for the summer temperature reconstruction. The comparison between the instrumental JJAS temperature data and the MLR calibration model is shown in Fig. 4.3. ($r^2 = 0.84$; period 1864 – 1950: 9-years smoothed, loess-detrended).

	1 variable	2 variables Trough; min690or700	3 variables Trough;min690or700; min480	4 variables Trough;min690or700; min480;R570d630	5 variables All except min690or700	6 variables all
$R_{590dR_{630}}$	0.142					
$R_{570dR_{630}}$	0.136					
Trough ₅₉₀₋₇₃₀	0.143					
MLR		0.116	0.102	0.100	0.098	0.098

Table 4.4. Comparison of leave one out cross-validated RMSEP for detrended variables. First the RMSEP of the univariate calibration using inverse regression is shown. Only the three variables significantly ($p_{ca} < 0.05$) correlated with detrended T JJAS were used for univariate calibration. Then RMSEP based on multiple linear regression models including two to six variables are shown.

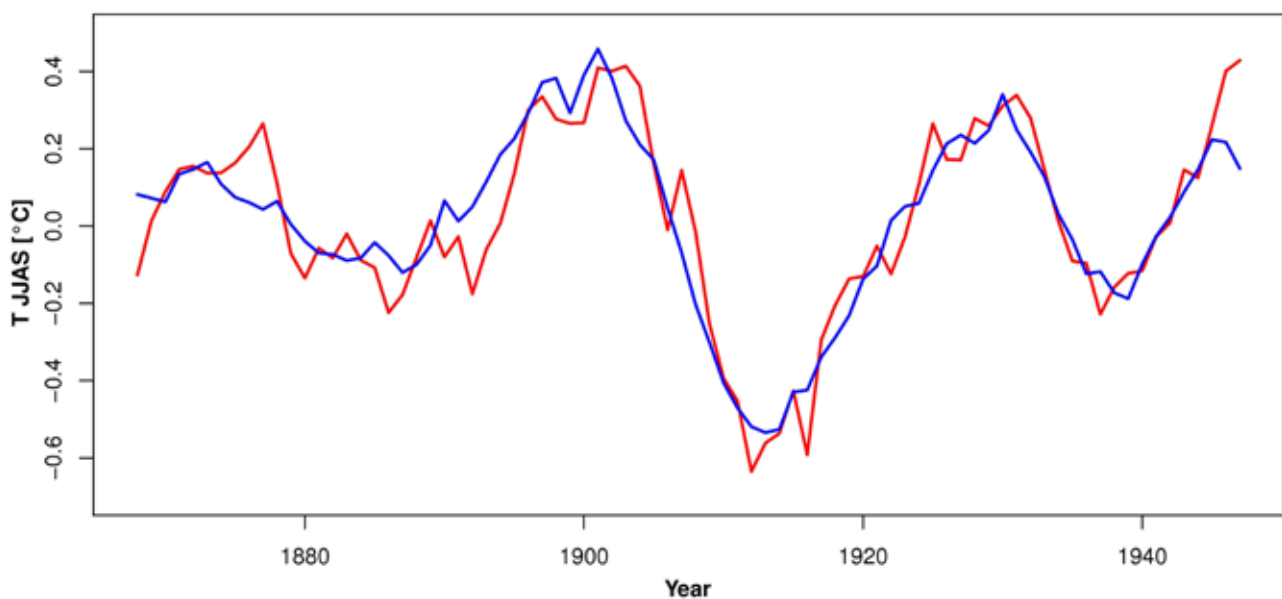


Fig. 4.3. Multivariate Calibration of detrended 9-year smoothed spectrum-derived variables (blue) with detrended 9-year smoothed TJJAS (red) $r^2=0.84$. The calibration model is based on multiple linear regression and includes three variables.

Running correlations with the summer (JJA) temperatures of Casty et al. (2005) were significant ($p_c < 0.1$) back to 1715 (time window 1615 – 1815) and remained positive for the time period back to 1500 (time window 1500 – 1700). The comparison with the tree ring (late-wood density) based reconstruction of Büntgen et al. (2006) showed significant ($p_c < 0.1$) correlations back to 1760 and between 1480 and 1550.

Fig. 4.4a and 4.4b show the comparison between the reflectance-based summer temperature reconstruction from Lake Silvaplana and two fully independent regional summer temperature reconstructions based on documentary data back to AD 1500 (Casty et al. 2005) and tree-ring data back to AD 1177 (Büntgen et al. 2006). Running correlations (200 years windows) are consistently positive and for large parts significant ($p_c < 0.1$; DF corrected for autocorrelation, Fig. 4.4c and 4.4d). The decadal-scale variability is well captured, in particular known extremely cold decades such as e.g. the decade AD 1810–1820 with strong negative volcanic forcing. The running correlations reveal that, even for longer periods (e.g. AD 1550 – 1650) the reflectance-based reconstruction performs much better than the tree-ring reconstruction when compared with the documentary data series. For other periods (e.g. AD 1200, 1450), there is a systematic offset of some years between the lake sediment and the tree-ring time series. This offset is smaller than the dating uncertainties of the age-depth model of the sediment core and, therefore, attributable to an imperfect chronology of the lake sediments.

4.5. Discussion

4.5.1. Reflectance-derived variables

Four of the six reflectance variables that were extracted from the reflectance spectra mirror the amount of chlorite and mica or combinations of these minerals in the lake sediment. A direct quantitative comparison of the variables with XRD measurements (Trachsel et al. 2008) was not possible for two reasons: (i) the XRD was measured in a semi-quantitative way that allows the calculation of mineral ratios only (peak intensity ratio) and (ii) the reflectance-derived variables are influenced by the reflectance spectra of several minerals overlaying each other.

Remarkable is the high autocorrelation (lag-1) of five out of six time series. This might be interpreted in three ways: (i) due light scattering on the polyethylene foil and on the wet sediment sur-

face, the area integrated in the reflectance measurement might be larger than the aperture of the sensor (diameter of 2.5 mm to which the light is emitted by the instrument); (ii) the variables indicative for illite, biotite and chlorite and min690or700 (unknown) have high persistence throughout the entire profile and reflect a multi-annual rather than an annual climate signal; (iii) the autocorrelation is enhanced by the trend in the time series of the variables R570d630, R590d690 and min690or700 (Venables and Ripley, 2002). Most likely these three effects interfere with each other, and it remains inconclusive whether the highest possible effective resolution is as small as the technical resolution (aperture = 2.5 mm) of the instrument.

The autocorrelation in the time series has considerable consequences for the subsequent statistical analysis (correlation and calibration): high autocorrelation decreases the number of independent observations and, in consequence, the Degrees of Freedom DF need to be adjusted when significance levels are calculated (Trenberth, 1984). Here, we recommend rigorous testing and careful assessment of significance levels rather than looking at correlation coefficients per se.

PCA reveals large similarities among a first group of variables that describe the slope of the spectra i.e. between R570dR630 and R590dR690 (Fig. 4.2). Although the segments are slightly different from each other they reflect generally the slope of the reflectance spectra between the maximum (at about 580 nm) and the minimum (at about 690 nm). The variable R570dR630 is well established in the literature and reflects the clastic compounds in particular chlorite, illite or biotite (Rein and Sirocco, 2002; Rein, 2003). A second group consists of the variables min690 and trough590-730, both being indicative of chlorite (USGS 2007). These variables describe the absorption band depth and the absorption area of the major reflectance minimum at 690 nm. Thus high similarity between the two variables is expected. The remaining two variables min480 and min690or700 (Table 4.1; indication unknown) are different from the other two groups. These variables are poorly or not correlated with climate variables and, therefore, not carried on for further analysis in the context of climate reconstructions.

4.5.2. Calibration and climate reconstruction

RDA revealed a strong influence of MAR on the reflectance data series. MAR is subject to a low-frequency trend related to glacier length fluctua-

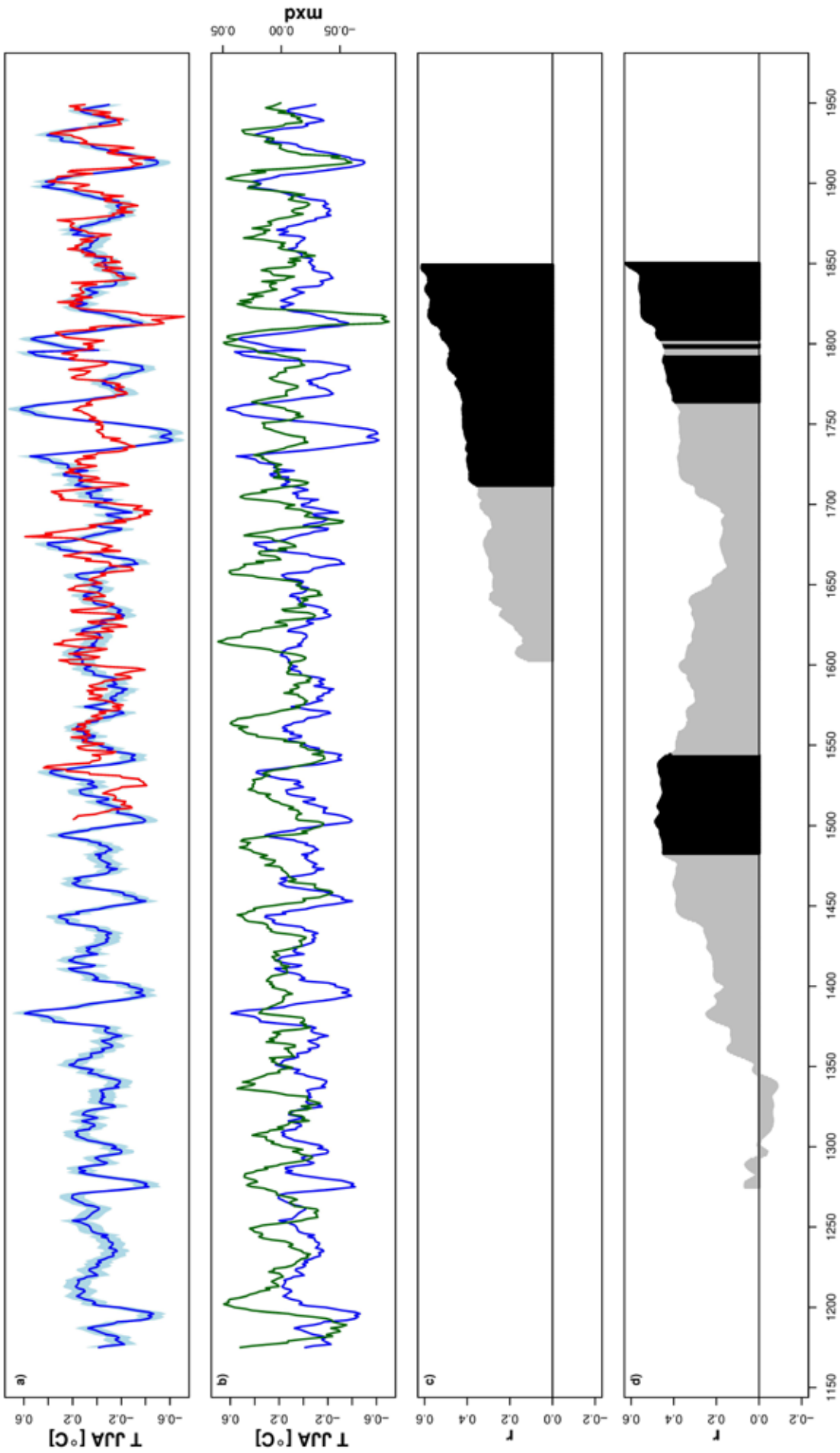


Fig. 4.4. (a) Comparison of reflectance inferred TJJAS reconstruction using multiple linear regression including 3 variables (blue), with the TJJAS reconstruction based on early-instrumental and documentary data (red) (Casty et al. 2005) (b) Comparison of reflectance inferred TJJAS reconstruction with the late-wood density (mxd) based TJJAS reconstruction (green) (Büntgen et al. 2006). 200-year running correlations of the reflectance inferred TJJAS reconstruction with (c) TJJAS reconstruction with (c) TJJAS reconstruction based (late-wood density) TJJAS reconstruction (Büntgen et al. 2006). Significant ($p_c < 0.1$) correlations are highlighted in black. For running correlation the year indicated is the central year of the 200-year-time window.

tions (Blass et al. 2007a). To produce a summer temperature reconstruction that is not affected by the trends related to MAR, all variables (predictors and predictands) need to be detrended for these effects as well (glacier length variations and MAR). RDA for detrended time series is clearly showing that temperature is the main factor influencing the reflectance-derived variables.

Significant correlations between summer temperature and reflectance-derived variables are found for min480, min690 and trough590-730 for raw (not detrended) 9-year smoothed data and for R570d630 R590d690 and trough590-730 for detrended 9-year data (Table 4.3). Beside the unknown variable min480, the other significant variables considered here are indicative of chlorite or mica (Rein, 2003; USGS, 2007). In our case study Lake Silvaplana, the variables indicative for these minerals are positively correlated with summer temperatures (Table 4.3, Trachsel et al. 2008): it has been established that, due to the particular geological setting of the catchment (Spillmann, 1993), the amount of chlorite and mica is highest in the sediment transported by glacial melt-water (Ohlendorf, 1998, Trachsel et al. 2008). During warm summers, glacier melt water runoff is enhanced and more mica and chlorite bearing sediment from the glaciated part of the catchment is transported into the lake.

Hence the next step was to calibrate one or a combination of several of the reflectance variables with summer temperature. Because RDA showed a high influence of MAR on raw variables we performed the calibration only on detrended variables.

Multivariate calibration is found to yield consistently better results than univariate calibration (criterion: small Leave-one-out cross-validated RMSEP). This result is expected since the PCA showed that three PCs (although not all significant) were found to explain the variability in the data set.

Given the fact that this is the first methodological attempt to calibrate scanning in-situ reflectance data (380 - 730 nm) from minerogenic lake sediments with meteorological time series, the calibration statistics are remarkable: individual reflectance variables correlate highly with summer temperature data during the calibration period AD 1864 – 1950 ($r > 0.71$ for 5-years smoothed series; $r > 0.82$ for 9-years smoothed series; both highly significant $p_{ca} < 0.05$, p corrected for autocorrelation and multiple testing). The RMSEP of a multivariate calibration model (including the three varia-

bles trough590-730, min690or700 and min480) is as small as 0.1°C ($r^2=0.84$). This is rarely found in quantitative paleolimnology and shows the great potential of this novel rapid technique. However, it should be noted that the quality of the calibration model and the calibration statistics (i.e. the final product used as a basis for the climate reconstruction) rely critically on a highly precise chronology (here: varve counts), a very good knowledge of the mineralogical composition of the individual varves (here: determined by XRD) and a sound understanding of the processes (meteorology in the catchment, sediment transport and deposition) that lead to a specific signature in the varves. To test the skill of the reflectance-derived variables to yield high-quality climate reconstructions, we compared our data with fully independent reconstructions following a running correlation approach. The stable significant ($p_c < 0.1$) running correlation with the summer temperatures of Casty et al. (2005) indicates the high stability of the calibration model back in time. The periods with systematic offsets on the order of a few years suggest that the correlation coefficients could further be enhanced by improving the chronology of the sediment core (time series of the reflectance data). For the purpose of the study here (methodology of scanning reflectance spectroscopy rather than climate reconstructions) we leave the chronology in its raw form. However, it is evident that, given the high temporal resolution of the data acquired, the precision of the chronology is critically important. It is recommendable to perform the non-destructive scanning reflectance spectroscopy on the same sediment half-core that is used afterwards to establish the age-depth model.

4.6. Conclusions and outlook

In this study we tested the potential of scanning in-situ reflectance spectroscopy in the visible spectrum (380 – 730 nm) as a novel method to produce quantitative high-resolution (annual – subdecadal) climate reconstructions from minerogenic lake sediments. For this methodological study, we have chosen proglacial, annually laminated Lake Silvaplana because the sedimentology, the mineralogy, geochemistry, and chronology of the sediments are very well known from previous studies that used established analytical paleolimnological methods (XRD, biogenic silica, Mass Accumulation Rate etc.) on individual varves. This knowledge allows for a sound interpretation of the reflectance spectra that are measured directly on the surface of split sediment cores. Furthermo-

re, a very long instrumental meteorological time series (back to AD 1864) located adjacent to the lake allows for a long calibration period prior to anthropogenic eutrophication of the lake (AD 1950), and independent climate reconstructions (climate field, tree-ring based) allow for the verification of the climate reconstruction inferred from reflectance variables back to AD 1177.

Using multiple linear regression (MLR) we establish a calibration model that explains 84% of the variance of summer (JJAS) temperature during the calibration period 1864-1950. The correlation of individual variables (indicative for Chlorite and Mica) were as high as $r=0.84$. Previous experimental work (XRD) has shown that the amount of Chlorite and Mica in individual varves is indicative of warm season temperature in Lake Silvaplana.

We propose that a series of numerical methods and statistical tests be performed to extract a robust climate signal and proper calibration from the multivariate reflectance spectra data set. We first tested the independence of the individual measurements calculating autocorrelation functions, and then assessed the degree of variance common to the reflectance-derived variables applying a Principal Component Analysis PCA. We then tested the influence of several potential climate and sediment parameters (here: temperature, precipitation and MAR) on the reflectance variables by means of Redundancy Analysis RDA. We found in our case study of lake Silvaplana that the Mass Accumulation Rate MAR influences the reflectance data. In our case study, MAR is subject to a low-frequency trend (glacier length variations); hence we had also to remove that trend from the reflectance-derived variables prior to calibration in order to retain a proper temperature signal.

We then tested whether one individual reflectance variable or a combination of several of them would yield a better calibration with climate data. Thus we compared the calibration statistics (criterion: RMSEP) of systematic univariate and multivariate calibration approaches and found that a calibration model using multiple linear regression including three variables performs best (smallest RMSEP). We then reconstructed summer temperatures back to AD 1177 applying this calibration model. This reconstruction was validated by comparing it to two fully independent regional reconstructions (multi-proxy reconstruction mainly based on early instrumental and documentary data, Casty et al. 2005); tree ring late-wood density reconstruction, Büntgen et al. 2006). Running correlation analysis showed high consistency back to at least AD 1600

between the data series compared. The decadal-scale structure and amplitude of summer temperature variability is well captured; so are shorter periods with cold summers after large tropical volcanic eruptions (e.g. around AD 1256, 1275, 1450, 17th century and the decade AD 1810-1820).

From this methodological study we draw the following recommendations for the practical work using scanning in-situ reflectance spectroscopy on mineroclastic sediments: non-destructive reflectance spectroscopy should be performed on the same split core that is used subsequently to establish the age-depth model and chronology of the sediment core. That is most critical, because a high chronological accuracy is fundamental when calibrating the reflectance data set against climate data. Prior to interpreting the reflectance spectra, the general mineralogical composition and geochemistry of the sediment should be measured by means of established analytical methods (e.g. XRD). This is the basis for a sound interpretation of the reflectance spectra with absorptions of the minerals that are actually present in the sediment.

In this study we could clearly show the high potential of scanning in-situ reflectance spectroscopy for the application on mineroclastic sediments. From a methodological point of view the robustness of reflectance characteristics should be further assessed. For the moment it remains open to which extent variables such as water content on the split core sediment surface, degree of oxidation of the sediment surface, or even the temperature could modify the reflectance measurements. Systematic tests are under way to assess the robustness, the reproducibility and technical performance of the scanning reflectance spectroscopy in the visible spectrum. However, one indisputable advantage of this novel method is the very inexpensive and very rapid data acquisition: several thousands of data points (corresponding to several meters of sediment core) can be generated in one day; this would also allow to systematically study the spatial representation of a sediment core in a given lake (intra-lake variability), which is very hard to perform with traditional analytical methods. A further avenue of research could involve systematic testing of the method on a variety of lakes with different sediment types and proportions of clastic, biogenic and even chemical components. While von Gunten et al. (2009) have demonstrated the skill of the new method on sediments with high proportions of organic matter in a eutropic lake,

the method needs to be tested in an environment with volcanoclastic or chemical sediment (evaporates) or in lakes with limestone bedrock.

Acknowledgments

We would like to thank Alex Blass, Thomas Kulbe, Michael Sturm and Alois Zwyssig for their help during fieldwork. Project grants were provided by European Union FP6 project "Millennium" (Contract 017008), NF-200021-106005/1 _ENLARGE' and the NCCR Climate.

References

- Begert M, Schlegel T, Kirchhofer W (2005) Homogeneous temperature and precipitation series of Switzerland from 1864 to 2000. *International Journal of Climatology* 25: 65-80.
- Benjamini Y, Hochberg Y (1995) Controlling the false discovery rate: a practical and powerful approach to multiple testing. *Journal of the Royal Statistical Society. Series B (Methodological)* 57: 289-300.
- Bigler C, von Gunten L, Lotter A.F, Hausmann S, Blass A, Ohlendorf C, Sturm M (2007) Quantifying human-induced eutrophication in Swiss mountain lakes since AD 1800 using diatoms. *The Holocene* 17: 1141 - 1154.
- Birks HJB (1998) Numerical tools in palaeolimnology – Progress, potentialities, and problems. *Journal of Paleolimnology* 20: 307-332.
- Blass A, Grosjean M, Troxler A, Sturm M, (2007a) How stable are twentieth-century calibration models? A high-resolution summer temperature reconstruction for the eastern Swiss Alps back to AD 1580 derived from proglacial varved sediments. *The Holocene* 17: 51 – 63.
- Blass A, Bigler C, Grosjean M, Sturm M (2007b) Decadal-scale autumn temperature reconstruction back to AD 1580 inferred from the varved sediments of Lake Silvaplana (southeastern Swiss Alps). *Quaternary Research* 68: 184-195.
- Büntgen U, Frank, DC, Nievergelt D, Esper J, (2006) Summer Temperature Variations in the European Alps, A.D. 755–2004. *Journal of Climate* 19: 5606–5623.
- Casty C, Wanner H, Luterbacher J, Esper J, Boehm R (2005) Temperature and precipitation variability in the European Alps since AD 1500. *International Journal of Climatology* 25: 1855–1880.
- Caviezel G (2007) Hochwasser und ihre Bewältigung anhand des Beispiels Oberengadin 1750 – 1900. MSc thesis. University of Bern, Bern.
- Cleveland WS, Devlin SJ (1988) Locally Weighted Regression - An Approach to Regression-Analysis by Local Fitting. *Journal of the American Statistical Association* 83: 596 - 610.
- Dawdy DR, Matalas NC (1964) Statistical and probability analysis of hydrologic data, part III: Analysis of variance, covariance and time series. In: Chow VT Handbook of Applied Hydrology, a Compendium of Water-Resources Technology. McGraw-Hill, New York, pp. 8.68-8.90.
- Francus P, Bradley RS, Abbott MB, Patridge W, Keimig F (2002) Paleoclimate studies of minerogenic sediments using annually resolved textural parameters. *Geophysical Research Letters* 29.
- Frontier S (1976) Etude de la décroissance des valeurs propres dans une analyse en composantes principales: comparaison avec le modèle du bâton brisé. *J. exp. Mar. Biol. ecol.* 25 : 67–75.
- Gensler G, Schüepp M (1991). Witterungsklimatologie von Graubünden. In: Elsasser H, Boesch M Beiträge zur Geographie Graubündens. Fotorotar, Egg.
- Heegaard E, Birks HJB, Telford RJ (2005) Relationships between calibrated ages and depth in stratigraphical sequences: an estimation procedure by mixed-effect regression. *The Holocene* 15: 612 – 618.
- Hotelling H (1933) Analysis of a complex of statistical variables into principal components. *Journal of Educational Psychology* 24: 417-441, 498-520.
- Kalugin I, Daryin A, Smolyaninova L, Andreev A, Diekmann B, Khlystov O (2007) 800-yr-long records of annual air temperature and precipitation over southern Siberia inferred from Teletskoye Lake sediments. *Quaternary Research* 67: 400 - 410.
- Kamenik C, Van der Knaap WO, Van Leeuwen JFN, Goslar T (2009) Pollen/climate calibration based on a near-annual peat sequence from the Swiss Alps. *Journal of Quaternary Science* 24: 529-546.
- Kaufman DS, Schneider DP, McKay NP, Ammann CM, Bradley RS, Briffa KR, Miller, GH, Otto-Blies-

- ner BL, Overpeck JT, Vinther BM, Arctic L (2009) Recent Warming Reverses Long-Term Arctic Cooling. *Science* 325: 1236 - 1239.
- Larocque-Tobler I, Grosjean M, Heiri O, Trachsel M, Kamenik, C (in review) 1000 years of climate change reconstructed from chironomid subfossils preserved in varved-lake Silvaplana, Engadine, Switzerland. *Quaternary Science reviews*.
- Legendre P, Legendre L (1998) *Numerical ecology*. Elsevier, Amsterdam.
- Mckay NP, Kaufman DS, Michelutti N (2008) Biogenic silica concentration as a high-resolution, quantitative temperature proxy at Hallet Lake, south-central Alaska. *Geophysical Research Letters* 35.
- Michelutti N, Blais JM, Cumming BF, Paterson AM, Ruehland K, Wolfe AP, Smol JP (2009) Do spectrally inferred determinations of chlorophyll a reflect trends in lake trophic status? *Journal of Paleolimnology* (online)
- Ohlendorf C (1998) *High Alpine Lake Sediments as Chronicles for Regional Glacier and Climate History in the Upper Engadine, Southeastern Switzerland*. PhD thesis. ETH Zürich, Zürich.
- Rein B, Sirocko F (2002) In-situ reflectance spectroscopy - analysing techniques for high-resolution pigment logging in sediment cores. *International Journal of Earth Sciences* 91: 950-954.
- Rein, B (2003) *In-situ Reflektionsspektroskopie und digitale Bildanalyse – Gewinnung hochauflösender Paläoumweltdaten mit fernerkundlichen Methoden*. Habilitationsschrift, University of Mainz, Mainz.
- Rein B, Lueckge A, Reinhardt L, Sirocko F, Wolf A, Dullo W (2005) El Niño variability off Peru during the last 20,000 years. *Paleoceanography* 20: PA 4003.
- Rosen P, Dodbakk E, Renberg I, Nilsson M, Hall R (2000) Near-infrared spectrometry (NIRS): a new tool for inferring past climatic changes from lake sediments. *The Holocene* 10: 161 – 166.
- Spillmann P (1993) *Die Geologie des penninischen-ostalpinen Grenzbereichs im südlichen Berninagebirge*, PhD thesis. ETH Zürich, Zürich.
- Trachsel, M, Eggenberger, U, Grosjean, M, Blass, A, Sturm, M (2008) Mineralogy-based quantitative precipitation and temperature reconstructions from annually laminated lake sediments (Swiss Alps) since AD 1580. *Geophysical Research Letters* 35: L13707.
- Trachsel M, Grosjean M, Larocque-Tobler I, Schwikowski M, Blass A, Sturm M (in review) Quantitative summer temperature reconstruction derived from a combined biogenic Si and chironomid record from varved sediments of Lake Silvaplana (south-eastern Swiss Alps) back to AD 1177. *Quaternary Science Reviews*.
- Trenberth KE (1984) Some Effects of Finite Sample Size and Persistence on Meteorological Statistics. Part I: Autocorrelations. *Monthly Weather Review* 112: 2359-2368.
- USGS (2007) Digital Spectral Library, splib06a. <http://speclab.cr.usgs.gov/spectral-lib.html>.
- van der Wollenberg AL (1977) Redundancy analysis: an alternative for canonical correlation analysis. *Psychometrika* 42: 207–219.
- Venables WN, Ripley BD, (2002) *Modern Applied Statistics with S*. Springer, New York.
- von Gunten L, Grosjean M, Rein B, Urrutia R, Appleby P (2009) A quantitative high-resolution summer temperature reconstruction based on sedimentary pigments from Laguna Aculeo, central Chile, back to AD 850. *Holocene* 19: 873 - 881.
- Wolfe AP, Vinebrooke R, Michelutti N, Rivard B, Das B (2006) Experimental calibration of lake-sediment spectral reflectance to chlorophyll a concentrations: methodology and paleolimnological validation. *Journal of Paleolimnology* 36: 91-100.
- Zolitschka B, Mingram J, van der Gaast S, Jansen JHF, Naumann, R (2001) Sediment logging techniques. In: Last WM, Smol JP *Tracking environmental change using lake sediments: physical and chemical techniques*. Kluwer Academic Publishers, Dordrecht, pp 137-153.

Chapter 5



5. Quantitative summer temperature reconstruction derived from a combined biogenic Si and chironomid record from varved sediments of Lake Silvaplana (south-eastern Swiss Alps) back to AD 1177

M. Trachsel^{a,b}, M. Grosjean^{a,b}, I. Larocque-Tobler^{a,b,c}, M. Schwikowski^{b,d}, A. Blass^e, M. Sturm^e.

a Department of Geography, University of Bern, Erlachstrasse 9a, 3012 Bern, Switzerland.

b Oeschger Center for Climate Change Research, University of Bern, Zähringerstrasse 25, 3012 Bern, Switzerland

c INRS-ETE, 490 De La Couronne, Québec, Québec, Canada, G1K 9A9

d Department of Chemistry and Biochemistry, University of Bern & Paul Scherrer Institut, 5232 Villigen, Switzerland

e Surface Waters, EAWAG, Überlandstrasse 133, 8600 Dübendorf, Switzerland

Submitted to Quaternary Science Reviews

Abstract

High-resolution quantitative temperature records are needed for placing the recent warming into the context of long-term natural climate variability. In this study we present a quantitative high-resolution (9-year) summer (June to August) temperature reconstruction back to AD 1177 for the south-eastern Swiss Alps. This region is a good predictor for summer temperatures in large parts of western and central Europe. Our reconstruction is based on a combination of the high-frequency component of annually resolved biogenic silica (bSi flux) data and the low-frequency component of decadal chironomid-inferred temperatures from annually laminated well dated sediments (varves) from proglacial Lake Silvaplana, eastern Swiss Alps.

For the calibration (period AD 1864 – 1949) we assess systematically the effects of six different regression methods (Type I regressions: Inverse Regression IR, Inverse Prediction IP, Generalised Least Squares GLS; Type II regressions: Major Axis MA, Ranged Major Axis RMA and Standard Major Axis SMA) with regard to the predicted amplitude and the calibration statistics such as root-mean-square error of prediction (RMSEP), reduction of error (RE) and coefficient of efficiency (CE).

We found a trade-off in the regression model choice between a good representation of the amplitude (Type II regressions) and good calibration statistics (Type I regressions). Since the amplitude is the essence of climate variability we recommend using a Type II regression which accounts for an error on the predictor and the predictand. Here, a combination between MA and SMA (Type II regressions) performed best ($r=0.67$, $p<0.04$;

$RMSEP=0.26^{\circ}C$, $RE=0.22$, $\Delta Amplitude_{(predicted - observed)} = 0.03^{\circ}C$; $RMSEP/Amplitude=0.197$).

The band-pass filtered bSi flux record is in close agreement both in the structure and the amplitude with two fully independent reconstructions spanning back to AD 1500 and AD 1177, respectively. All known pulses of negative volcanic forcing are represented as cold anomalies in the bSi flux record. Volcanic pulses combined with low solar activity (Spörer and Maunder Minimum) are seen as particularly cold episodes around AD 1460 and AD 1690. The combined chironomid and bSi flux temperature record is in good agreement with the glacier history of the Alps. The warmest (AD 1190) and coldest decades (17th century; 1680-1700) of our reconstruction coincide with the largest anomalies in the Alpine tree ring based reconstruction; both records show in the decadal variability an amplitude of $2.6^{\circ}C$ between AD 1180 and 1950, which is substantially higher than the amplitude of hemispheric reconstructions. Our record suggests that the current decade is slightly warmer than the warmest decade in the pre-industrial time of the past 800 years.

5.1. Introduction

High-resolution, well calibrated temperature reconstructions are fundamental to put the current warming into a wider perspective. In this context, lake sediments are very important because they may provide very long records (eg. Sturm and Lotter, 1995; Zolitschka et al., 2000) and preserve the signals of low-frequency climate variability (eg. Moberg et al., 2005; Jansen et al., 2007).

Typically, quantitative temperature reconstructions from lake sediments are based on biological proxies (e.g. chironomids, Heiri et al., 2003)

using a transfer function (e.g., Birks 1998). In the recent past considerable efforts have been made to quantitatively assess the range, trends and amplitude of paleoclimate variability from high-resolution (annually resolved) geochemical proxies in lake sediments using methods from tree ring research (calibration-in-time approach; Francus et al., 2002; Kalugin et al., 2006; Blass et al., 2007a, b; McKay et al., 2008; Trachsel et al., 2008; von Gunten et al., 2009; Kaufman et al., 2009). The quantitative assessment of paleoclimate parameters from geochemical lake sediment proxies may, however, be challenged by the complex and often non-linear responses of lacustrine systems to climate change (eg. Ohlendorf, 1998), possible anthropogenic influences (e.g. Gobet et al., 2004; Geirsdottir et al., 2009), difficulties with precise dating of lake sediments (e.g. Goszlar et al., 2009; von Gunten et al., 2009), long-term trends due to the natural lake evolution (Blass et al., 2007b), and the appropriate choice of the statistical calibration and reconstruction method. This latter problem is particularly often overlooked, but it affects substantially characteristics and amplitudes of the paleoclimate reconstructions (e.g. Esper et al., 2005; Bürger et al., 2006; Riedwyl et al., 2008; Kamenik et al., 2009).

In this study we present an 800-years long annually resolved record of biogenic silica bSi from proglacial Lake Silvaplana, eastern Swiss Alps. A long temperature record from this area is climatically highly significant because this region is an excellent predictor for summer temperatures in large parts of Western and Central Europe, and the northern Mediterranean (Fig. 5.1, inset map). The sediment of Lake Silvaplana is annually laminated (varved; Leemann and Niessen, 1994; Ohlendorf et al., 1997; Blass et al. 2007a) and provides an excellent age control. Blass et al. (2007b) established that, in this lake, biogenic silica bSi flux is a proxy for summer (JJA) and June to November temperatures, which corresponds to the ice-free period of the lake (Livingstone, 1997).

In this study we place particular emphasis on testing systematically the robustness of trends and amplitudes of reconstructed climate variability in different frequency domains. Correct amplitudes of variability are fundamental to assess, for instance, the (regional) climate sensitivity to a particular forcing or whether or not specific periods (e.g. during the Medieval Warm Period) were warmer/colder than the last few decades (Bradley et al. 2003). Since the amplitude of a climate reconstruction is depending on the choice of the

statistical reconstruction method (e.g. Esper et al. 2005), we calibrate our data set with six different regression methods (inverse regression, inverse prediction, generalised least squares, Major Axis regression, Ranged Major Axis regression and Standard Major Axis regression). The goal is to assess the influence choice of the method on the amplitudes of the calibrated time series and calibration statistics (root mean squared error of prediction RMSEP, reduction of error RE and coefficient of efficiency CE) and, finally, the reconstruction. The regression methods are briefly reviewed and the calibration statistics are discussed in the light of our goal to assess the 'real' amplitude of decadal to centennial-scale climate variability over the past 800 years.

Potential non-climatic trends in paleolimnological data sets and their influence on climate reconstructions are generally very difficult to assess and to quantify. Blass et al. (2007b) found a low-frequency (>100 years domain), non-climatic trend in the biogenic silica flux data of Lake Silvaplana. This non-climatic trend has been removed and the bSi-based decadal-scale temperature variability is compared with two fully independent summer temperature reconstructions: the multi-proxy climate field reconstruction and the tree ring late-wood density reconstructions (Casty et al., 2005; Büntgen et al., 2006).

Establishing the low frequency (centennial-scale) domain of climate variability is arguably one of the most difficult but important challenges (Moberg et al., 2005; Jansen et al., 2007). In the following we combine the high-resolution bSi-based decadal-scale reconstruction with a lower-resolution centennial-scale chironomid-based summer temperature reconstruction from the same lake and sediment core (Larocque-Tobler et al., in review). The chironomid-based temperature reconstruction has been established using a transfer function (Heiri et al., 2003), which is much more robust against long-term trends. As a final product we present a combined summer temperature reconstruction for the Alps for the past 800 years that has assessed skills in the sub-decadal to multi-centennial range of climate variability.

5.2. Regional Setting

Lake Silvaplana (Lej da Silvaplauna, Fig. 5.1) is located in the Engadine, south-eastern Swiss Alps, at an altitude of about 1800 m a.s.l. The lake has a maximum depth of 77 m and a volume of 127×10^6 m³ (Blass et al., 2007a and references therein), and is usually ice-covered between Ja-

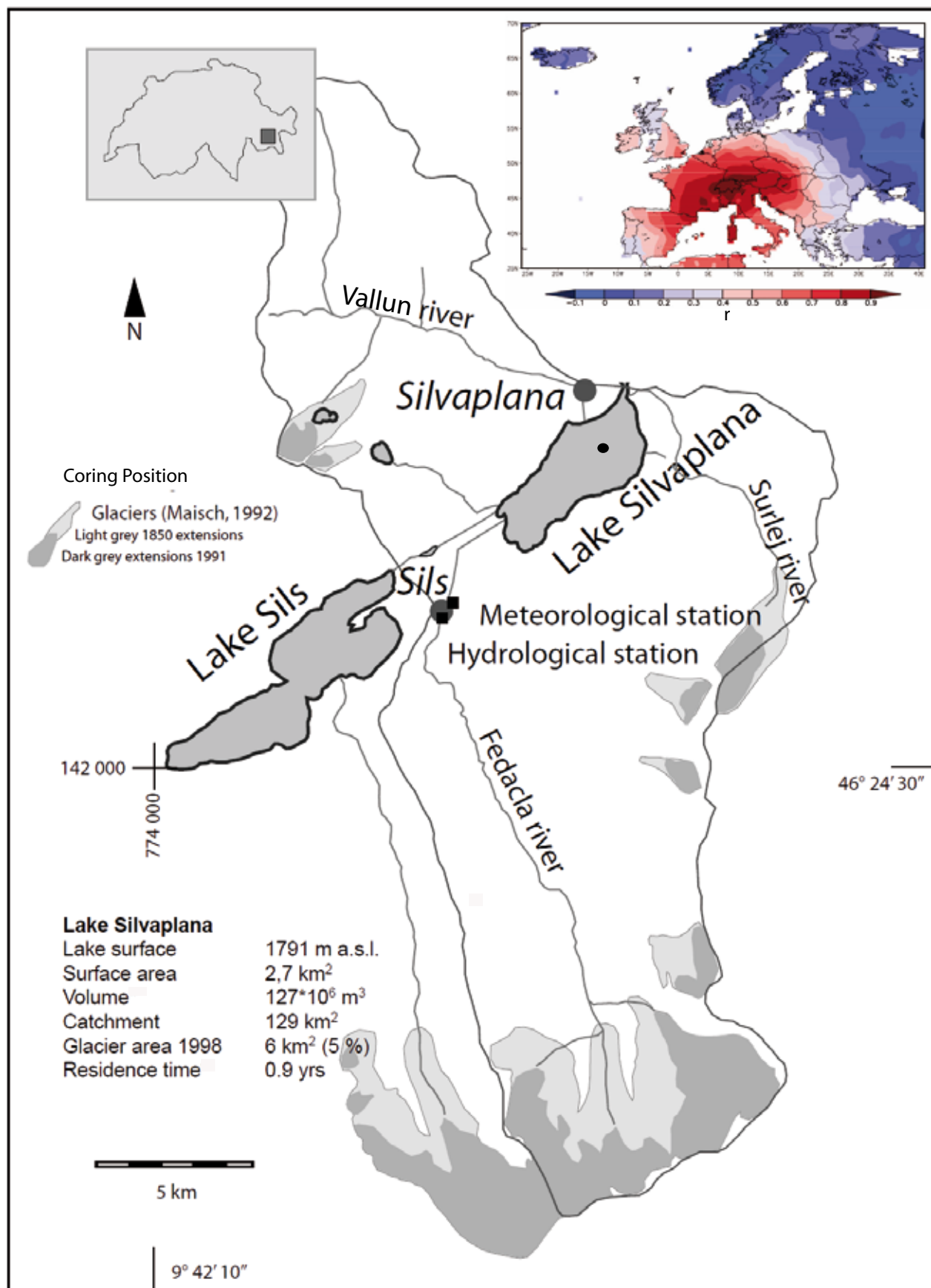


Fig. 5.1: Overview map of the Lake Silvaplana catchment area, including the coring position, meteorological station and the glacier extent during the Little Ice Age and in 1991 (redrawn from Blass et al., 2007a). The spatial correlation of Engadine summer temperatures is shown in the inset map (Trachsel et al., 2008)

nuary and May. Lake Silvaplana is a dimictic lake with a rather short period of spring mixing after the ice break-up that is followed by a period of summer stratification lasting from June to November. Strong local valley winds develop on sunny days between around 11 h and late afternoon if the synoptic-scale upper airflow is weak. This results in a generally well-mixed epilimnion during the summer stagnation (Blass et al., 2007b). The second overturn of the year occurs usually in December. The mean water residence time is only 8 months because of the high rate of inflow of glacial melt water during summer. Lake Silvaplana is oligotrophic with $<10 \mu\text{g l}^{-1}$ orthophosphate in the water column (Bigler et al., 2007). Oxygen concentrations are consistently $>5\text{mg l}^{-1}$ in near-bottom waters and the pH is around 7.8 (Bigler et al., 2007).

The catchment area of the lake extends over 129 km². In 1998, about 6 km² (5%) of the catchment area were glaciated (Blass et al. 2007a). The most important inflow is the Fedacla River, which has a mean discharge rate of $1.5 \text{ m}^3 \text{ s}^{-1}$, is fed mainly by glacial meltwater and carries a high load of suspended sediment. A second inflow is the Inn River, which connects Lake Silvaplana to Lake Sils. This river has a mean discharge rate of $2 \text{ m}^3 \text{ s}^{-1}$ but carries almost no suspended sediment. The discharge rates of the Vallun and Surlej Rivers are 0.7 and $0.3 \text{ m}^3 \text{ s}^{-1}$, respectively.

The Engadine is an inner-alpine dry valley with a mean annual precipitation rate of 978 mm (SMA, 2002; climatology 1961–1990). The annual precipitation maximum occurs in August (121 mm) and the minimum in February (42 mm). Thunderstorms are relatively infrequent (20 days per year, SMA, 2002). The area lies in a meteorological boundary zone and receives precipitation mainly from the south (Brunetti et al., 2006). Monthly mean temperatures range from $-7.8 \text{ }^\circ\text{C}$ in January to $10.8 \text{ }^\circ\text{C}$ in July.

5.3. Materials and methods

5.3.1. Material and chronology, climate data

Two piston cores of 9 meters length were recovered in winter 2005/2006 to extend two previously recovered freeze cores (Blass et al., 2007b). Using marker layers, the piston cores were stratigraphically correlated to the freeze cores. The sediment cores were frozen with liquid nitrogen and individual varves were sampled in a freeze laboratory (-12°C). Biogenic silica bSi concentration in the sediment was determined using alkaline leaching

(Mortlock and Froehlich, 1989) and ICP-OES, and corrected for lithogenic Si according to Ohlendorf and Sturm (2007). The annual Mass Accumulation Ratio MAR was calculated from varve thickness, water and organic matter content according to Berner (1971) and Niessen et al. (1992). For further details see Blass et al. (2007b).

The existing chronology from AD 1580 to AD 1949 (Blass et al., 2007a; varve counting and documented flood layers) was refined with additional historically documented floods from the upper Engadin (Caviezel, 2007). The chronology was then extended back to AD 1177 using varve counting of thin sections and digital images, and two historically documented very large flood events AD 1566 and AD 1177 (Sturm and Matter, 1978; Blass et al. 2007b; Fig. 5.2), which confirmed the varve counting.

For the calibration of the lake sediment proxies, we used monthly mean values of the homogenised meteorological data from nearby station Sils Maria (1864 to 1949, Begert et al., 2005) and the mean value of the entire Alpine gridded temperature reconstruction (mainly early instrumental data AD 1760 - 1949; Casty et al., 2005). The period AD 1950 – 2005 was not used for calibration because of varve counting difficulties and eutrophication effects (Blass et al., 2007b).

In order to account for dating uncertainties (varve-counting errors, e.g. Besonen et al., 2007) we tested the calibration also with 5-years and 9-years running means applied to the annually resolved bSi flux and meteorological data series prior to the correlation analysis. For the same reason (chronological uncertainties) the reconstruction is displayed as the 9-year (15-year) running mean back to AD 1500 (AD 1177).

5.3.2. Statistical methods

We applied six different regression methods to assess the effect of the method choice on the amplitudes of reconstructed temperatures. The methods were: ordinary least squares (OLS) regression with three variants (i) inverse regression (Venables and Ripley, 2002 and (ii) inverse prediction (Sokal and Rohlf, 2001), (iii) generalised least squares regression (Venables and Ripley, 2002), (iv) Major Axis regression (Legendre and Legendre, 1998), (v) Ranged Major Axis regression (Legendre and Legendre, 1998), and (vi) Standard Major Axis regression (Legendre and Legendre, 1998; Sokal and Rohlf, 2001).

(i) Inverse regression IR is the most commonly used regression type based on the equation

$$(1) y = a + b \cdot x + e$$

where y , the dependent variable is the climate data and x , the independent variable is the climate proxy data, a being the intercept, b the slope of the regression and e the normally distributed residuals.

$$\text{i.e. } T = a + \text{Proxy} \cdot b + \varepsilon$$

The amplitude of inverse regression is the correlation coefficient times the amplitude of scaling (Esper et al., 2005).

(ii) Inverse prediction IP is as well based on equation (1) but now y being the climate proxy and x being the climate data (e.g. temperature T):

$$\text{Proxy} = a + b \cdot T + \varepsilon$$

Solving for 'temperature' (to be predicted by the proxy) we get

$$T = \frac{(\text{Proxy} - a)}{b}$$

(iii) Generalised least squares regression GLS accounts for serial correlation of the residuals applying an autoregressive (AR1) model for the residual series (Venables and Ripley, 2002).

(iv) Major Axis regression MA: the regression line is the first principal component of the scatter of points (Legendre and Legendre, 1998); here, the square of the Euclid distance between the points and the regression line is minimised.

(v) Ranged Major Axis regression RMA is similar to Major Axis regression, but prior to extracting the first principal component, the variables x and y are transformed into x' and y' . The transformation (ranging) is depending on the scale of the variables (i.e. relative or interval scaled variables). By ranging, the variables are transformed into numbers between 0 and 1 (Legendre and Legendre, 1998). In our example bSi flux is a relative scale variable (absolute zero value) whereas temperature in °C is an interval scale variable (zero value set arbitrarily). With detrended bSi flux data both variables are interval-scaled variables.

(vi) Standard Major Axis regression SMA regression (scaling, geometric mean regression, reduced Major Axis regression), is again similar to Major Axis regression but prior to minimising the Euclid distances both variables are standardised. SMA is the geometric mean of the slope parameters b of inverse regression and inverse prediction (geometric mean regression), and can be obtained from inverse regression by dividing the regressi-

on coefficient b with r and, subsequently adjusting the intercept a , or by adjusting mean and variance of the proxy to mean and variance of the climate data (scaling, e.g. Esper et al., 2005).

OLS regression (i – iii) is referred to as Type I regression which is minimising the squared errors on the x or the y axis, whereas in Type II regressions (iv – vi; variants of Major Axis regression) the squares of the Euclid distances are minimised (Legendre and Legendre, 1998). Type II regression should be applied if there is a random error on both variables x and y . This is the case in our example with the two variables 'temperature' and 'biogenic silica flux'.

In theory these six regression methods may only be applied to normally distributed data. We therefore carried out a set of shapiro-wilk (Shapiro and Wilk, 1965) tests to test our data for normality.

For the calibrations in the long period (AD 1760 – 1949; early instrumental data from Casty et al., 2005) we calculated the reduction of error (RE) and the coefficient of efficiency (CE) statistics following Cook et al. (1994). When calibrating the 9-year smoothed bSi record for the shorter period with instrumental data (AD 1864 to 1949, Blass et al., 2007b) we did not divide the data set into a calibration and a verification period (cross-validation) due to the low number of independent observations (i.e. degrees of freedom; Trenberth, 1984). In this case, we calculated a RE statistics comparing our temperature reconstruction with the mean observed temperature of the calibration period.

We used Pearson correlation coefficients and the significance levels were calculated after correction for the degrees of freedom DF according to Dawdy and Matalas (1964); the DF-corrected p -value is indicated as p_{corr} .

Statistical analysis was performed using the open-source software R (r-project.org).

5.3.3. Detrending methods

Blass et al. (2007b) detected a non-climate trend in the bSi flux data and band-pass filtered the data series. Following this method, we used the residuals of a 100-year loess filter Cleveland and Devlin (1988). The span was set to represent 100 years in our annually resolved data set. Subsequently we applied a 9-years running mean (low-pass; calibration period and reconstruction from AD 1500 onwards) or 15-years running mean (reconstruction from AD 1177 onwards) to the residuals to account for the varve counting uncertainties (Blass

et al., 2007a). The independent data sets used for comparison and validation (Casty et al., 2005; Büntgen et al., 2006) were treated in the same way.

To represent the full decadal to centennial-scale spectra of climate variability in our record, we combined the band-pass filtered bSi summer (JJA) temperature data with the low-frequency component of the chironomid-inferred temperature series. Since chironomids are representing mostly July temperatures (Larocque-Tobler et al., in review) we had to convert the chironomid-inferred July temperature record into summer (JJA) temperature to make it comparable with the bSi record. We used the mean and variance values of instrumental July and summer (JJA) temperatures (1864 – 2002) to scale the chironomid-inferred July temperatures to JJA temperatures. The scaled chironomid record was then 100-year loess filtered to retain the centennial scale variability.

5.4. Results

5.4.1. Chronology

Fig. 5.2 shows the refined chronology AD 1177 to 1949 with the turbidite layers of the documented

floods in 1987, 1951, 1834, 1828 (Blass et al., 2007b) and the new additional floods reported for AD 1868, 1793, 1772, 1706, 1566 and 1177 (corrected ages according to Caviezel, 2007). The 1793 flood coincides with the massive sediment sequence from 90 to 95 cm depth where Blass et al. (2007b) found varve counting to be inconclusive. Here we interpret this sediment sequence as one event layer. This is supported by anomalous grain size medians and mineralogical composition (Blass et al., 2007a; Trachsel et al., 2008). In summary the freeze core reaches back to AD 1604 (previously AD 1577); the entire record covers the time since AD 1177. The flood of AD 1177 caused a huge turbidite deposit of 30 cm thickness. Therefore, we decided to end our record before this hiatus.

5.4.2. Biogenic silica as a temperature proxy: calibration, detrending and reconstruction

Blass et al. (2007b) demonstrated the high correlation of the bSi flux record with instrumental summer and autumn temperature data for the calibration period between 1864 and 1949. As a consequence of the refined chronology during the

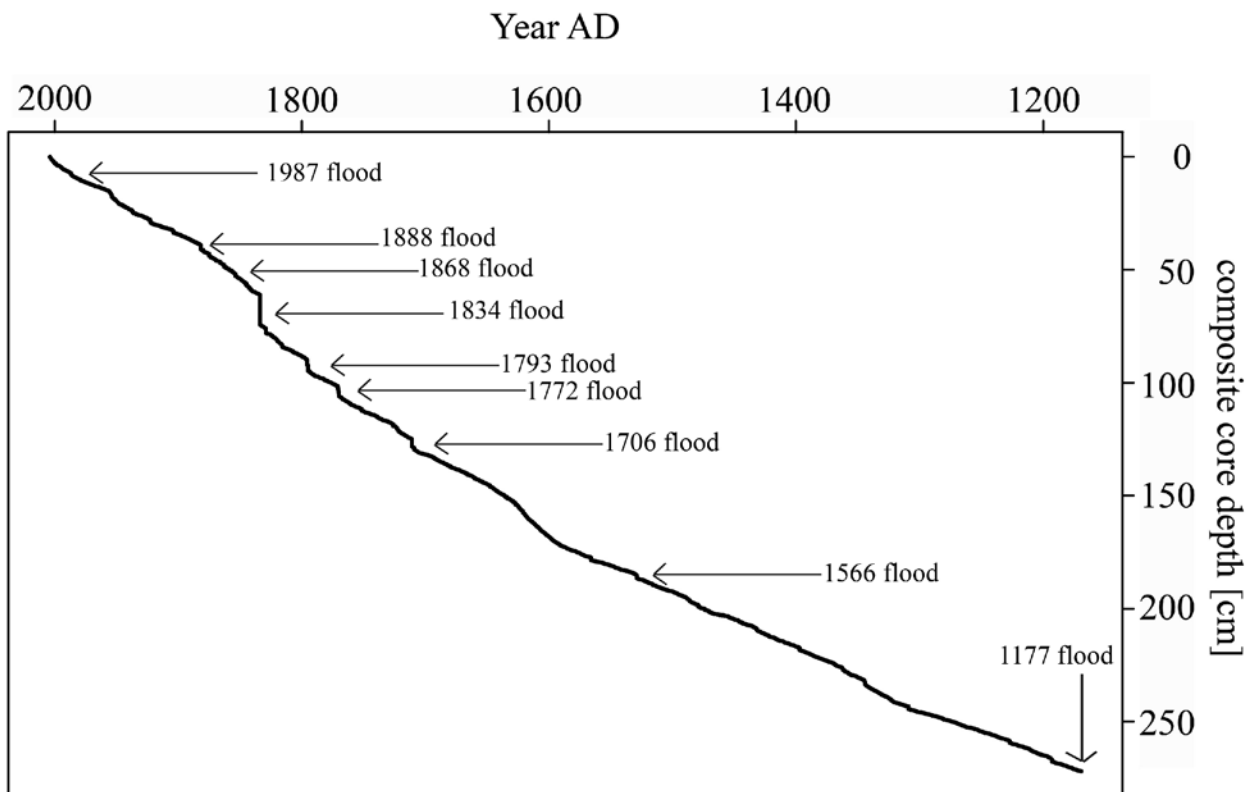


Fig. 5.2: Varve-count based composite age-depth model of the five cores SVP 04-11, SVP 05-1, SVP 06-3 I, SVP 06-2 II and SVP 06-3 II. Ten marker layers of historic floods (Caviezel, 2007) are used to constrain the varve-counting chronology.

(a)		MAM	JJA	JJAS	JJASON	SON	Year
bSi flux	r	r	r	r	r	r	r
	0.12	0.05	0.22	0.32	0.36	0.31	0.31
bSi flux 5-year running mean	0.02	0.06	0.56	0.55	0.6	0.51	0.45
bSi flux 9-year running mean	-0.32	0.08	0.67	0.67	0.69	0.6	0.47
(b)		1500-1950	1560-1950	1600-1950	1760-1950	1850-1950	
season	r	r	r	r	r	r	
JJA (Casty et al. 2005)	0.5	0.56	0.58	0.58	0.58	0.58	
JJASON (Casty et al. 2005)	0.5	0.5	0.6	0.58	0.66	0.66	

Table 5.1. (a) Matrix of correlation coefficients between biogenic silica (bSi) flux and seasonal air temperature measured at Sils from AD 1864 to 1949; the correlations were calculated for original (annually resolved) data, the 5-year and the 9-year running means. (b) correlations between the band-pass filtered bSi flux data and band-pass filtered temperature data (Casty et al., 2005). Significance levels $p < 0.05$ are bold, significance levels $p < 0.01$ are bold and italic.

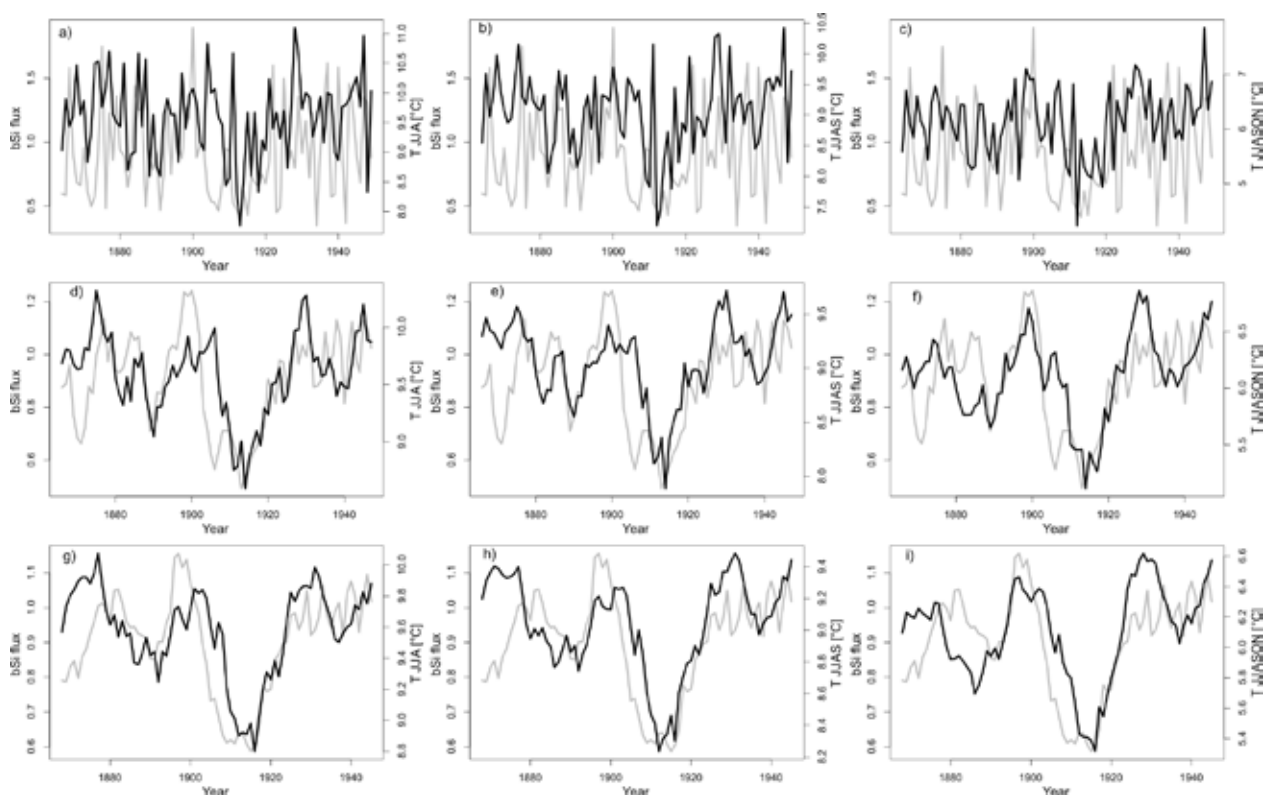


Fig. 5.3: Comparison of annual biogenic silica flux (grey) with instrumental temperatures (Sils Maria, black) for the summer season (JJA; left row; Figs. 5.3a,d,g), prolonged summer season (JJAS; Figs. 5.3b,d,h) and summer/autumn season (JJASON; Figs. 5.3c,e,i). The top panels show annually resolved data (Figs. 5.3a,b,c), the middle panels show 5-year smoothed data (Figs. 5.3d,e,f) and the bottom panels show 9-year smoothed data (Figs. 5.3g,h,i). Correlation coefficients are displayed in Table 5.1.

calibration period we needed to recalibrate the bSi flux data.

With the new annually resolved data five significant ($p < 0.05$) correlations with meteorological data (Table 5.1a, Fig. 5.3) were obtained. The highest correlation was found for T JJASON ($r = 0.36$, $p < 0.01$). The 5-years running mean bSi flux was also highly correlated with T JJASON ($r = 0.6$, $p_{\text{corr}} = 0.012$); the correlation of the 9-year smoothed series with T JJASON amounted to $r = 0.69$ ($p_{\text{corr}} = 0.043$). These

correlations were very similar to the values presented by Blass et al. (2007b) confirming the summer and autumn temperature signal preserved in the bSi flux data from the sediment of Lake Silvaplana. Generally, the accordance between the bSi flux data and the instrumental temperature data is excellent after AD 1878, whereas considerable mismatches in the calibration period are found between AD 1868 and 1878 (Fig. 5.3).

Since we are calibrating univariate, normally dis-

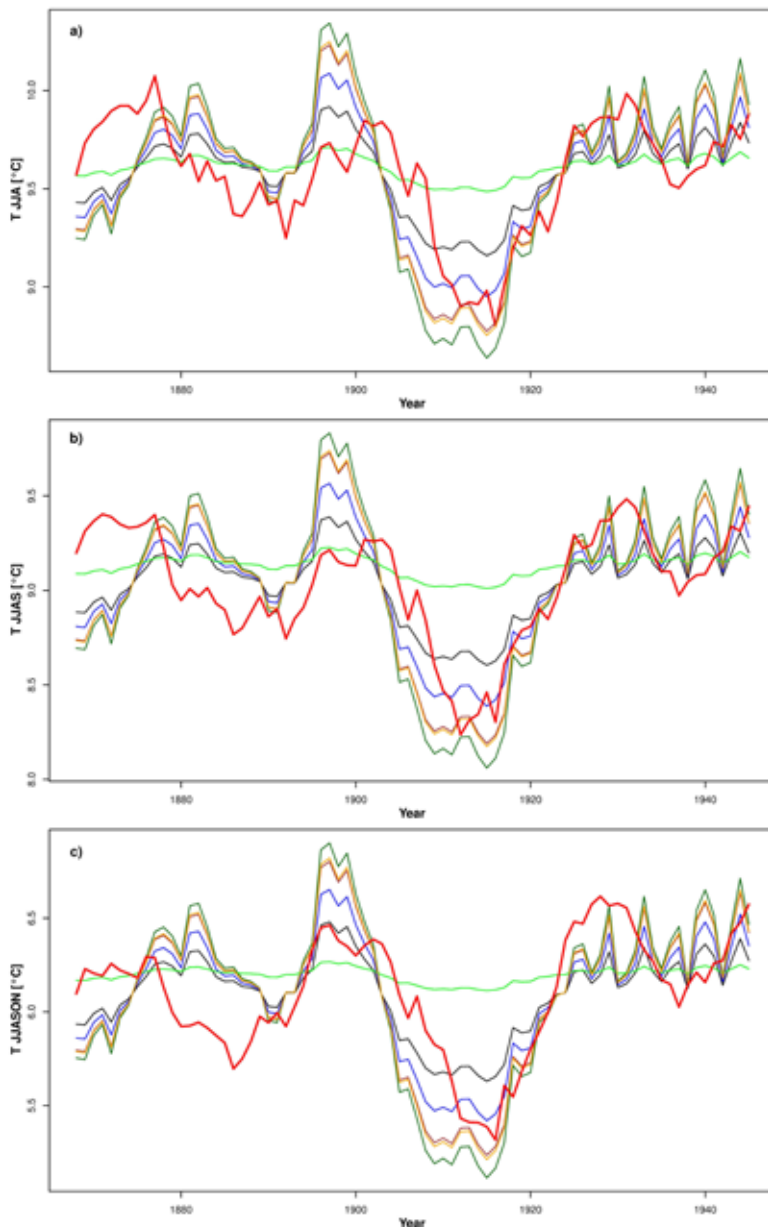


Fig. 5.4: Comparison of meteorological data (red; Sils Maria) and bSi-inferred temperatures 9-years smoothed (a) top panel JJA; b) middle panel JJAS, c) bottom panel JJASON) calculated with six different regression methods: Inverse Regression (black), Inverse Prediction (green) and Generalised Least Squares (brown), Standard Major Axis (geometric mean) regression (blue), Ranged Major Axis regression (orange) and Major Axis regression (red). Inverse Prediction predicts systematically the largest amplitude compared with the instrumental data (red); SMA and RMA regressions are closest to the amplitude of the instrumental record, Inverse Prediction and Generalised Least Squares regression underestimate the amplitude.

tributed data, the choice of the calibration method does not affect the shape of the reconstruction but the amplitude and, thereby, the calibration statistics (Fig. 5.4). Table 5.2 shows the Reduction of Error RE statistics, the Root Mean Square Error of Prediction RMSEP, the Amplitude predicted by the different regression methods, and the ratio between the RMSEP and the calibrated Amplitude. With regard to RE and RMSEP statistics and for the entire calibration period (1864 -1949), Inverse Regression IR performs best (RMSEP is lowest and RE is highest) followed by Standard Major Axis SMA regression. RMSEP of General Least Square GLS, Major Axis MA and Ranged Major Axis RMA regression are very close, but RE performs poorly: RE values of MA and RMA regression are close to zero. The RMSEP of inverse prediction IP is highest and RE is negative.

With regard to the amplitude (Fig. 5.4), the RMA regression is slightly overestimating the predicted amplitude compared with the observed amplitude of the instrumental data (true values, red line in Fig. 5.4) whereas SMA regression is slightly underestimating the amplitude. Large differences are found with IP and MA regression (largely overestimating the amplitude), and inverse regression and GLS regression (largely underestimating the amplitude). The ratio between the RMSEP and the Amplitude is lowest for IP closely followed by RMA, MA and SMA regression. This ratio is considerably higher for IR and the even larger than 1 for the GLS regression, which means that the amplitude is smaller than the RMSEP.

The overall best representation of interannual and decadal-scale amplitude and closest match with instrumental data was obtained by averaging

Raw Data						
(a)						
Instrumental target	T JJA Sils Maria	Calibration 1864-1949				
Regression method	RMSEP [°C]	Amplitude [°C]	RMSEP/Amplitude	RE		
Inverse regression	0.22	0.76	0.28	0.44		
Inverse prediction	0.32	1.71	0.19	-0.25		
Generalised least Squares	0.29	0.22	1.14	0.21		
SMA	0.25	1.14	0.21	0.33		
RMA	0.29	1.46	0.19	0.07		
MA	0.3	1.49	0.19	0.02		
Mean (RMA and SMA)	0.26	1.3	0.2	0.22		
Amplitude of the instrumental target		1.27				
Detrended data						
(b)						
Instrumental target	T JJA Casty et al. (2005)	Calibration 1760-1949				
Regression method	RMSEP [°C]	Amplitude [°C]	RMSEP/Amplitude	RE		
inverse regression	0.19	0.53	0.36	0.16		
Inverse prediction	0.33	1.65	0.2	-1.6		
Generalised least Squares	0.19	0.32	0.59	0.17		
SMA	0.22	0.94	0.23	-0.14		
RMA	0.21	0.83	0.25	-0.02		
MA	0.24	1.12	0.22	-0.4		
Amplitude of the instrumental target		1.11				
(c)						
Instrumental target	T JJA Casty et al. (2005)	Calibration 1760-1851				
Regression method	RMSEP [°C]	Amplitude [°C]	RMSEP/Amplitude	RE	CE	Amplitude verification
Inverse regression	0.20	0.47	0.43	0.22	0.2	0.34
Inverse prediction	0.35	1.39	0.25	-0.18	-0.2	1
Generalised least Squares	0.20	0.42	0.47	0.21	0.19	0.3
SMA	0.24	0.81	0.29	0.21	0.19	0.59
RMA	0.22	0.69	0.32	0.23	0.22	0.49
MA	0.25	0.87	0.28	0.19	0.17	0.63
Amplitude of the instrumental target		1.04				0.88
(d)						
Instrumental target	T JJA Casty et al. (2005)	Calibration 1852-1949				
Regression method	RMSEP [°C]	Amplitude [°C]	RMSEP/Amplitude	RE	CE	Amplitude verification
Inverse regression	0.17	0.49	0.35	-0.02	-0.04	0.68
Inverse prediction	0.31	1.56	0.2	-5.04	-5.12	2.18
Generalised least Squares	0.19	0.09	1.96	0.09	0.08	0.02
SMA	0.2	0.87	0.23	-1.03	-10.6	1.21
RMA	0.2	0.87	0.23	-1.01	-1.04	1.21
MA	0.25	1.22	0.20	-2.69	-2.74	1.7
Amplitude of the instrumental target		0.88				1.04

Table 5.2. Calibration statistics of (a) 9-year smoothed *bSi* flux with 9-year smoothed temperature data from Sils, indicating the calibration period, not cross-validated RMSEP, the amplitude predicted by the specific regression method, and RE comparing the MSE (mean squared error) between prediction and target on the entire instrumental period with the MSE of between the target and the mean temperature of the instrumental period, (b) similar to (a) but calibration of the band-pass filtered *bsi* flux and the band-pass filtered JJA temperature of Casty et al. (2005) (c) Calibration statistics of band-pass filtered data, indicating the calibration period, RMSEP during the calibration period, the amplitude in the calibration and in the verification period and RE and CE calculated as described in Cook et al. 1994. (d) Calibration of band-pass filtered data, calibration period 1852-1949.

the results from SMA and RMA regression for not trend-adjusted data (Mean RMA and SMA; Table 5.2).

Although in theory, the length and choice of the calibration period should be a random choice, in practice it is determined by the availability of instrumental data. The choice of the calibration period greatly influences the calibration statistics (Table 5.2). For instance, the reduction of the calibration period to 1874 - 1949 (instead of 1864 - 1949) results in large changes of the calibration statistics (data not shown).

According to Blass et al. (2007b) the long-term, non-climate trend in the bSi flux data series needs to be removed. We followed a purely statistical approach and applied a 9 - 100-years band pass filter on the raw annual bSi flux data to (i) account for varve counting errors (9 years low-pass) and (ii) to remove the long-term trend (100-year high-pass; Blass et al. 2007b). In consequence, the target and significance of the bSi-based temperature reconstruction were reduced exclusively to the decadal- and multi-decadal frequency domain of variability. The detrended temperature data are normally distributed for the period 1760 - 1949

and 1760 - 1851, they are differing from a normal distribution 1852 - 1949.

Fig. 5.6 a and b show the comparison of the bSi flux-based temperature reconstruction with two fully independent climate reconstructions: the climate field reconstruction for the Alpine Region back to AD 1500 (Casty et al., 2005) and a tree-ring based (late-wood density) temperature reconstruction for the Swiss Alps (Büntgen et al., 2006). The three data sets show a very good agreement both in the structure and the amplitude. Despite a considerable mismatch between AD 1530 and 1590, the correlation between the bSi record and the climate field reconstruction is highly significant and amounts to $r=0.45$, ($p_{\text{corr}}=0.0005$, period AD 1500 - 1950; $r=0.5$, $p_{\text{corr}}=0.0009$ for the period AD 1560 -1950). Comparing the bSi record with the late-wood density record from AD 1177 to 1530, we find a correlation of $r=0.54$ ($p_{\text{corr}}=0.01$). The 16th century, however, seems enigmatic: between AD 1500 and 1600 the agreement between tree-ring data, bSi data and the multi-proxy reconstruction is strikingly poor. After AD 1600, the accordance is again very good: between AD 1600 and 1950 the correlation between bSi and the tree-ring record amounts to $r=0.42$ ($p_{\text{corr}}=0.03$)

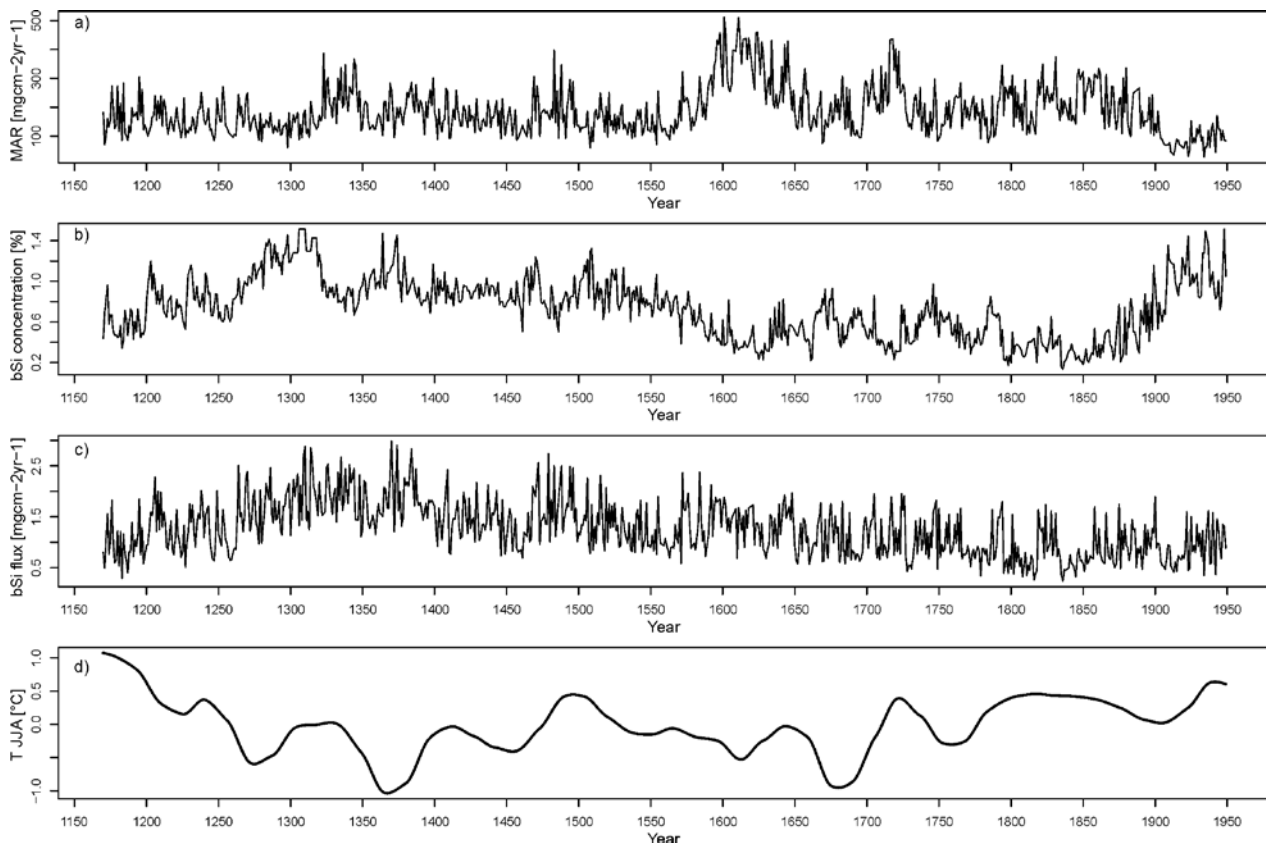


Fig. 5.5: showing the original data sets: a) Annually resolved mass accumulation rate (MAR); b) Annual biogenic silica concentration; c) Annual biogenic silica flux, and d) Low frequency (100-years low pass) component of the chironomid-inferred summer temperature (mean and variance adjusted to JJA temperatures)

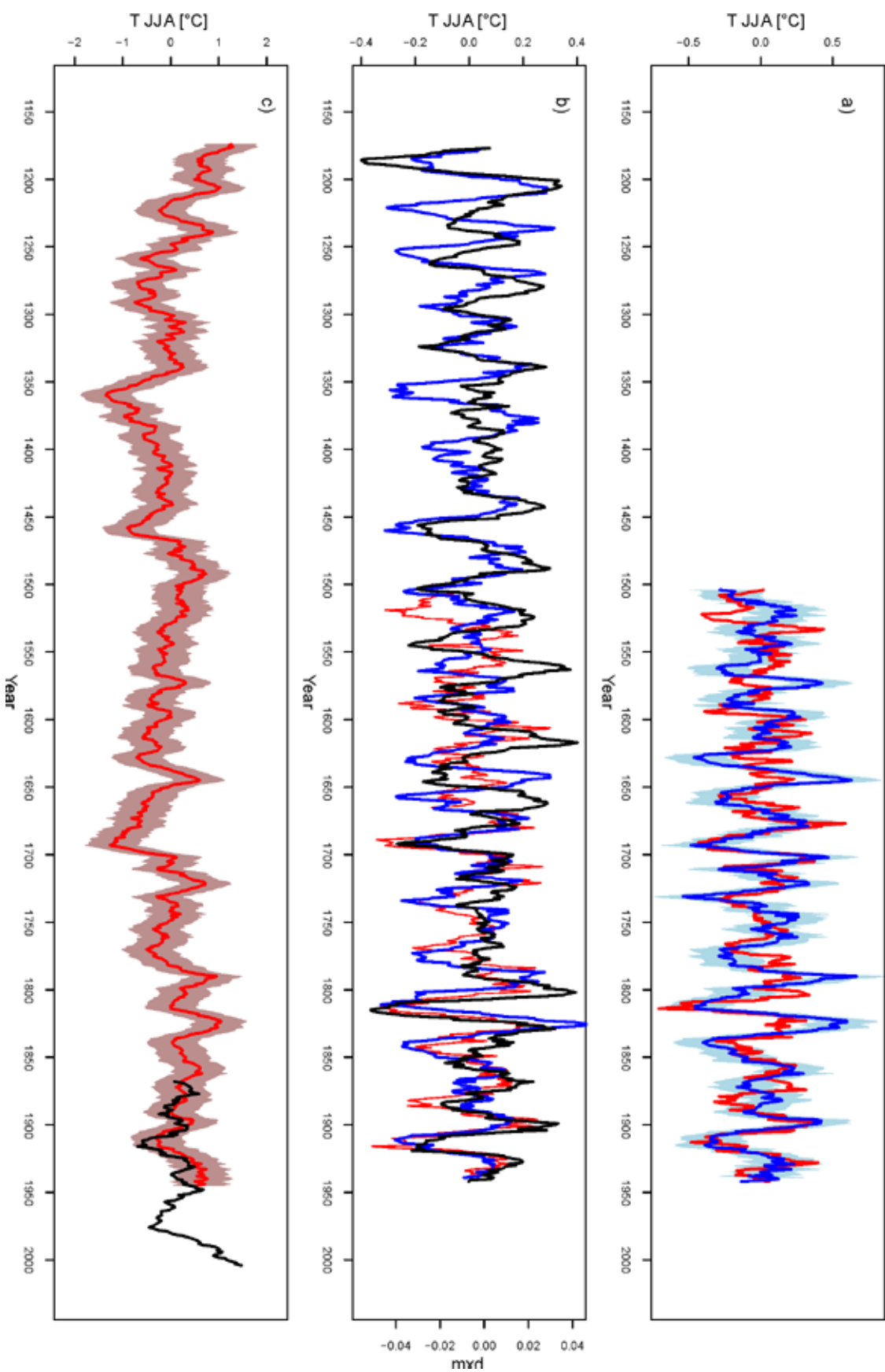


Fig. 5.6: (a) 100-year high-pass filtered and 9-year smoothed (9-100 years band-pass filtered) bSi flux-based temperature reconstruction AD 1500 – 1949 (blue, light blue indicating the RMSEP) and multi-proxy summer temperature reconstruction (red; Cas ty et al. 2005, data filtered in the same way). (b) 15-100 years band-pass filtered bSi temperature reconstruction AD 1177 – 1949 (blue), Cas ty et al. (2005) JJA temperature reconstruction (red) and tree ring based Alpine summer temperature reconstruction (Bür tgen et al. 2006) (black). (c) Combined chironomid and bSi flux-based summer temperature reconstruction (9-year running mean, red, light red indicating the uncertainty) and 9-year running mean of summer (JJA) temperature from adjacent station Sls Maria (black). All anomalies are given with respect to the period 1961 – 1990).

5.4.3. The combined temperature reconstruction

To reintegrate the low-frequency component of climate variability into our 9-100-year band-pass-filtered bSi record, we added the 100-year low-pass component of a chironomid-inferred summer temperature reconstruction from Lake Silvaplana (Fig. 5.5d, Larocque-Tobler et al. in review; bSi and chironomid data are from the same core). The combined record (Fig. 5.5c; 9-years smoothed) shows pronounced (multi)decadal-scale variability superposed with long-term trends: warm temperatures around AD 1200 are followed by a cooling with minima around AD 1260 and 1360. Afterwards, cold summers followed with a next minimum around AD 1460. The 16th century appears slightly warmer, particularly at the beginning. The 17th century exhibits two severe minima around AD 1630 and 1690; these were interrupted by a short warm interval around AD 1650. The 19th and 20th century show a long-term warming with pronounced warm decades around AD 1730, AD 1790 and 1830. The latter two warm decades were interrupted by a severe cold interval centred on AD 1815-1820. At decadal scale, the extremes are observed with highest values in the late 12th century and the lowest values in the late 14th and the late 17th century. The amplitude of the combined record over the past ca. 800 years (AD 1180 – 1949) is in the order of 2.6 °C.

The values reconstructed for the warmest pre-industrial decade of the past 800 years (i.e. in the late 12th century) are 0.6°C warmer than the values for the 1940.

5.5. Discussion

5.5.1. Calibration (model choice)

The six tested regression methods entail large differences in amplitude, RMSEP and RE statistics during the calibration period. Each of the method has its strengths and weaknesses and is, given the distribution and errors of the predictor and predictand, theoretically more or less adequate (Legendre and Legendre 1998). In theory, total least squares (TLS) regression would be the most appropriate method since it accounts for errors in x and in y (Venables and Ripley, 2002) The uncertainties of the instrumental data are, however, not known.

Inverse regression IR, the most commonly used regression, minimises the error of the predictand with the least squares method assuming an error-free predictor (the proxy). In our case study, this

assumption is obviously not valid and, therefore, IR is not a method of first-choice: according to Legendre and Legendre (1998) IR should not be applied when the uncertainty of x (here: the proxy) is much larger than the uncertainty of y (here: the temperature data).

IR is also known to underestimate the slope of the regression (parameter b ; Legendre and Legendre, 1998, Esper et al. 2005), which underestimates the amplitude of the target (here: temperature variability in the calibration and reconstruction). This is consistent with our results (Fig. 5.4). The advantage of inverse regression is the good RE and CE statistics. This is expected because the predicted values are dragged towards the mean value of the target to which they are compared calculating the RE and CE statistics (Cook et al. 1994).

Inverse Prediction IP would be the correct method since the proxy (y) is depending on temperature (x). However, IP enhances the slope of the regression (parameter b), and thus the amplitude (Sokal and Rohlf, 2001). This is in line with our results showing that IP does not perform well in reproducing climate variability during the calibration period. In light of the homogenisation problems with the meteorological data used (Begert et al. 2005) it remains also debatable to which extent the assumption is valid that temperature measurements (x) are error-free. IP yields poor RE and CE results; in summary, IP is not a good choice here.

The Generalised Least Squares regression GLS is a special inverse regression type (Venables and Ripley, 2002) and is, thereby also known to underestimate the slope of a regression and thus to underestimate the amplitude (Legendre and Legendre, 1998). Other than inverse regression, GLS regression allows the regression residuals to be autocorrelated, which further reduces the amplitude. Indeed, GLS regression produces a summer temperature reconstruction that exhibits almost no variability, which is not realistic.

Major Axis MA, Ranged Major Axis RMA and Standard Major Axis SMA regressions (Type II regressions) should be used if we can assume an identical and random error of both the predictor and the predictand (here: bSi and temperature) (Legendre and Legendre, 1998). MA regression should be used when both variables are expressed in the same units or are dimensionless, or when the variance of the random errors of both parameters is equal. This is consistent with our finding that MA regression is able to reproduce quite well the

amplitude of the detrended data (i.e. the residuals are transformed), whereas the amplitude is largely overestimated when the two variables are in their original form (raw data, not detrended), MA is however overestimating the amplitude for the calibration period where the data are not normally distributed. RMA regression should be used in this case. SMA regression (scaling, geometric mean regression) should be used if the ratio of the variance of the error and the variance of the measured data is similar for the two compared variables. RMA and SMA perform best regarding the amplitude for raw data and for the detrended data that are not normally distributed. For the raw data the difference between modelled and observed amplitudes is smaller than 0.13°C for the calibration period AD 1864 and 1949 (Table 5.2). Also the ratio RMSEP/Amplitude is small suggesting that the modelled amplitude (reconstructed temperature variability) is significant in the light of RMSEP. On the other hand, RMA and SMA do not perform best with regard to RE and CE statistics. For detrended data in two calibration periods MA performs best regarding the amplitude, in the third calibration period RMA and SMA again have the best performance.

Given the characteristics of sedimentary bSi flux as a warm season temperature proxy in Lake Silvaplana and the characteristics of instrumental meteorological data, our empirical findings about the advantages and disadvantages of the six calibration methods tested are consistent with theoretical considerations (Legendre and Legendre, 1998). Obviously there is a trade-off in the calibration methods choice between the RE/CE statistics and the correct assessment of the amplitude of the reconstruction (slope of the regression model). The method with the best performance in RE/CE statistics (IR) shows poor performance in modelling the amplitude. Thus the question arises: how can the quality of a calibration be evaluated? There are a number of different measures of “quality”: the RE and CE calibration statistics (Cook et al., 1994), smallest RMSEP (e.g. Kamenik et al., 2009), the ratio between the RMSEP and the amplitude (which indicates the proportion of uncertainty on the amplitude, e.g. Birks, 1998), or the ‘correct’ representation of the amplitude of the target variable (Legendre and Legendre, 1998). Assessing the ‘correct’ amplitude of climate change in the various frequency domains is arguably one of the prime challenges to detect forced and unforced variability. This is especially the case for the past millennium, when forcing factors are

relatively well documented (Jansen et al., 2007) and regional responses to perturbations may be investigated quantitatively (detection and attribution). In consequence, we place utmost care on the ‘correct’ amplitude of climate variability and favour for our summer temperature reconstruction (Fig. 5.6) Type II regressions, whereby MA performs best for the detrended data in the calibration period 1760 – 1949. Placing too much emphasis on good RE and CE statistics while neglecting the performance of the amplitude might result in problematic climate reconstructions.

5.5.2. Comparing the biogenic silica flux record with independent temperature reconstructions

The band-pass filtered bSi flux series, the multi-proxy reconstruction for the Alpine area of Casty et al. (2005; AD 1500 onwards) and the late-wood density MXD data of the Alpine summer temperature reconstruction (Büntgen et al. 2006) (Fig. 5.6a,b) show overall an excellent agreement among each other both in the structure and the amplitudes. All of the three data sets are fully independent. Agreement is expected since the distribution of summer temperatures in Central Europe and the Alps is mostly uniform (Fig. 5.1 inset map). The residuals, however, might be attributed to differential ecosystem responses to a specific combination of forcings or boundary conditions (e.g. drought), or to errors in the data sets. In the following, the three different time series are compared, and put into perspective of internal and forced variability as found in ensemble model simulations for European summers of the past 1000 years (Goosse et al., 2005, and references therein; forcings after Jansen et al., 2007).

The characteristic features of decadal-scale climate variability between AD 1500 and 1949 are consistently found in the three archives: the cold anomaly at the end of the 16th century (e.g. Dobrovolny et al., 2009; Glaser and Riemann, 2009) coincided with marked negative volcanic forcing; the very cold summers in the Late Maunder Minimum centred on AD 1690 (Glaser and Riemann, 2009) coincided with low solar irradiance and strong negative volcanic forcing; the same combination is found for the very pronounced cold spell during the Dalton Minimum and the negative volcanic forcing around 1815-20 (Tambora eruption). Negative temperature anomalies are found during the Damon solar minimum around 1910; the relatively warm phases in the middle of the 18th century (Glaser and Riemann, 2009) are also

well captured by all the three records.

Interesting is the disagreement among the three records in the 16th century. The cold anomaly centred on AD 1505 and the warm anomaly around AD 1525 are found in the tree ring and lake sediment data while the multi-proxy data (Casty et al., 2005) show an opposite structure. The cold decade around AD 1545 is found in the tree ring and multi-proxy series, while the sediments suggest a warming. All the three archives differ vastly until AD 1595 when they line up again during a cold anomaly with strong negative volcanic forcing. The 16th century was a period with broad absence of negative volcanic forcing and relatively low solar irradiance. We may speculate that the three archives responded with different sensitivities to this particular combination of forcings. The different behaviour of the tree ring record between 1635 and 1665 is also enigmatic, where both the sediment record and the multi-proxy record show consistent decadal trends and negative temperature anomalies coinciding with negative volcanic forcing peaking around AD 1630 and 1660. The multi-proxy and sediment records seem to respond more sensitively to volcanic forcing, at least during that period. The same accordance between the multi-proxy and the sediment records is found during the cold anomaly around 1775 but not recorded in the tree ring MXD data. The minor discrepancies between 1780 and 1810 were attributed to an anomalously high NAO index (Blass et al. 2007b) which influences temperatures during summer only in the Southern Alps (location of Lake Silvaplana). Another explanation might be overestimation of temperatures during the early instrumental period (Frank et al., 2007; Böhm et al., 2009).

The sediment record and the tree ring record provide insight into climate variability between AD 1177 and 1500. The temporal offset between both records (sediments lead the tree rings by 4 – 6 years) is likely attributable to varve counting errors since there is no stratigraphic flood marker in that section of the core that could help to constrain the sediment chronology in more detail (Fig. 5.2). On purpose we did not match the wiggles and keep both records fully independent. The recorded cold anomaly centred on AD 1453; is very well represented; the Kuwae eruption produced the third largest negative volcanic forcing of the past 1000 years (Jansen et al., 2007), which is accurately captured in the ensemble model simulations (Goosse et al., 2005). A very pronounced cooling is recorded after the volcanic eruption of AD 1256,

one of the two strongest negative forcings of the past 1000 years. A further negative temperature anomaly around 1220 is also attributable to volcanic forcing. It seems that all of the volcanic eruptions with major negative forcing are represented as pronounced short-lived pulses with negative summer temperature anomalies in the decadal-to multi-decadal-scale reconstructions suggesting that volcanic forcing is a major source of forced variability during summer in the (multi)decadal frequency band. This is consistent with model experiments (Goosse et al., 2005) and observations of composite temperature responses to volcanic forcing in Europe (Fischer et al., 2007).

Of particular interest is the massive and prolonged cooling recorded in the sediments around AD 1360 (Fig. 5.6b and c). This cooling is hardly visible in the tree ring series. Solar irradiance is around average and volcanic forcing is unimportant, and the model simulations show only an insignificant cooling (Goosse et al. 2005). However, this cooling is real, massive and regionally very well documented in the enormous and very rapid advances of the Great Aletsch and the Gorner Glacier to maximum Little Ice Age stages around AD 1370-90 (Holzhauser et al. 2005; the response lag of 2-3 decades to the initial cooling is characteristic for the glaciers). In the absence of sufficiently strong forcings, we consider a reduced Atlantic Meridional Overturning Circulation during that time (Bianchi and McCave 1999) as a possible explanation. Reduced AMOC leads to generally cool conditions in Europe, which is consistent with our observations but needs further investigation. We may speculate whether this phenomenon might be an expression of internal variability and serve as a case for stochastic resonance (Alley et al., 2001).

The combined summer temperature record of Lake Silvaplana (9-100 years band-pass biogenic Si and 100 years low-pass chironomid; Fig. 5.6c) shows strikingly similar characteristics in the multi-decadal and centennial variability domain compared with the tree-ring late-wood density inferred summer temperature series (Büntgen et al., 2006). The warmest decades superposed on the long-term centennial temperature trends, are found in both records around AD 1200 and in the late 20th century, whereas the coldest decades are observed around AD 1690, in the 17th century in general. The first decade of the 21st century are 0.2°C warmer than the warmest decade of the pre-industrial time for the past 800 years, which is not significant given the reconstruction

errors. The overall amplitude between the warmest and coldest decades during the past 800 years amounts to $\Delta 2.8^{\circ}\text{C}$ in both the Alpine tree ring (Büntgen et al. 2006) and the sediment records (this study). This amplitude at the regional scale is about at least two times larger than other hemispheric or global reconstructions (Jansen et al., 2007): for instance the 9-year smoothed Northern Hemispheric reconstruction by Moberg et al. (2005) suggests an amplitude of 1°C between 1177 and 1950 compared to 2.6°C in this study. Our results confirm the finding by Hunt (2004) suggesting that the amplitude of climate variability is much enhanced at the regional scale compared with hemispheric or global scales. This has, indeed, significant implications when impacts of climate change are concerned: natural and managed ecosystems experience enhanced variability of the local or regional climate.

5.6. Conclusions

In this study we present multi-decadal to sub-centennial biogenic silica (bSi)-inferred summer (JJA) and summer-autumn (JJASON) temperature reconstructions back to AD 1177. We combined the decadal-scale bSi record with the low-frequency component (100 years low-pass) of chironomid-inferred summer temperatures to produce a record that has defined skill in a broad spectrum of climate variability.

One of the most critical issues in past climate research and climate reconstructions is the correct assessment of amplitudes of climate variability. Here we tested systematically six different regression methods (Type I regressions: Inverse Prediction, Inverse Regression and General Least Squares; Type II regressions: Major Axis, Ranged Axis and Standard Major Axis). We used a number of indicators to assess the quality of the calibration: RE and CE statistics, the ratio RMSEP/Amplitude and the correct representation of the modeled amplitude compared with observed data. The six methods revealed very different results whereby those methods that show good skills in the RE and CE statistics (Type I regressions) perform very poorly with regard to the amplitude, and vice versa (Type II regressions). There seems to be a trade-off, and the optimum model choice depends on the objective of the research. Obviously the correct amplitude is the prime target for climate reconstructions; in our case, i.e. for band-pass filtered data, a regression model based on Major Axis regression performed best. We used this regression model for the climate reconstruc-

tion and conclude that a focus on RE and CE statistics alone might be myopic and eventually lead to problematic reconstructions.

Our sediment-based summer temperature reconstruction reveals very good agreement with two independent summer temperature reconstructions (multi-proxy reconstruction from Casty et al. (2005) and tree-ring inferred Alpine temperatures from Büntgen et al. (2006)) both in the structure and the amplitudes. We found that all the major episodes of negative volcanic forcing are represented in negative summer temperature anomalies. This is particularly pronounced in periods when negative volcanic forcing coincides with low solar irradiance as e.g. during the Maunder Minimum around AD 1690, the Spörer Minimum around AD 1450, and possibly at the very end of the Wolf Minimum around AD 1360. Volcanic forcing seems to be a major source of summer temperature variability in the decadal-scale frequency band.

The period around AD 1360 appears to be a very interesting phase with strongly negative summer temperature departures during a time when negative solar and volcanic forcings are absent, and the tree-ring temperature series does not show a major cooling. This negative summer temperature anomaly found in the lake sediments, however, is real and well documented in massive glacier advances in the Alpine area. In a first approximation, we consider internal variability related to North Atlantic SSTs as a possible explanation. To our knowledge a systematic investigation of that phenomenon remains to be carried out.

We find also periods of disagreement and inconsistencies among the three archives considered here. These inconsistencies may help to identify uncertainties and errors in the data sets (e.g. response lags due to chronological uncertainties in the varve counting) or differential responses and memory effects of the ecosystems to a certain combination of forcings. The prime target to study such effects seems to be the 16th century, when the three reconstructions differ markedly from each other.

The warmest and coldest decades of the past 800 years coincide in the sediment record and the tree-ring record, showing that the decadal-scale variability superposed on the centennial-scale variability is robust. The current decades are only slightly warmer (ca. 0.2°C) than the warmest pre-industrial decade since AD 1180. Warm season temperature amplitudes between the warmest and the coldest decades amount to $\Delta 3^{\circ}\text{C}$ over that

period in both records, which is very large compared with hemispheric or global reconstructions of temperature variability. These large temperature amplitudes at regional scale are particularly significant when impacts of climate change are considered.

5.7. Acknowledgements

We would like to thank Thomas Kulbe for his help during field work. We are grateful to Daniela Fischer, Philipp Grob and Silvia Köchli for their help with laboratory work, and to Christian Pfister for discussion on floods in the Medieval period. We acknowledge Jörg Leuenberger, Karl Schroff and Gerhard Furrer for making the freeze laboratory at ETH Zürich available. We are grateful to Christian Kamenik for discussion on statistics. Project grants were provided by European Union FP6 project "Millennium" (Contract 017008), NF-200021-106005/1 'ENLARGE' the NCCR Climate and the MHV NSF grant to I. Larocque-Tobler.

5.8. References

- Alley, R.B., Anandakrishnan, S., Jung, P., 2001. Stochastic resonance in the North Atlantic. *Paleoceanography* 16, 190–198.
- Bahrenberg, G., Giese, E., Nipper, J., 1999. *Statistische Methoden in der Geographie*, fourth ed. Teubner, Stuttgart.
- Begert, M., Schlegel, T., Kirchhofer, W., 2005. Homogeneous temperature and precipitation series of Switzerland from 1864 to 2000. *International Journal of Climatology* 25, 65–80.
- Berner R.A., 1971. *Principles of chemical sedimentology*, McGraw-Hill Book Company, New York.
- Besonen, M., Patridge, W., Bradley, R., Francus, P., Stoner, J., Abbott, M., 2008. A record of climate over the last millennium based on varved lake sediments from the Canadian High Arctic. *The Holocene* 18, 169–180.
- Bianchi, G.G., and McCave, I.N., 1999. Holocene periodicity in North Atlantic climate and deep-ocean flow south of Island. *Nature* 397, 515–517.
- Bigler, C., von Gunten, L., Lotter, A. F., Hausmann, S., Blass, A., Ohlendorf, C., Sturm, M., 2007. Quantifying human-induced eutrophication in Swiss mountain lakes since AD 1800 using diatoms. *The Holocene* 17, 1141–1154.
- Birks, H.J.B., 1998. Numerical tools in palaeolimnology: progress, potentials, and problems. *Journal of Paleolimnology* 20, 307–332.
- Blass, A., Grosjean, M., Troxler, A., Sturm, M., 2007a. How stable are twentieth-century calibration models? A high-resolution summer temperature reconstruction for the eastern Swiss Alps back to AD 1580 derived from proglacial varved sediments. *The Holocene* 17, 51–63.
- Blass, A., Bigler, C., Grosjean, M., Sturm M., 2007b., Decadal-scale autumn temperature reconstruction back to AD 1580 inferred from the varved sediments of Lake Silvaplana (southeastern Swiss Alps). *Quaternary Research* 68, 184–195.
- Böhm, R., Jones, P.D., Hiebl, J., Brunetti, M., Frank, D., Maugeri, M., 2009. The early instrumental warm bias: A solution for long central European temperatures series 1760- 2007. *Climatic Change* (in press).
- Bradley, R.S., Hughes, M.K., Diaz, H.F., 2003. Climate in Medieval Time. *Science* 302.
- Brunetti, M., Maugeri, M., Nanni, T., Auer, I., Böhm, R., Schöner, W., 2006. Precipitation variability and changes in the greater Alpine region over the 1800–2003 period. *Journal of Geophysical Research* 111, D11107.
- Büntgen U., Frank, D.C., Nievergelt D., Esper J., 2006. Summer Temperature Variations in the European Alps, A.D. 755–2004. *Journal of Climate* 19, 5606–5623.
- Bürger, G., Fast, I., Cubasch, U., 2006. Climate reconstruction by regression - 32 variations on a theme. *Tellus series a – dynamic meteorology and oceanography* 58, 227–235.
- Casty, C., Wanner, H., Luterbacher, J., Esper, J., Boehm, R., 2005. Temperature and precipitation variability in the European Alps since AD 1500. *International Journal of Climatology* 25, 1855–1880.
- Caviezel, G., 2007. Hochwasser und ihre Bewältigung anhand des Beispiels Oberengadin 1750 – 1900. MSc thesis . University of Berne.
- Cleveland, W.S., Devlin, S.J., 1988. Locally Weighted Regression: an Approach to Regressi-

- on Analysis by Local Fitting. *Journal of the American Statistical Association* 83, 596–610.
- Cook, E.R., Briffa, K.R., Jones, P.D., 1994. Spatial regression methods in dendroclimatology: A review and comparison of two techniques. *International Journal of Climatology* 14, 379–402.
- Dawdy, D. R., Matalas N.C., 1964. Statistical and probability analysis of hydrologic data, part III: Analysis of variance, covariance and time series, In: Chow, V.T., (Ed.), *Handbook of Applied Hydrology, a Compendium of Water-Resources Technology*. McGraw-Hill, New York, pp. 8.68-8.90.
- Dobrovolny, P., Moberg, A., Brazdil, R., Pfister, C., Glaser, R., Wilson, R., van Engelen, A., Limanowka, D., Kiss, A., Halickova, M., Mackova, J., Riemann, D., Luterbacher, J., Böhm, R., 2009. Monthly and seasonal temperature reconstructions for Central Europe derived from documentary evidence and instrumental records since AD 1500. *Climatic Change* (in press).
- Esper, J., Frank, D.C., Wilson, R.J.S., Briffa, K.R., 2005. Effect of scaling and regression on reconstructed temperature amplitude for the past millennium. *Geophysical Research Letters*, L07711.
- Fischer, E., Luterbacher, J., Zorita, E., Tett, S.F.B., Casty, C., Wanner, H., 2007. European climate response to tropical volcanic eruptions over the last half millennium. *Geophysical Research Letters* 34, L05707.
- Francus, P., Bradley, R. S., Abbott, M.B., Patridge, W., Keimig, F., 2002. Paleoclimate studies of minerogenic sediments using annually resolved textural parameters. *Geophysical Research Letters* 29, GL015082.
- Frank, D., Büntgen, U., Böhm, R., Maugeri, M., Esper, J., 2007. Warmer early instrumental measurements versus colder reconstructed temperatures: shooting at a moving target. *Quaternary Science Reviews* 26, 3298–3310.
- Geirsdóttir, Á., Miller, G., Thordarson, T., Ólafsdóttir, K., 2009. A 2000 year record of climate variations reconstructed from Haukadalsvatn, West Iceland. *Journal of Paleolimnology* 41, 95–115.
- Glaser R., Riemann D., 2009. A thousand-year record of temperature variations for Germany and Central Europe based on documentary data. *Journal of Quaternary Science* 24, 437–449.
- Gobet E., Hochuli, P.A., Ammann, B., Tinner, W., 2004. Vom Urwald zur Kulturlandschaft des Oberengadins. *Vegetationsgeschichte der letzten 6200 Jahre. Jahrbuch der Schweizerischen Gesellschaft für Ur- und Frühgeschichte* 87, 255–270.
- Goslar, T., Van der Knaap, W.O., Kamenik, C., Van Leeuwen, J.F.N., 2009. Age-depth modelling of an intensively dated modern peat profile. *Journal of Quaternary Science* 24, 481–499.
- Goosse, H., Renssen, H., Timmerman, A., Bradley, R.S. 2005. Internal and forced climate variability during the last millennium: a model-data comparison using ensemble simulations. *Quaternary Science Reviews* 24, 1345–1360.
- Heiri, O., Lotter, A.F., Hausmann S., Kienast F., 2003. A chironomid-based Holocene summer air temperature reconstruction from the Swiss Alps. *The Holocene* 13, 477–484.
- Hunt B.G., 2004. The stationarity of global mean climate. *International Journal of Climatology* 24, 795–806.
- Jansen E., et al. 2007. Palaeoclimate. In: *Climate Change 2007: The Physical Science Basis. Contribution of Working Group I to the Fourth Assessment Report of the Intergovernmental Panel on Climate Change*. In: Solomon, S., Qin, D., Manning, M., Chen, Z., Marquis, M., Averyt, K.B., Tignor M., Miller H.L., (Eds.), Cambridge University Press, Cambridge. pp. 435 – 498.
- Kalugin, I., Daryin, A., Smolyaninova, L., Andreev, A., Diekmann, B., Khlystov, O., 2007. 800-yr-long records of annual air temperature and precipitation over southern Siberia inferred from Teletskoye Lake sediments. *Quaternary Research* 67, 400–410.
- Kamenik, C., Van der Knaap, W.O., Van Leeuwen, J.F.N., Goslar, T., 2009. Pollen/climate calibration based on a near-annual peat sequence from the Swiss Alps. *Journal of Quaternary Science* 24, 529–546.
- Kaufman, D. S., Schneider, D.P., McKay, N.P., Ammann, C.M., Bradley, R.S., Briffa, K.R., Miller, G.H., Otto-Bliesner, B.L., Overpeck, J.T., Vinther,

- B.M., 2009. Recent Warming Reverses Long-Term Arctic Cooling. *Science* 325, 1236–1239.
- Larocque-Tobler I., Grosjean, M., Heiri, O., Trachsel, M., Kamenik, C., (in review) 1000 years of climate change reconstructed from chironomid subfossils preserved in varved-lake Silvaplana, Engadine, Switzerland. *Quaternary Science Reviews*.
- Leemann, A., Niessen, F., 1994. Holocene glacial activity and climatic variations in the Swiss Alps: reconstructing a continuous record from proglacial lake sediments. *The Holocene* 4, 259–268.
- Legendre, P. and Legendre, L., 1998. *Numerical ecology*, second ed. Elsevier, Amsterdam.
- Livingstone, D.M., 1997. Break-up dates of alpine lakes as proxy data for local and regional mean surface air temperatures. *Climatic Change* 37, 407–439.
- McKay, N.P., Kaufman, D.S., Michelutti, N., 2008. Biogenic silica concentration as a high-resolution, quantitative temperature proxy at Hallet Lake, south-central Alaska. *Geophysical Research Letters*, L05709.
- Moberg, A., Sonechkin, D.M., Holmgren, K., Datsenko, N.M., Karlen, W., 2005. Highly variable Northern Hemisphere temperatures reconstructed from low- and high-resolution proxy data. *Nature* 433, 613–617.
- Mortlock, R., Froelich, P., 1989. A simple method for the rapid determination of biogenic opal in pelagic marine sediments. *Deep-Sea Research* 36, 1415–1426.
- Niessen, F., Wick, L., Bonani, G., Chondrogiani, C., Siegenthaler, C., 1992. Aquatic system response to climatic and human changes—Productivity, bottom water oxygen status, and sapropel formation in Lake Lugano over the last 10,000 years. *Aquatic Sciences* 54, 257–276.
- Ohlendorf, C., Sturm, M., 2007. A modified method for biogenic silica determination. *Journal of Paleolimnology* 39, 137–142.
- Ohlendorf, C., Niessen, F., Weissert, H., 1997. Glacial varve thickness and 127 years of instrumental climate data: a comparison. *Climatic Change* 36, 391–411.
- Ohlendorf, C., 1998. High Alpine Lake Sediments as Chronicles for Regional Glacier and Climate History in the Upper Engadine, Southeastern Switzerland. PhD thesis. ETH Zürich, Zürich.
- Riedwyl, N., Luterbacher, J., Wanner, H., 2008. An ensemble of European summer and winter temperature reconstructions back to 1500. *Geophysical Research Letters*, L20707.
- SMA, 2002. Jahresbericht der Meteo Schweiz. *Annalen der Meteo Schweiz*.
- Sokal, R.R., Rohlf F.J., 2001. *Biometry the Principles and Practice of Statistics in Biological Research*, third ed. W. H. Freeman, New York.
- Sturm, M., Lotter, A.F., 1995. Lake sediments as environmental archives. *EAWAG News* 38E, 6–9.
- Sturm, M., Matter, A., 1978. Turbidites and varves in Lake Brienz (Switzerland): deposition of clastic detritus by density currents. In: Matter, A., Tucker, M. (Eds.), *Modern and ancient lake sediments*. Blackwell Scientific Publications, Bern, pp. 147–168.
- Trachsel, M., Eggenberger, U., Grosjean, M., Blass, A., Sturm, M., 2008. Mineralogy-based quantitative precipitation and temperature reconstructions from annually laminated lake sediments (Swiss Alps) since AD 1580. *Geophysical Research Letters* 35.
- Trenberth, K.E., 1984. Some Effects of Finite Sample Size and Persistence on Meteorological Statistics. Part I: Autocorrelations. *Monthly Weather Review* 112, 2359–2368.
- Venables, W.N., Ripley, B., 2002. *Modern Applied Statistics with S*, fourth ed. Springer, New York.
- Von Gunten, L., Grosjean, M., Beer, J., Grob, P., Morales, A., Urrutia R., 2009. Age modeling of young non-varved lake sediments: methods and limits. Examples from two lakes in Central Chile. *Journal of Paleolimnology* 42, 401–412.
- Zolitschka, B., Brauer, A., Negendank, J.F.W., Stockhausen, H., Lang, A., 2000. Annually dated late Weichselian continental paleoclimate record from the Eifel, Germany. *Geology* 28, 783–786.

Chapter 6



6. Is interannual temperature variability related to the mean temperature? Evidence from instrumental, early instrumental and proxy data in Europe since 1600 AD.

Mathias Trachsel, Pascal Hänggi and Martin Grosjean

Oeschger Center for Climate Change Research and Institute of Geography, University of Bern, Erlachstrasse 9a T3, 3012 Bern, Switzerland

In revision with *Climate Dynamics*

Abstract

Climate models project there will be an increase in the interannual variability of European summer temperatures as a consequence of warmer temperatures in the 21st century. This increase in variability has been attributed to an enhanced soil moisture-atmosphere feedback. An increase in variability would have significant impacts on climate extremes.

Here, we assess whether a relationship between the ‘mean’ and ‘variability’ of temperatures in Europe has existed in the past. Using the non-parametric measure of the first two L-moments (‘mean’ and ‘variability’), we investigate the climatology of interannual temperature variability in instrumental (1864–2007) and early instrumental (1760–1864) data in Europe. This period covers the cooler ‘Little Ice Age’ and the warming of the 20th century.

Only a few instrumental temperatures series show significant negative (mostly winter, sometimes autumn) or positive correlations between ‘mean’ and ‘variability’ since 1864 (referred to as ‘Mean versus Variability Change’ (MVC) of temperatures). These correlations are, not temporally stable, but are spatially coherent over synoptic-scale regions of Europe. The spatio-temporal evolution of MVC behaviour is consistent with changes in the relative frequency of predominant circulation modes in Europe.

Exploring the potential to extend the record back to AD 1000, we investigate whether the MVC behaviour of temperatures can be assessed using annually resolved tree-ring and lake-sediment proxy data. Out of the six investigated data series, only one tree-ring series showed a similar MVC behaviour as local instrumental data. It appears that the proxy series used do not sufficiently well record (i) seasonal extremes (‘variability’) and/or (ii) centennial-scale trends (‘mean’).

6.1. Introduction

Climate models predict there will be an increase in mean temperature for the current century. More importantly and particularly for summers, recent studies also suggest an increase in interannual variability (IPCC 2007; Schär et al. 2004; Seneviratne et al. 2006), which leads to a wider spread in the probability density functions (PDF) of summer temperatures. These changes in interannual variability are expected to have a much larger impact on ecosystems and society than the changes in mean temperature: adapting to very variable conditions with more frequent extremes is more difficult than adapting to increasing, but constant mean values (Seneviratne et al. 2006).

The concern about increasing interannual and intraseasonal variability and extremes of current and future European temperatures has stimulated a number of investigations. Scherrer et al. (2005) assessed PDF changes of European temperatures AD 1960–2004 and a set of IPCC scenarios, while Schär et al. (2004) and Seneviratne et al. (2006) examined future conditions for the 21st century using General Circulation Model (GCM) and Regional Climate Model (RCM) simulation data. They found a consistently significant increase in summer temperature variability in a warmer climate, which they attributed to an increase in the soil moisture–atmosphere feedback; Europe appears to be as the global hotspot for increasing warm-season temperature variability. The increase in variability with increasing mean summer temperatures has also been found at intraseasonal scales and daily maximum temperatures over the instrumental period (Della-Marta et al. 2007; Yiou et al. 2009). Also, Beniston (2009) discovered an increase in the frequency of warm/dry periods from 1901 to 2007.

Theoretical considerations and RCM experiments provide insight into the underlying mechanisms (e.g. Schär et al. 2004; Seneviratne et al. 2006; Fischer et al. 2007). The increasing variability of

summer temperatures is mainly attributed to rapid and non-linear increases in the Bowen ratio when, beyond a certain threshold of soil moisture depletion, the energy at the land surface is mainly transformed into sensible heat, which in turn warms up the regional atmosphere (i.e. the soil moisture–atmosphere feedback). Consequently, the highest interannual variability would be expected in a climate where the soil moisture–atmosphere feedback takes place every second summer on average (at a probability of 0.5). We hypothesise that the interannual summer temperature variability would be relatively small in a wetter (and cooler) or very dry (and very warm) climate when this feedback only takes place very rarely (all summers are cool) or very often (all summers are hot). In contrast to summer (convective processes) winter climate is mainly dominated by advective processes. Therefore winter climate variability is expected to be driven by large-scale circulation modes such as Westerly flow patterns or Russian high pressure systems.

Or more generally speaking, is variability among temperature series in Europe related to multi-decadal or even centennial-scale climate variability?

Here, we test this hypothesis using long instrumental temperature series (from 1659, 1760 and 1864 onwards) distributed across Central Europe. These records extend back to the Little Ice Age, thus covering a broad temperature range. We ask the following questions: (i) how does the interannual summer temperature variability during the Little Ice Age compare to the variability during the 20th century and the associated strong warming trend? (ii) How were the other seasons different? (iii) Are the observed changes in the interannual temperature variability of the different seasons related to the climatology and occurrence of synoptic-scale circulation types? (iv) Can natural proxies such as tree rings and annually laminated lakes sediments provide adequate information to address these questions? If yes, this would allow us to test the model projections for the end of the 21st century with proxy data extending back to the best warm analogues during the Medieval Warm Period or even the Roman Time.

6.2. Data and Methods

In this study, we assess changes in the PDF of 30-year running windows (climatology) for instrumental temperature data (seasonally resolved) and proxy data that are specifically sensitive to the warm season and are annually resolved. We

describe the PDF of 30-year running windows, calculating the first two moments (L-location and L-scale, synonymous to ‘mean’ and ‘variability’ respectively) of the PDF. As suggested by Del-la-Marta et al. (2007) PDF parameters were assessed using L-moments (Hosking 1990) which, in contrast to product-moments, do not assume normality, are non-parametric and, therefore, more robust. This is in line with Zhang et al. (2008) who argued that the soil moisture feedback enhances the warm extremes rather than the cold extremes, which leads to skewed PDFs (i.e. it is not normally distributed).

We eliminate trend-induced enhancement of variability (Räsänen 2002), applying segment-wise detrending according to Scherrer et al. (2005). Similar to Scherrer et al. (2005) and Scherrer et al. (2006) we standardised the mean and the variability of the floating climatologies (30-year windows) to the mean and the variability of the 1961 to 1990 reference period. The sensitivity of the mean and the variability of the 1961 to 1990 reference period to singular values (extreme values) was assessed using a bootstrap resampling with replacement. The 90% confidence interval of 5000 bootstrap replicates was used to determine PDFs differing significantly from the 1961 to 1990 standard period. The results (Figs. 6.2&6.3) are presented in Mean versus Variability Change plots (MVC plots, Scherrer et al. 2005).

After computing the first two L-moments we assessed connections between ‘mean’ and ‘variability’ by calculating Spearman’s rank correlation. The degrees of freedom of the autocorrelated time series were corrected according to Dawdy and Matalas (1964).

Fifty-year running correlations were calculated to assess the stability of the correlations between ‘mean’ and ‘variability’. The year indicated (e.g. in Fig. 6.4) is the central value of the investigated period (e.g. 1925 reflects the correlation of the data series 1901 to 1950).

We assessed the connection between the proxy data and the instrumental data by correlating (Spearman) the ‘mean’ (‘variability’) of the 30-year running windows of the proxy data with the ‘mean’ (‘variability’) of the 30-year running windows of the nearby instrumental series. Thus, the positions of the individual data points on the x-axis (y-axis) in the MVC-plots were compared. When comparing proxy and instrumental data we distinguish between the correlation in the ‘mean’ and the correlation in the ‘variability’.

The dataset used for this study includes 10 homo-

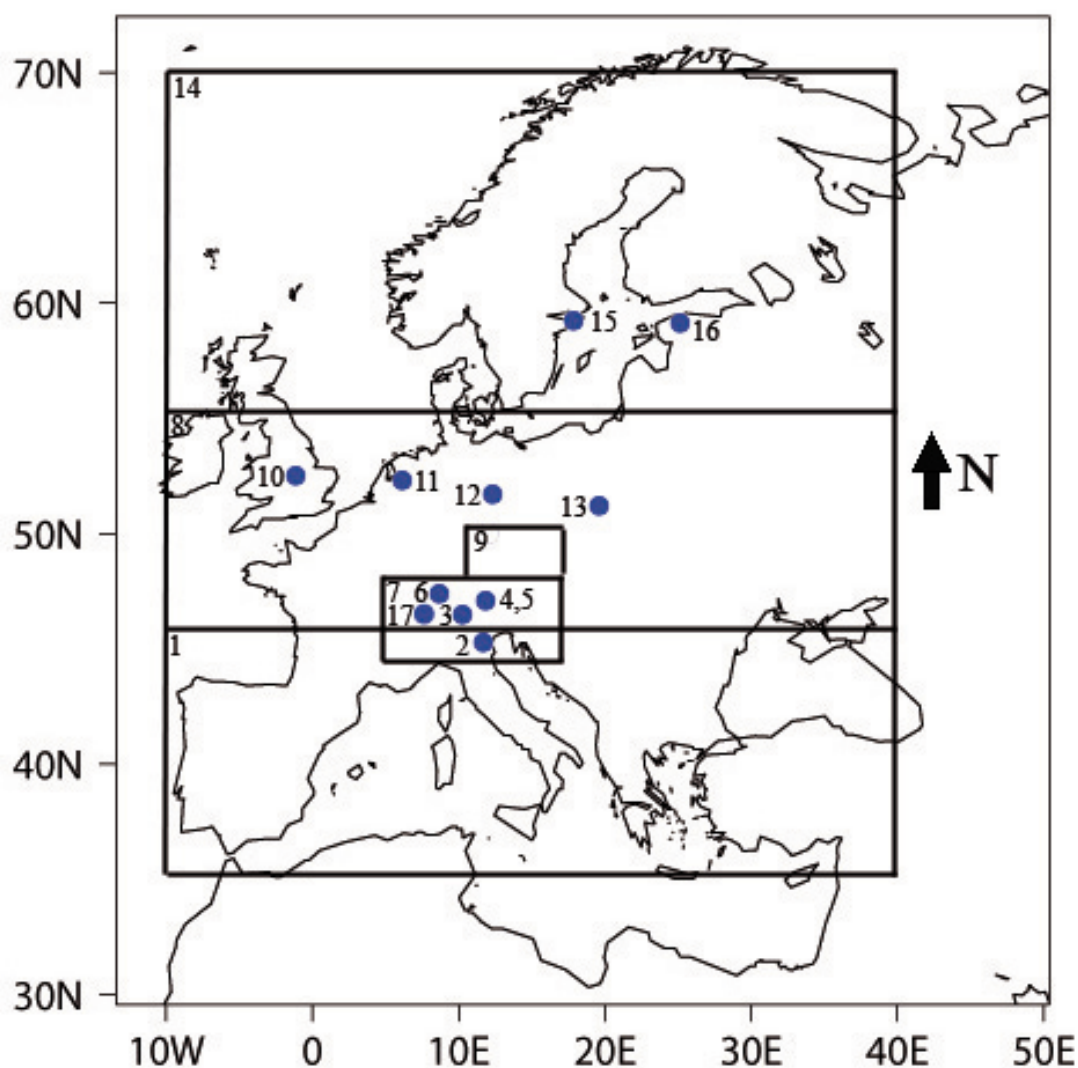


Fig. 6.1. Spatial distribution of the meteorological data series used in this study: 1 Mediterranean (35° – 45° N; 10° W– 40° E), 2 Padova, 3 Southern Alps (Lugano), 4 Central Alps (Sils Maria), 5 Central Alps–AUER (46° N, 9° E, Auer et al. 2007), 6 Northern Alps (mean of Basel, Bern, Geneva and Zurich), 7 Alps–CASTY (Casty et al. 2005), 8 Central Europe (45° – 55° N; 10° W– 40° E), 9 Central Europe–Dobrovolny (Dobrovolny et al. 2009), 10 Central England, 11 de Bilt, 12 Berlin, 13 Warsaw, 14 Northern Europe (55° – 70° N; 10° W– 40° E), 15 Tallinn, 16 Stockholm, 17 mxd (late-wood density) Swiss Alps (Büntgen et al. 2006), 18 trw (tree-ring width) Swiss Alps (Büntgen et al. 2005), 19 trw (tree ring width) Greater Alpine Region (Frank and Esper 2005; corresponding with Nr 7), 20 mxd (late-wood density) Greater Alpine Region (Frank and Esper 2005; corresponding with Nr 7), 21 Qz/Mi (Quartz/Mica) Central Alps (Lake Silvaplana, Trachsel et al. 2008; corresponding with 4), 22 bSi (biogenic silica flux) Central Alps (Lake Silvaplana, Blass et al. 2007; corresponding with 4).

genised instrumental time series, a composite of early instrumental measurements and three gridded temperature reconstructions (Fig 6.1., Table 6.1) The stations were selected in areas that are expected to respond most sensitively to summer temperature variability (Seneviratne et al. 2006). Furthermore, we investigated six natural proxy data series that are sensitive to warm-season temperatures. The tree-ring width series for the Swiss Alps (trw Swiss Alps) correlates best with JJA temperatures (Büntgen et al. 2005). The late-wood density series from the same area (mxd Swiss Alps) correlates best with JJAS temperatures (Büntgen et al. 2006), while the series covering the entire Alpine region (Frank and Esper 2005; here: Gre-

ater Alpine Region GAR) correlates with JJA temperatures (tree ring width, trw GAR) and AMJJAS temperature (late-wood density, mxd GAR). The two proxy series from annually laminated Lake Silvaplana, Eastern Swiss Alps AD 1580-1940 are biogenic silica flux (bSi Central Alps; correlates with SON, JJA and JJASON temperatures; Blass et al. 2007) and the XRD peak intensity ratio of quartz to mica (Qz/Mi Central Alps) in individual varves is negatively correlated with MJJAS temperatures (Trachsel et al. 2008). Both data series end in the first half of the 20th century (bSi Central Alps 1949; Qz/Mi Central Alps 1920). Thus, the comparison between proxy data and instrumental data spans from 1864 to 1920/1949.

Full Name	Location	Starting Year	Ending Year	Reference
Mediterranean	35° N - 45° N; 10° W - 40° E	1760	2000	Luterbacher et al. 2004;
Padova	45° 24' N; 11° 52' E	1774	1990	Xoplaki et al. 2005 Küttel 2009
Southern Alps	46° N; 8° 57' E	1864	2008	Begert et al 2005
Central Alps	46°26' N; 9°45' E	1864	2008	Begert et al 2005
Central Alps-AUER	46° N, 9°30' E	1760	2003	Auer et al. 2007
Northern Alps	47° N; 7°30' E	1864	2008	Begert et al. 2005
Alps-CASTY	43° N - 48° N; 4° E - 16° E	1760	2000	Casty et al. 2005 Luterbacher et al. 2004;
Central Europe-Dobrovolny	46° N - 50° N; 6° E - 16° E	1760	2007	Xoplaki et al. 2005 Dobrovolny et al. (in press);
Central Europe	45° N - 55° N; 10° W - 40° E	1760	2000	Luterbacher et al. 2009.
Central England	52° N; 0° E	1659	2008	Manley 1974
de Bilt	52°7' N; 5°11' E	1760	2007	Küttel 2009
Berlin	52°31' N; 13°24' E	1760	2007	Küttel 2009
Warsaw	52°13' N; 21°E	1779	2007	Küttel 2009 Luterbacher et al. 2004;
Northern Europe	55° N - 70° N; 10° W - 40° E	1760	2000	Xoplaki et al. 2005
Tallinn	59°25' N; 24°46' E	1760	2007	Küttel 2009
Stockholm	59°20' N; 18° E	1760	2007	Küttel 2009

Table 6.1: List of the 16 investigated instrumental (or climate field) data sets

6.3. Results

First we discuss the correlations between ‘mean’ and ‘variability’ of seasonal and annual temperatures for the entire instrumental period (1864-2007/2000). Then we assess whether natural climate proxies are suitable for reconstructing past changes in temperature PDFs. Next we investigate the temporal stability of the connections between ‘mean’ and ‘variability’ using 50-year running correlations for the early-instrumental and the instrumental period, and finally we investigate potential regional patterns.

6.3.1. Instrumental data 1864-2007/2000

Out of the 80 time series analyzed (of which 16 temperature series were analyzed for the four seasons and the annual mean), 12 series show correlations ($p_{\text{corr}} < 0.1$) between the ‘mean’ and the ‘variability’ (30-year moving windows) over the entire instrumental period (Table 6.2 and Fig. 6.2): six for winter (DJF), four for autumn (SON), one for spring (MAM) and one for mean annual temperature.

The DJF Southern Alps and the DJF Mediterranean time series show a significant decrease of the ‘variability’ ($-0.7 \cdot s_0$, $-0.5 \cdot s_0$ respectively) with increasing temperatures ($3.5 \cdot s_0$, $2.5 \cdot s_0$ respectively). In the Central Alps–AUER, winter temperature variability is only greater than in the reference period (exceeding s_0 confidence bounds) for a short period during the beginning of the 20th century. In two of the winter (DJF) time series (Central Alps and Alps–CASTY) and the SON Northern Europe series, the computed ‘variability’ does not exceed the confidence bound of the 1961-1990 reference

period for ‘variability’ (Fig. 6.2). The autumn SON Northern Alpine and the autumn SON Southern Alpine series show a decrease in variability ($-0.6 \cdot s_0$) with warmer mean temperatures ($3.5 \cdot s_0$).

Tallinn spring temperatures constantly show very high variability until the middle of the 20th century, followed by a rapid decrease in the variability ($-0.3 \cdot s_0$), which coincides with warmer mean temperatures ($3 \cdot s_0$). Increasing variability ($0.4 \cdot s_0$) in a warming mean climate ($1.5 \cdot s_0$) is found for Central European annual temperatures.

Increasing variability in a climate with warmer summers is not conclusive from the time series over the entire instrumental period from 1864 to 2007. The three Swiss series (Northern, Central and Southern Alps) and the Alps–CASTY data show two phases with high variability: around 1910 and the second half of the 1940s. Both phases are, however, not phases with particularly warm mean summer temperatures. Also, the record hot summer of 2003 leads to an increase in variability, but the variability of this period does not exceed the confidence bounds of the reference period 1961-1990. Similar results are found for the larger European regions (Northern and Central Europe, Mediterranean): there is no significant ($p_{\text{corr}} > 0.1$) change in summer temperature variability compared to the 1961-1990 reference period throughout the entire instrumental period (1864-2007). Although Warsaw and Berlin record the highest variability synchronously with the highest mean values, ‘mean’ and ‘variability’ for the summer temperatures is not correlated ($p_{\text{corr}} < 0.1$) for both stations.

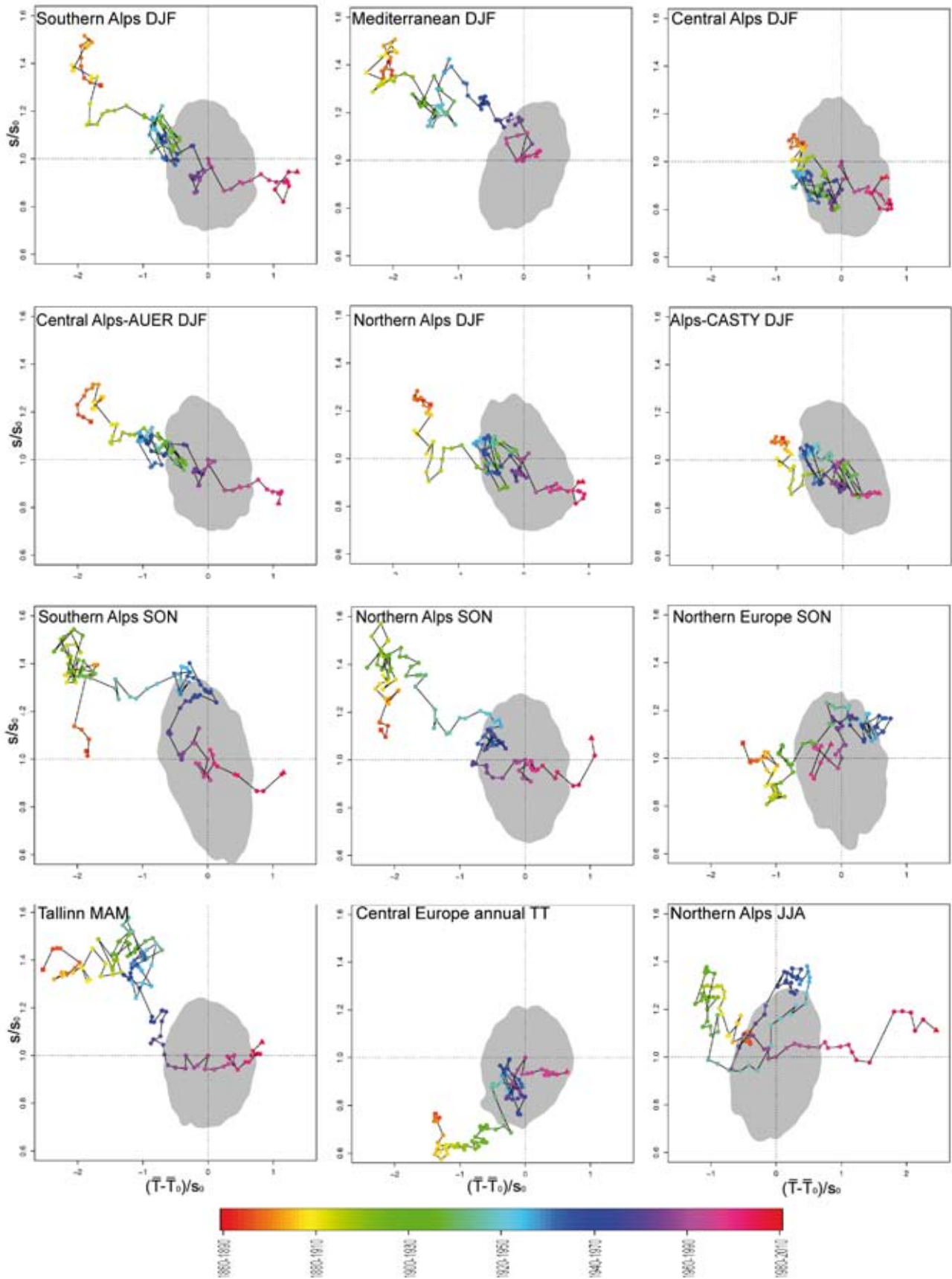


Fig. 6.2. Mean and Variability Change (MVC) plots of the time series with a correlation between 'mean' and 'variability' ($\rho_{corr} < 0.1$). In addition the MVC plot of summer temperatures of the Northern Alps is displayed. The grey shaded area indicates the 90% confidence range of the 1961-1990 standard period.

	DJF		MAM		JJA		SON		Annual	
	r	p	r	p	r	p	r	p	r	p
Mediterranean	-0.81	0.02	0.56	0.15	0.16	0.84	-0.14	0.76	0.72	0.11
Padova	-0.54	0.13	0.72	0.27	0.63	0.37	-0.28	0.58	0.35	0.44
Southern Alps	-0.87	0.02	0.72	0.13	0.12	0.70	-0.68	0.09	0.00	0.99
Central Alps	-0.59	0.06	0.72	0.25	-0.13	0.68	-0.51	0.19	-0.32	0.39
Central Alps-AUER	-0.91	0.00	0.72	0.30	0.34	0.42	-0.74	0.06	-0.06	0.91
Northern Alps	-0.77	0.01	0.72	0.29	-0.08	0.81	-0.85	0.06	-0.20	0.64
Alps CASTY	-0.70	0.01	0.72	0.16	0.18	0.66	-0.55	0.33	0.60	0.12
Central Europe	0.10	0.79	0.72	0.33	-0.27	0.55	-0.27	0.72	0.74	0.09
Central Europe-Dobrovolny	-0.46	0.18	0.72	0.32	-0.09	0.79	-0.69	0.20	0.30	0.51
Central England	-0.56	0.11	0.72	0.86	-0.19	0.65	-0.42	0.35	-0.45	0.26
de Bilt	-0.06	0.89	0.72	0.60	-0.03	0.96	-0.44	0.33	0.37	0.26
Berlin	-0.37	0.36	0.72	0.49	0.23	0.23	-0.79	0.11	0.09	0.85
Warsaw	-0.04	0.90	0.72	0.93	0.38	0.40	-0.46	0.54	0.41	0.42
Northern Europe	-0.13	0.76	0.72	0.18	-0.15	0.66	0.75	0.08	0.12	0.79
Tallinn	-0.17	0.64	0.72	0.10	-0.50	0.25	0.37	0.47	0.02	0.95
Stockholm	-0.35	0.44	0.72	0.21	-0.17	0.57	0.49	0.27	0.40	0.32

Table 6.2: Correlations (Spearman) between 'mean' and 'variability' of 30-years moving windows for the four seasons and the annual mean during the instrumental period (1864–2007/2000). Significant correlations ($p_{corr} < 0.1$) are bold.

6.3.2. Comparison between instrumental and proxy data 1864 to 1940/2000

The MVC-plots of the tree ring and lake sediment proxies are shown in Fig. 6.3. The four tree ring series (late-wood density and ring width from the Swiss Alps and the Greater Alpine Region GAR) show a different behaviour and are internally not consistent. It needs to be noted that the data from the GAR end in 1988 (Frank and Esper 2005) and do not contain the last decades with the strong warming.

Both sediment proxy series show higher variability with higher mean values. Because the Qz/Mi Central Alps series is negatively correlated with temperature, the connection between 'mean' and 'variability' is negative for Qz/Mi-derived temperature. The bSi Central Alps data remain mostly within the 90% confidence area of the reference period.

Table 6.3 shows the correlations of the 'mean' and 'variability' between the proxy data and the corresponding instrumental data. Most of the proxy series show a correlation ($p_{corr} < 0.1$) with the instrumental data for at least one of the two L-moments ('mean' or 'variability'), except for trw GAR and Qz/Mi Central Alps, which do not correlate with the corresponding temperature series. The only series with positive correlations ($p_{corr} < 0.05$) in both 'mean' and 'variability' is the tree ring width series from the Swiss Alps (trw Swiss Alps, compared with the nearby station Sion Table 6.3; Begert et al. 2005). Both late-wood density series show

<u>MXD Swiss Alps</u>	<u>Sion JJAS</u>	<u>p-value</u>
r ,mean'	0.19	0.81
r ,variability'	0.78	0.02
<u>TRW Swiss Alps</u>	<u>Sion JJA</u>	<u>p-value</u>
r ,mean'	0.74	0.02
r ,variability'	0.59	0.05
<u>TRW Greater Alpine Area</u>	<u>Alps CASTY JJA</u>	<u>p-value</u>
r ,mean'	0.92	0.26
r ,variability'	0.51	0.13
<u>MXD Greater Alpine Area</u>	<u>Alps CASTY AMJJAS</u>	<u>p-value</u>
r ,mean'	0.89	0.29
r ,variability'	0.77	0.04
<u>biogenic silica Central Alps</u>	<u>Central Alps JJA</u>	<u>p-value</u>
r ,mean'	0.78	0.07
r ,variability'	-0.81	0.01
<u>biogenic silica Central Alps</u>	<u>Central Alps SON</u>	<u>p-value</u>
r ,mean'	0.22	0.51
r ,variability'	-0.63	0.07
<u>biogenic silica Central Alps</u>	<u>Central Alps JJASON</u>	<u>p-value</u>
r ,mean'	0.76	0.02
r ,variability'	-0.65	0.06
<u>Quartz/Mica Central Alps</u>	<u>Central Alps JJA</u>	<u>p-value</u>
r ,mean'	0.82	0.17
r ,variability'	0.6	0.29

Table 6.3: Correlations of 'mean' and 'variability' (30-years running windows) between the proxy series and corresponding instrumental data. Significant correlations ($p_{corr} < 0.1$) are bold. The correlations span from 1864 to the end of the proxy data series i.e. 2005 for mxd Swiss Alps, 2002 for trw Swiss Alps, 1989 for trw Greater Alpine Area GAR, 1987 for mxd GAR, 1920 for Quartz/Mica Lake Silvaplana (Qz/Mi Central Alps) and 1949 for biogenic silica flux (bSi Central Alps).

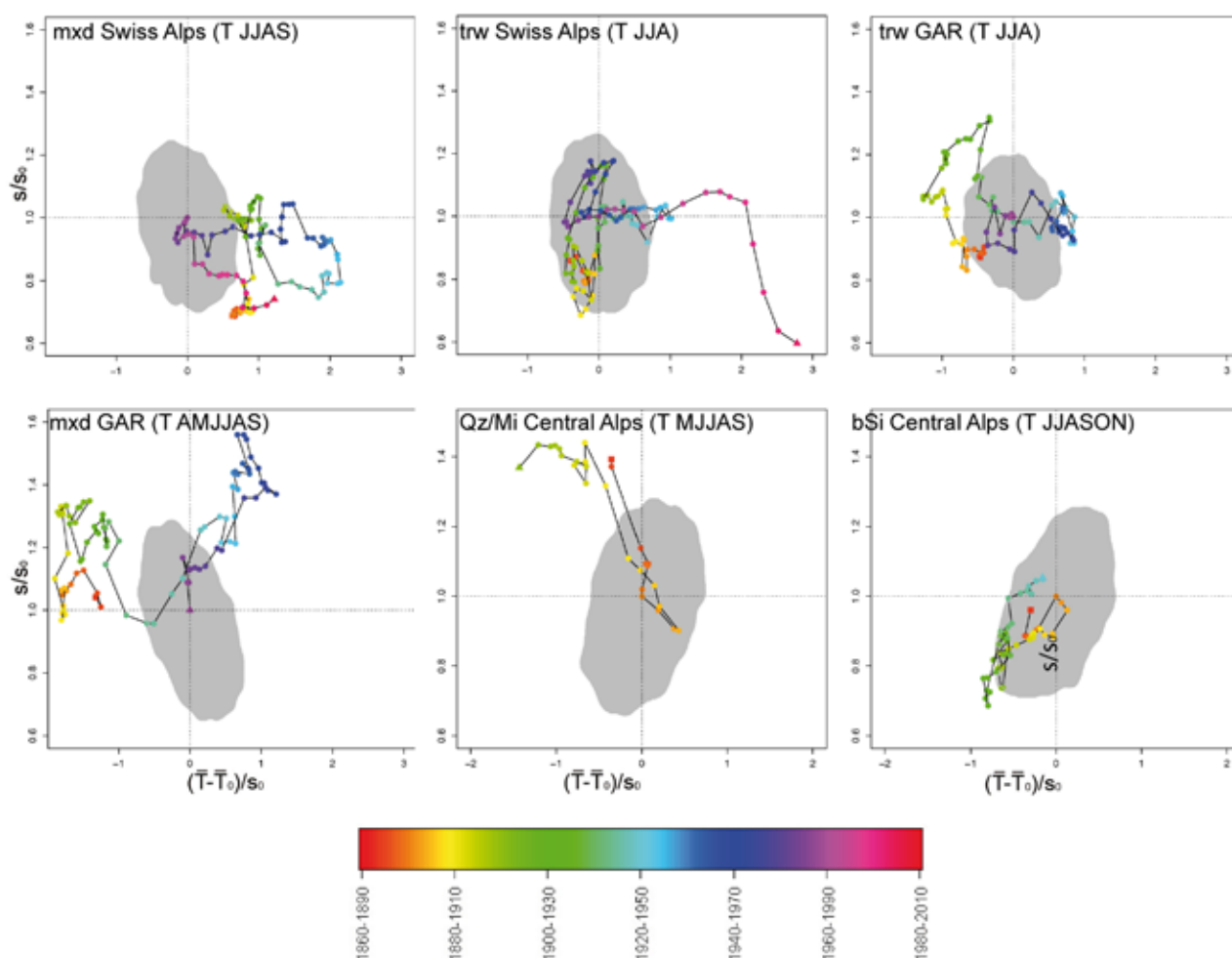


Fig. 6.3. MVC plots of the six proxy data series. The grey shaded area indicates the 90% confidence range of the 1958-1987 (1871-1900) standard period for tree-rings (sedimentological proxies).

a significant correlation in ‘variability’, but not in the ‘mean’. The correlation between the tree-ring widths of the Greater Alpine Region (GAR) series and the JJA temperature for Alps–CASTY is high, but not significant in ‘mean’.

The bSi Central Alps series is positively correlated with JJASON and JJA temperature in the ‘mean’, but negatively correlated with JJA, SON and JJA-SON temperature in ‘variability’. There is no correlation in the ‘mean’ between biogenic silica flux and T SON. The Qz/Mi Central Alps time series does not exhibit any correlation ($p_{\text{corr}} < 0.1$) with instrumental JJA Central Alps in ‘mean’ or ‘variability’.

6.3.3. Temporal stability of correlations between ‘mean’ and ‘variability’

6.3.3.1. Significant instrumental time series (1900 onwards); the period with the warming trend

The temporal stability of the relationship between ‘mean’ and ‘variability’ was assessed using 50-year running correlations (Spearman). The results

are shown in Fig. 6.4.

For winter in the 20th century, the negative relationship between ‘mean’ and ‘variability’ (i.e. greater variability in a climate with colder winters) is consistently found in Northern Italy (Padova), in the Southern, Central and Northern Alps, and in Central Europe–Dobrovolny (Winter Nr 2-13 in Fig. 6.4). It is most significant in the Southern and Central Alps. Northern Europe, including Stockholm and the Mediterranean (Winter Nr 1, 14 and 16 in Fig. 6.4), show decadal scale changes with a reversal around 1930 (positive connection: larger variability in a climate with warmer winters).

For autumn in the 20th century, stations in Central Europe (de Bilt and Berlin, Autumn Nr 11 and 12 in Fig. 4) show consistently negative correlations from the beginning of the century (large variability in a climate with cooler autumns), while the onset of consistently negative relationship in Central England and the entire Alpine Region starts from 1910-1920 onwards (Autumn Nr 3-7, 10 in Fig. 6.4). Northern Europe and Stockholm in particular, and to some extent the Mediterranean (except around 1940) show mostly positive connection

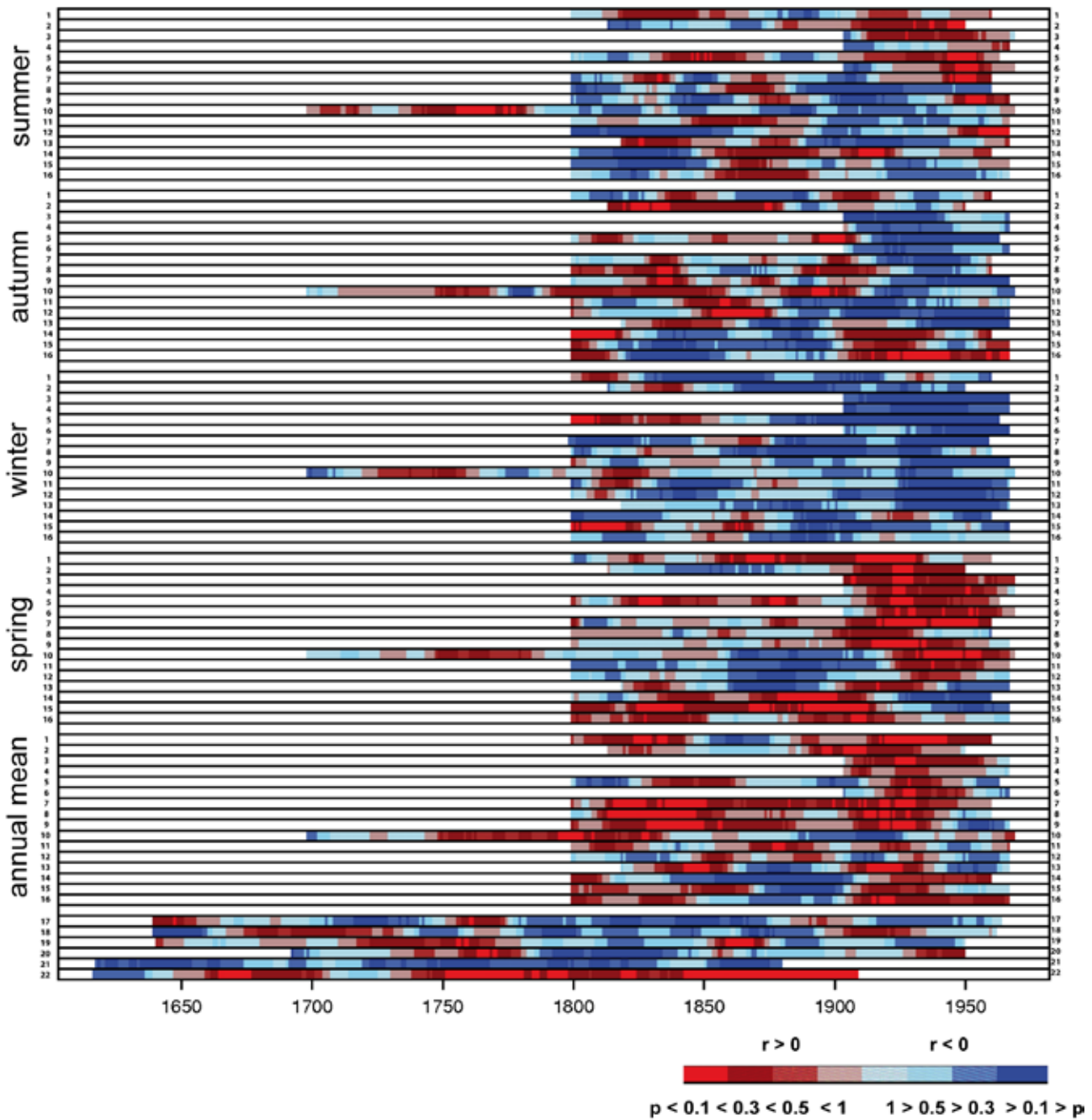


Fig. 6.4. 50-years Spearman running correlations between 'mean' and 'variability' of the 16 temperature series for the four seasons and the annual mean temperatures, and the six proxy data series. Positive (negative) correlations are indicated in red (blue). Numbering of the data series: 1 Mediterranean, 2 Padova, 3 Southern Alps (Lugano), 4 Central Alps (Sils Maria), 5 Central Alps–AUER, 6 Northern Alps, 7 Alps–CASTY, 8 Central Europe, 9 Central Europe–Dobrovolny, 10 Central England, 11 de Bilt, 12 Berlin, 13 Warsaw, 14 Northern Europe, 15 Tallinn, 16 Stockholm, 17 mxd Swiss Alps, 18 trw Swiss Alps, 19 trw Greater Alpine Region, 20 mxd Greater Alpine Region, 21 Qz/Mi Central Alps (Lake Silvaplana), 22 bSi Central Alps (Lake Silvaplana). For references see Table 6.1.

(i.e. low variability in a climate with cool autumns, Nr 1, 2 and 14, 16 in Fig. 6.4).

The Mediterranean, Alps and Central Europe have seen generally positive relationships for the spring season: low variability in a climate with cool springs (Spring Nr 1-9 in Fig. 6.4). Noteworthy is the sea-saw pattern between Northeastern Europe (including Stockholm, Warsaw and Tallinn) and

the area of Central England, de Bilt and Berlin (and to some extent the Northern Alps): the latter area started with a few decades of positive connection followed by negative relationship from ca. 1920-1940 onwards, and vice versa. This change is clearly visible in Fig. 6.2 (Tallinn MAM).

For summer in the 20th century, Northern Italy and the Southern Alps show generally positive connec-

tion (enhanced variability in a climate with warmer summers; Summer Nr 2,3 in Fig. 6.4), while the Mediterranean, Central and Northern Alps remain inconclusive. Central and Northern Europe remain in the domain of generally negative connection (low variability in a climate with warmer summers) until ca. 1960 when a reversal to positive relationship (high variability in a climate with warmer summers) is observed. However, all positive correlations become very weak towards the end of the investigated period.

The annual temperatures show an overall positive correlation in the Mediterranean, the Alps and Northern Europe throughout the 20th century (high variability in a warmer climate), while Central England and the stations in Central Europe show a less consistent pattern, with mostly negative relation from 1930-1940 onwards (i.e. until 1975).

6.3.3.2. Seasonal patterns in instrumental, early instrumental and proxy data: a focus on the 19th century

The extensions of these records back to the early instrumental period (1800, 1700 in Central England) show that the patterns established for the 20th century are not stable in time. Instead they show spatially coherent arrangements with decadal-scale fluctuations between positive and negative relationships (blue and red colours in Fig. 6.4).

In the second half of the 19th century, summers in Northern and Central Europe (Nr 7-9 and 11-16 in Fig. 6.4) seem to have experienced generally positive connection (increasing variability in a climate with warmer summers) peaking around 1860-1870 (i.e. the 50-year moving windows covering the time period between 1835 and 1895), while mostly negative connections prevailed in that area (except in Warsaw) during the first half of the 19th century. Central England (and to some extent Berlin) shows a different behaviour with mostly negative connections prevailing throughout the 19th century (decreasing variability in a climate with warmer summers).

The picture of autumn in the 19th century is heterogeneous in the Mediterranean. Spatially consistent arrangements appear in Central Europe and Central England with mostly positive relationship between 1810 and 1840, while Northern Europe and Tallinn show negative connections during that time. Data for the individual stations de Bilt, Berlin and Warsaw are inconsistent with the regional data set (Central Europe) for the second half of the 19th century.

The 50-year running correlations show the most consistent picture for winter temperatures. From 1875 onwards the entire European area shows negative relation (lower variability in a climate with warmer winters), except for a short reversal in Northern Europe around 1920. Two decades with positive relationship are found in Central England, in Central European stations, the Central Alps and Northern Italy (Padova) between 1810 and 1830. Again, individual stations in Central Europe show a mismatch with the regional data for Central Europe (Winter Nr 10-13 versus 8-9 in Fig. 6.4).

For spring temperature, Northern Europe and Tallinn show positive correlations between 'variability' and 'mean' (higher variability in a climate with warmer springs) throughout the 19th century, whereas Central England and Central European stations show largely negative relationship (most significantly de Bilt; although an exception is Warsaw around 1830).

Annual temperatures during the 19th century are slightly dominated by positive connections except for the Mediterranean area between 1850 and 1880, the Central European stations between 1820/30 and 1850, and Northern European stations data in the second half of the 19th century, which show negative relationship.

Interestingly, all six proxy data series considered in this study show a very different behaviour of connection between 'variability' and 'mean'. The tree ring data (ring width and late-wood density) from the Swiss Alps and the Greater Alpine Region are internally not consistent and hardly compare with the corresponding instrumental data. They show, however, multi-decadal to centennial-scale oscillations between positive and negative relationship. Overall, positive relationship (higher variability in a climate with warmer summers) are found 1760-1770 and consistently negative relationship from 1805 to 1825. The lake sediment data show higher variability with higher mean values (higher variability of bSi Central Alps with higher mean bSi Central Alps values; bSi is a proxy for warm season temperature in Lake Silvaplana, Engadine, Blass et al. 2007) except for two phases in the first half of the 17th century and around 1710-1730. The XRD peak intensity ratios of Qz/Mi Central Alps of individual varves show a consistently positive relationship between 'mean' and 'variability'. Remarkably, this relationship (Nr 21 in Fig. 6.4) does not show any reversal throughout the entire record.

6.4. Discussion

6.4.1. Methods

We made our results comparable with previous studies applying the methods exactly as described by Scherrer et al. (2005) and Della Marta et al. (2007). However the question arises whether a linear regression is the most suitable method for detrending the individual segments. Linear detrending is a parametric method and, therefore, sensitive to outliers, whereas for example a Theil–Sen (Theil 1950; Sen 1968) trend estimate would be non-parametric and, hence, more robust against outliers. Furthermore, within a 30-year time period increasing and decreasing trends may occur. These decadal trends cannot be removed with a linear trend estimate spanning the entire 30-year period. Non-linear smoothing, such as locally weighted regression or spline-smoothing, could remove the positive and negative trend segments that originate from decadal-scale variability. However, testing these different detrending methods and their implications is beyond the scope of this article.

As noted by Scherrer et al. (2005), large discontinuities are observed if an extreme value enters or leaves the 30-year moving window (climatology) under consideration. Although we have assessed the ‘variability’ of a PDF with the more robust second L-moment, effects of individual extreme values are still visible in the data. For example, the extremely cold spring temperature of Tallinn in 1942, the cold winter of 1962/63, the hot summer of 2003 and the very warm autumn of 2006 in the Swiss data series. The most critical factor is the effect of an extreme value. If a particular year is positioned at one of the tail ends of the 30-year running window, then it has the greatest effect on the slope of the linear trend.

6.4.2. Instrumental and early instrumental data

The question arises from the synopsis presented in Fig. 6.4 whether the spatio-temporal patterns and changes in the temperature PDFs might be related to changes in the climatology of large-scale circulation modes and associated within-mode variations over Europe (Küttel 2009). Here, we compare our analysis with the classifications of the modes back to 1760 for winter (Jacobeit et al. 2003; Küttel 2009) and summer (Jacobeit et al. 2003).

Intuitively, one would argue that an increase in interannual temperature variability (large spread in

the PDF) is observed if different modes with their inherent temperature distributions are well mixed and occur at similar probabilities. Hence, cold and warm conditions change frequently. On the other hand, a decrease in interannual variability (narrow spread in the PDF) is expected for phases with only one dominant and persistent mode, which leads to rather similar (cold or warm) temperatures in the climatology. Generally, rather warm conditions are expected for winters with Westerly flow (W mode), while cold winters are characteristic for the Russian High (RH mode). Large-scale advective circulation patterns (mostly winter) lead to spatially more homogenous conditions than convective patterns (mostly summer).

The most stable relationship between ‘mean’ and ‘variability’ is the negative correlation for winter temperatures (blue colour in Fig. 6.4). This is true for all stations and temperature fields after 1860 except for the series from Northern Europe. As expected, this relationship is explained by changes in prevailing circulation patterns: between 1840 and 1870 the Russian High mode is as frequent as the Westerly flow pattern (W mode; Jacobeit et al. 2003). Hence, the temperature is rather cold, but the interannual variability is high for the mid 19th century. After 1900, especially between 1910 and 1930, Westerly flow is prevailing (Küttel 2009; Jacobeit et al. 2003): temperatures warm up while the variability decreases (cold winters are less frequent). From 1940 to 1960, the Westerly Mode and the Russian High mode are again equally frequent, which results in colder temperatures and in a higher variability. From 1970 onwards, the Russian High mode becomes rare in winter (Küttel 2009). For the very beginning of the 19th century, the Westerly flow (W mode) is most important, followed by the RH mode, while the L mode (Low pressure) is almost absent. This leads in some areas of Europe to relatively warm conditions with high interannual variability (red colours in Fig. 6.4).

For summer, the association of the temperature PDF with circulation patterns is less conclusive. This might be related to the greater importance of convective processes. However, the positive correlations between ‘mean’ and ‘variability’ after 1870, but especially from 1950 onwards, can be associated with a relative increase in the Atlantic Ridge (AR) pattern (Jacobeit et al. 2003). This leads to warm and dry summers and, potentially, to a higher probability of triggering the soil moisture–atmosphere feed back. According to Schär et al. (2004), this would lead to high variability. How-

ver, the variability of summer temperatures seems to be mainly driven by a few extreme years rather than by changes in circulation patterns. As pointed out by Scherrer et al. (2005), the largest discontinuities in variability are calculated if an extreme year is included in the 30-year moving window (climatology). For instance, the record hot summer of 2003 alone increases the variability in the Northern Alps data series immediately by $0.2 \cdot s_0$. Our data suggest that the increase in summer temperature variability, as expected from model studies for the 21st century, has not yet been observed north of the Alps, while the areas south of the Alps (e.g. in Northern Italy) show this effect. According to the proposed underlying mechanism (the soil moisture–atmosphere feedback; Fischer et al. 2007), we would expect that the area of highest sensitivity, which today is in the Southern Alps/Mediterranean, would move northward in the next few decades.

The autumn temperature series show a change from positive to negative correlations around 1910. This is mainly due to a decrease or even absence of cold autumns after 1922 and an increase in autumn temperatures around 1930 and after 1970.

The positive correlation of the spring temperatures around 1925 is associated with increasing mean temperatures between 1900 and 1950 and a related increase in variability. The negative correlation in the time series located in Scandinavia (50°N) is caused by an increase in mean temperature from 1830 to 1900 and a concomitant reduction of cold years.

The annual mean temperatures generally show an increase in ‘variability’ coupled with increasing ‘mean’. This is mainly attributed to a strong warming trend from 1890 to 1960 and a concomitant increase in variability. The warming trend after 1980 is not associated with an increase in variability, which leads to negative correlations towards the end of the time series.

6.4.3. Comparison between instrumental data and proxy data

The only correlation of a proxy series with an instrumental series (30-year running windows), which yielded a significant positive correlation ($p_{\text{corr}} < 0.05$) in ‘mean’ as well as in ‘variability’ is the correlation between trw Swiss Alps (Büntgen et al. 2005) and JJA Sion (Begert et al. 2005). However, the correlation of the ‘variability’ only explains about 35% of the variance. In general, the level of significance for the correlation coefficients is lo-

wer for ‘variability’ than for the ‘mean’, because the serial correlation of ‘variability’ is lower than for the ‘mean’.

The lack of correlation ($p_{\text{corr}} < 0.1$) in the ‘mean’ between the mxd Swiss Alps series (Büntgen et al. 2006) and the JJAS temperature of the nearby station Sion is due to differences in the low frequency domain of the two data series.

The late-wood density data series in the Greater Alpine Region (mxg GAR, Frank and Esper 2005) shows a high correlation ($r = 0.89$, 1864–1987) with the AMJJAS temperature of Alps–CASTY in the ‘mean’, but this correlation is not significant ($p_{\text{corr}} = 0.29$, Table 6.3). This shows the important effect of the very high lag–1 autocorrelation of a time series of 30-year running means (typical values are on the order of 0.95), which requires an adjustment (here a reduction to 5% of the original DF) of the degrees of freedom to assess the significance of the correlation (Dawdy and Matalas 1964). The same is valid for the correlation in ‘mean’ between trw Alps and JJA temperatures of Alps–CASTY.

However, the largest problem in this context might be that tree rings often show non-linear growth responses to climate, which affects both the ‘mean’ and the ‘variability’ of the time series (Esper and Frank 2009), additionally the variance of tree-ring time series is stabilized and/or adjusted (Frank and Esper, 2005).

The negative correlation between the variability of temperatures from Sils Maria and the bSi Central Alps data are difficult to explain. The bSi time series experiences a strong heterostedasticity. Thus, the variability increases as soon as the ‘mean’ value increases. This heterostedasticity is quite stable throughout the time series. Therefore, we suspect that heterostedasticity might instead be related to system-internal positive feedbacks, which makes it difficult to assess past temperature variability changes based on this proxy series.

The systematic negative connection of ‘variability’ between biogenic silica flux in Lake Silvaplana and the nearby meteorological data (Table 6.3) is mainly due to an increase in temperature variability from 1890 to 1900, followed by a decrease between 1920 and 1940, while the variability of the biogenic silica flux shows the opposite behaviour. In fact, the lack of relationship between the sedimentological proxies and instrumental data was not surprising. Blass et al. (2007) and Trachsel et al. (2008) have pointed out that the correlation of proxy data from individual annual sediment layers with meteorological data series is highly suscep-

tible to varve counting errors and imperfect sampling of the individual varves for geochemical analyses (i.e. minute admixtures of sediment material from the varves of adjacent years). In order to account for these effects they applied a 5-year triangular filter before comparisons between proxy data and meteorological data were made. For the raw data at annual resolution, the explained variance between proxy data and climate data hardly exceeded 15% (Blass et al. 2007).

Overall, it seems very difficult to assess changes of the seasonal and annual temperature distributions ('mean' versus 'variability' change behaviour, MVC) from proxy data series. We spot two major problems, both of which have their origin primarily in the calibration of the proxy data against climate data. The first is that natural archives often respond non-linearly to meteorological conditions (e.g. Loehle 2009). Thus, scaling and regression-based calibration procedures (Esper et al. 2005) have their limits. This is particularly problematic for the reconstruction of extreme events, which in turn determine the behaviour of 'variability' in the MVC analysis. Secondly, it is very difficult to correctly reconstruct the low frequency (centennial-scale) climate variability from proxy series and thus to assess the 'mean' correctly (i.e. in absolute terms). This depends largely on the properties of the calibration period, such as the length of the calibration period, beginning and end, statistical pre-treatment of the raw proxy data, and the presence of long-term trends in the proxy archives (e.g. Esper and Frank 2009; Loehle 2009; Blass et al. 2007).

6.5. Conclusions

Climate model simulations project a significant increase in the interannual variability of summer temperatures in the warmer climate of the 21st century. Europe has been found to be the global hotspot for increasing variability. The associated raise in hot extremes is expected to have major impacts on ecosystems and society. Using the non-parametric measure of the first two L-moments ('mean' and 'variability') we investigated changes of the temperature distributions in the instrumental (AD 1864-2007) and early instrumental (AD 1760-1864) data across Europe. This period covers the generally cooler 'Little Ice Age' and the warming trend in the 20th century. In order to explore the potential to extend the record back to AD 1000 we investigated whether changes in interannual temperature distributions can be assessed using annually resolved proxy data (tree rings and var-

ved lake sediments). This would allow us to test the model projections for the 21st century with the nearest analogues from the warm Medieval Period or the Roman Times.

In order to make our results comparable with previous investigations we have used the methodology as described by Scherrer et al. (2005). We note that the procedure for detrending the individual segments (here a 30-year period) is highly sensitive to outliers. We propose to test in a future study a non-parametric and thus more robust method (e.g. Theil-Sen trend estimate). Locally weighted regression or spline-smoothing could be used to remove the trends induced by decadal-scale climate variability.

For the winters after 1860 (i.e. end of the Little Ice Age) we found a general decrease in interannual variability with the warming trend. The spring season (except in Northern Europe) and the annual mean temperatures generally show the opposite: an increasing variability with the warming trend of the 20th century. While summers in the Southern Alps and Northern Italy have experienced greater variability with warmer temperatures during the 20th century and partly the 19th century, this effect is observed north of the Alps only during the last two decades (statistically weakly significant, $p_{\text{corr}} < 0.3$). However, in all these series the warming after 1980 was not associated with a further increase in variability.

In the 19th century (i.e. before the strong warming of the 20th century), the relationship between 'mean' and 'variability' fluctuates between positive and negative values. These fluctuations are consistent with changes of the occurrence of synoptic-scale patterns across Europe: winter periods with a well-balanced mix between the Westerly Mode and the Russian High mode (e.g. 1830-1880) lead to very high variability with cold and warm extremes while the decrease in the frequency of the Russian High after 1940-1950 resulted in less frequent cold extremes (and thus in a decrease of variability in a warmer climate).

While the effect of the soil moisture-atmosphere feedback during summer (increase in variability) may be in place south of the Alps today, it is not yet clearly visible north of the Alps. However, consistent with the model projections, it is expected to migrate northward to Central Europe in the current and next few decades.

A more systematic investigation is needed to assess whether annually resolved proxy data (tree-ring and varved lake sediment data) could be used to assess the MVC behaviour of climate

further back in time. For example, to investigate the warm periods of the past (Medieval Warm Period and/or Roman Times). Our data (tree-ring widths and late-wood density from the Swiss Alps and the Greater Alpine Region; biogenic silica and mineralogical composition of individual varves in Lake Silvaplana, Engadine Eastern Swiss Alps) do not show consistent results in comparison with the corresponding meteorological data series. We spot two major obstacles in the proxy data series that have a great impact on the MVC behaviour. Firstly, it is very difficult to reconstruct the amplitude of extreme events and thus 'variability' from proxy data (non-linear responses). Secondly, it is very difficult to reconstruct the correct absolute value for the 'mean' from proxy data. Both the 'mean' and the 'variability' are critically important to assess the MVC behaviour.

Acknowledgements

Project grants were provided by European Union FP6 project "Millennium" (Contract 017008), NF-200021-106005/1 'ENLARGE' and the National Center of Competence in Research Climate. We acknowledge Marcel Küttel and Jürg Luterbacher for providing temperature reconstructions and instrumental data series, and David Frank for providing tree ring data.

References

Auer I et al (2007) HISTALP – historical instrumental climatological surface time series of the Greater Alpine Region. *Int J Climatol* 27:17–46.

Begert M, Schlegel T, Kirchhofer W (2005) Homogeneous temperature and precipitation series of Switzerland from 1864 to 2000. *Int J Climatol* 25:65–80.

Beniston M (2009) Trends in joint quantiles of temperature and precipitation in Europe since 1901 and projected for 2100. *Geophys Res Lett* 36. doi:10.1029/2008GL037119.

Blass A, Bigler C, Grosjean M, Sturm M (2007) Decadal-scale autumn temperature reconstruction back to AD 1580 inferred from the varved sediments of Lake Silvaplana (southeastern Swiss Alps). *Quat Res* 68:184–195.

Büntgen U, Esper J, Frank DC, Nicolussi K, Schmidhalter M (2005) A 1052-year tree-ring proxy for Alpine summer temperatures. *Clim Dyn* 25:141–153.

Büntgen U, Frank DC, Nievergelt D, Esper J (2006) Summer temperature variations in the European Alps, AD 755–2004. *J Clim* 19:5606–5623.

Casty C, Wanner H, Luterbacher J, Esper J, Böhm R (2005) Temperature and precipitation variability in the European Alps since 1500. *Int J Climatol* 25:1855–1880.

Dawdy DR, Matalas NC (1964) Statistical and probability analysis of hydrologic data. Part III Analysis of variance, covariance and time series. In: Chow VT (Ed.) *Handbook of applied hydrology*, McGraw-Hill Book Company, New York, pp 68–90.

Della-Marta PM, Haylock MR, Luterbacher J, Wanner H (2007) Doubled length of western European summer heat waves since 1880. *J Geophys Res* 112. doi:10.1029/2007JD008510.

Dobrovolný P, Moberg A, Brázdil R, Pfister C, Glaser R, Wilson R, van Engelen A, Limanówka D, Kiss A, Halíčková M, Macková J, Riemann D, Luterbacher J, Böhm R (In Review) Monthly and seasonal temperature reconstructions for Central Europe derived from documentary evidence and instrumental records since AD 1500. *Clim Change*.

Esper J, Frank DC, Wilson RJS, Briffa KR (2005) Effect of scaling and regression on reconstructed temperature amplitude for the past millennium. *Geophys Res Lett* 32. doi:10.1029/2004GL021236.

Esper J, Frank DC (2009) Divergence pitfalls in tree-ring research. *Clim Change* 94:261–266.

Fischer EM, Seneviratne SI, Vidale PL, Lüthi D, Schär C (2007) Soil moisture-atmosphere interactions during the 2003 European summer heat wave. *J Clim* 20:5081–5099.

Frank D, Esper J (2005) Temperature reconstructions and comparisons with instrumental data from a tree-ring network for the European Alps. *Int J Climatol* 25:1437–1454.

Hosking JRM (1990) L-Moment – Analysis and Estimation of Distributions Using Linear-Combinations of Order-Statistics. *J Royal Stat Soc Series B-Methodological* 52:105–124.

IPCC (2007) *Climate Change, The Scientific Basis*. Cambridge Univ. Press, Cambridge.

- Jacobeit J, Wanner H, Luterbacher J, Beck C, Philipp A, Sturm K (2003) Atmospheric circulation variability in the North–Atlantic–European area since the mid–seventeenth century. *Clim Dyn* 20:341–352.
- Küttel M (2009) European climate dynamics and long-term variations over the past centuries. Dissertation, University of Bern.
- Loehle C (2009) A mathematical analysis of the divergence problem in dendroclimatology. *Clim Change* 94:233–245.
- Luterbacher J, Dietrich D, Xoplaki E, Grosjean M, Wanner H (2004) European seasonal and annual temperature variability, trends, and extremes since 1500. *Science* 303:1499–1503.
- Manley G (1974) Central England temperatures: monthly means 1659 to 1973. *Q J Royal Met Soc* 100:389–405.
- Räisänen J (2002) CO₂–induced changes in interannual temperature and precipitation variability in 19 CMIP2 experiments. *J Clim* 15:2395–2411.
- Schär C, Vidale PL, Lüthi D, Frei C, Häberli C, Liniger MA, Appenzeller C (2004) The role of increasing temperature variability in European summer heatwaves. *Nature* 427:332–336. doi:10.1038/nature02300.
- Scherrer SC, Appenzeller C, Liniger MA, Schär C (2005) European temperature distribution changes in observations and climate change scenarios. *Geophys Res Lett* 32. doi:10.1029/2005GL024108.
- Scherrer SC, Appenzeller C, Liniger MA (2006) Temperature trends in Switzerland and Europe: Implications for climate normals. *Int J Climatol* 26:565–580.
- Sen PK (1968) Estimates of the regression coefficient based on Kendall's tau. *J Am Stat Assoc* 63:1379–1389.
- Seneviratne SI, Lüthi D, Litschi M, Schär C (2006) Land–atmosphere coupling and climate change in Europe. *Nature* 443:205–209. |doi:10.1038/nature05095.
- Theil H (1950) A rank–invariant method of linear and polynomial regression analysis. *Netherlands Akad. Wetensch. Proc.* 53:386–392 (part I), 521–525 (part II), 1397–1412 (part III).
- Trachsel M, Eggenberger U, Grosjean M, Blass A, Sturm M (2008) Mineralogy–based quantitative precipitation and temperature reconstructions from annually laminated lake sediments (Swiss Alps) since AD 1580. *Geophys Res Lett* 35. doi:10.1029/2008GL034121.
- Xoplaki E, Luterbacher J, Paeth H, Dietrich D, Steiner N, Grosjean M, Wanner H (2005) European spring and autumn temperature variability and change of extremes over the last half millennium. *Geophys Res Lett* 32. doi:10.1029/2005GL023424.
- Yiou P, Dacunha–Castelle D, Parey S, Hoang TTH (2009) Statistical representation of temperature mean and variability in Europe. *Geophys Res Lett* 36. doi:10.1029/2008GL036836.
- Zhang JY, Wang WC, Leung LR (2008) Contribution of land–atmosphere coupling to summer climate variability over the contiguous United States. *J Geophys Res* 113. doi:10.1029/2008JD010136.

Chapter 7



7. Concluding remarks and outlook

7.1. Quantitative climate reconstruction from Lake Silvaplana

One of the main goals of this thesis was to produce high-resolution quantitative temperature reconstructions from the sediments of Lake Silvaplana. Ideally, these records should span the last 1000 years. To achieve this goal a high-precision chronology is fundamental (e.g. Blass, 2006; Grosjean et al. 2009). For the calibration-in-time approach an accurate chronology is crucial because chronological error will reduce the correlation between the proxy and the instrumental target. Moreover a good dating control is important for the comparison of climate records among each-other. As for the calibration period statistical analysis will fail as soon as the quality of the chronology drops below a certain level. Therefore the strengths of the chronology of Lake Silvaplana are summarised prior to summarising the reconstruction studies.

7.1.1. Chronology

The sediment of Lake Silvaplana is annually laminated (varved) for the last 3300 years (Leemann and Niessen, 1994). Varve counts are known as powerful method to establish chronologies (e.g. Lamoureux, 2001). In central Europe major floods of the last 1000 years have been documented. For the Engadine Valley a flood history based on historical documents (Caviezel, 2007) including floods as far back as 1566 has recently become available. These documents regarding the Upper Engadine Valley gave us the opportunity to refine and even improve the chronology proposed by Blass et al. (2007a). Floods of known age could be attributed to flood deposits in the sediment. This allowed us to corroborate the varve counts (e.g. Sturm and Matter, 1978) and to test the accuracy of varve counts. The major flood 1342 (e.g. Röthlisberger, 1991) was dated to 1344 by varve counts. Due to these constraining flood deposits it was possible to estimate the maximum uncertainty of the chronology to amount to ± 8 years.

7.1.2. Lake Silvaplana as an archive for high-resolution quantitative climate reconstructions

In the first part of this chapter the study testing scanning in-situ reflectance spectroscopy for climate reconstruction on clastic sediments is reviewed. Then, the summer temperature reconstruction based on the combination of the

high-frequency, climate related signal of bSi flux and the low-frequency component of a chironomid-based summer temperature reconstruction is discussed.

Here the potential of in-situ reflectance spectroscopy to detect amount and composition of clastics has been tested for the very first time. We therefore thoroughly assessed the measured data by means of autocorrelation functions and principal component analyses.

We further tested the influence of different climate and sediment parameters on reflectance data using redundancy analysis.

Due to the special geological setting in the catchment of Lake Silvaplana, the amount of mica and chlorite in the sediment is positively correlated with summer temperature (Trachsel et al. 2008). The reflectance-derived variables representing the amount of chlorite and biotite are highly correlated to summer temperatures (TJJAS) during the calibration period from 1864 to 1950 ($r=0.82$). We increase the correlation during the calibration period to $r = 0.93$ using multiple linear regression.

The accordance of reflectance inferred T JJAS reconstruction with fully independent reconstructions (e.g. Casty et al. 2005) was assessed by means of running correlation. Back to AD 1500 running correlations are positive and mostly significant ($p<0.1$, two-sided test).

We could show the high-potential of in-situ reflectance spectroscopy for applications on clastic sediments. A further avenue of research could involve systematic testing of the method on a variety of lakes with different sediment types and proportions of clastic, biogenic and even chemical components.

The objectives of this study presented in chapter five were to: (i) refine and extend an existing bSi flux based temperature reconstruction. (ii) test the effects of different calibration methods on predicted amplitudes.

As mentioned above (chapter 7.1.1.) the chronology was refined between AD 1600 and AD 2000. This resulted in chronological changes in the calibration period. These modifications changed the main temperature signal from autumn (Blass et al. 2007b) to summer (JJA and JJAS) and summer-autumn (JJASON).

The non-climate trend in the bSi flux data (Blass et al. 2007b) was removed applying a loess-filter. The band-pass filtered (9 to 100 years) bSi record

is in good accordance ($r \approx 0.5$; $p < 0.05$) with fully independent climate reconstructions (Casty et al. 2005 back to AD 1500 and Büntgen et al. 2006 back to AD 1177).

When combining the bSi flux derived summer temperature reconstruction with the low-frequency component of the chironomid derived summer temperature reconstruction, we find an amplitude of climate between 1177 and 1950 that amounts to 2.6°C. Extension of the record to 2008 by adding the summer temperatures of Sils, the warmest decade in the last 800 years is found in the last 10 years. It is 0.2 °C warmer than the warmest decade in the reconstruction period (the decade around 1180). However, this difference of 0.2 ° is within the uncertainty bands of the reconstruction.

To achieve these quantitative statements about past climate variability we tested the effects of six univariate regression methods (inverse regression, inverse prediction, generalised least squares regression, major axis regression, standard major axis regression, ranged major axis regression) on the predicted amplitude. Differential calibration resulted in massive differences for the predicted (reconstructed) amplitude. In our study Major Axis regression was best representing the amplitude of the instrumental target and was chosen for calculating the calibration model between bSi flux and instrumental data.

Based on this sensitivity study we could show weaknesses of calibration measures RE and CE (Cook et al. 1994). RE and CE favour calibration methods that underestimate the amplitude of natural climate variability during the calibration period. Thereby, the amplitude of past climate variability is as well underestimated. This shows the need for alternative calibration measures if we want to assess the amplitude of past climate variability.

Hence in this study two points with general implications for paleo-climatology arose:

(i) Even minor changes in the chronology of the calibration period can result in changes in the calibration statistics and can even change the season to which the correlation of the proxy is highest. Therefore a good age control of the proxy record is fundamental.

(ii) The statistical method applied for calibration is affecting the amplitude of the climate reconstruction. Therefore, the calibration method has to be chosen thoroughly. This choice must not only be based on conventional measures for the quality of a calibration. The most widely used calibration measures (RE and CE) bias the choice of the

calibration method towards methods that underestimate the amplitude of climate variability. We therefore propose to use the correct representation of the amplitude of the instrumental target as an additional criterion for the quality of a calibration.

7.2. The changes of mean and variance of seasonal temperatures over Europe in the last 250 years

In this study, we asked the following questions: (i) is the interannual summer temperature variability related to the mean value. Climate models project an increase in interannual variability of summer temperatures going along with the projected increase in mean temperature. (ii) can natural proxies such as tree rings and annually laminated lakes sediments provide information about changes in interannual climate variability?

Lake sediment derived proxies assessed in this study do not represent changes in interannual climate variability. They show strong heteroscedasticities (increasing variance with increasing mean). These heteroscedasticities might be explained in two ways. (i) a natural system reacts more dynamically when it is on a high level (high mean value). For MAR two main processes control the sediment transport to the lake: the sediment availability and the runoff. If the sediment availability is high the MAR will react more dynamically to changes in runoff than with low sediment availability. With low sediment availability runoff is always sufficient to transport all sediment. Hence sediment availability is the only factor contributing to MAR. With high sediment availability runoff is a limiting factor for sediment transport. Depending on the situation runoff or sediment availability are the limiting factor. Thus, more processes are influencing sediment transport, resulting in a more variable MAR during phases with generally increased sediment availability. (ii) The accordance of unsmoothed proxy data with unsmoothed meteorological data is low and is explaining 20% of the variance at maximum. Therefore, 80% of the variance of unsmoothed proxy data is not directly related to climate. These 80% of variance are explained by other factors influencing a proxy (e.g. nutrient availability for bSi flux) and sampling, analytical and chronological uncertainties. Most probably, we find a combination of the two factors listed.

The processes leading to an increase in mean and variability of summer temperatures (e.g. soil-moisture feedback) have not yet been important

enough to be visible in the instrumental data on a seasonal basis. Significant correlations between mean values and variability have been reported for daily data (Della-Marta et al. 2007; Yiou et al. 2009), and models have shown the importance of soil-moisture feedback for heat-waves (Fischer et al. 2007a; Fischer et al. 2007b).

In our study, we found the strongest and most consistent changes in PDFs of seasonal data for winter temperatures. This could possibly be attributed to changes in large-scale atmospheric circulation patterns which are most important in winter (e.g. Küttel, 2009).

7.3. Outlook

This part of the thesis is structured in three parts: (i) publications in preparation about Lake Silvaplana and further research on Lake Silvaplana and other Swiss lakes, (ii) possible improvements in the study assessing changes in probability density functions (iii) general progress that has to be made to gain further insight into past climates.

(i) In this PhD-thesis a substantial amount of data that has not yet been fully interpreted and published has been generated. Additionally, a few points which should be further investigated in Lake Silvaplana arise from this study.

A few manuscripts are in preparation: Blass et al. (2007a) demonstrated the accordance of the high-frequency component of MAR with temperature. This connection is further tested with the new chronology in the calibration period and should be extended back in time. The same applies to the mineralogy based temperature and precipitation reconstructions presented by Trachsel et al. (2008). In addition, the potential of changes in grain-size to reflect hydro-meteorological conditions should be tested. Currently a manuscript comparing sedimentary records of Lake Silvaplana with glacier reconstructions is under way.

A further topic is to investigate the reasons for the long-term trend in the bSi flux data, which is most probably not climate related. It can not be attributed to human-induced nutrient input, since this input seems to be constant prior to AD 1800 (Westover and Bigler, 2009). This is however unexpected because human influence in the Upper Engadine has been recorded on longer time scales (Gobet et al. 2003) and population has varied considerably during early modern times (Mathieu, 1998).

Another interesting point is to further investigate in-situ reflectance spectroscopy measurements on clastic sediments: Reflectance spectra are only understood on very broad lines. The exact proc-

esses driving reflectance spectra of clastic sediments are not yet clearly understood. Currently measurements and investigations in this direction are in progress.

In the Upper Engadine we have the unique situation to have many different proxies which are all summer temperature sensitive (Esper et al. 2008; Kamenik et al. 2009; Larocque et al. 2009a; Trachsel et al. 2008; Trachsel et al. (in review)). These proxies have different strength and weaknesses and record climate in different frequency domains. This allows us to combine these records and to thereby test the effects of different methods when combining records (different filters, different calibrations and so forth). First steps in this direction have already been made by Christian Kamenik (personal communication, 2009).

In the frame of the SNF-funded project ENLARGE the existing records of Lake Silvaplana are extended back in time and the potential of other lakes for high-resolution, quantitative climate reconstruction is assessed.

(ii) For the comparison of changes in 'mean' and 'variance' a few details in the methodology can be improved. A methodological point largely affecting the evolution of mean and variability is the detrending applied to data series prior to the calculation of mean and variability. Trend-induced variability can only be removed calculating a linear trend when the time series experience a monotonic linear trend. When increasing and decreasing trends are found in the same time window variability will be increased but linear detrending will fail in reducing this variability. It appears however very difficult to make the choice of the detrending (filter) objective.

Moreover numerous measures for location (mean) and spread (variability) could be tested. As with the filter-choice the choice of measure for the moments is arbitrary and will therefore not yield conclusive results.

Lake sediment derived climate proxies experience strong heteroscedasticity. In a next step, the question if this is indicative for climate impacts should be addressed.

(iii) from a more general point of view, several points which should be improved in the field of climate reconstructions could be identified in this thesis:

One of the most fundamental challenges in paleoclimate research is the assessment of the 'real' amplitude of natural climate variability. The widely

used calibration measures RE and CE (Cook et al. 1994) are favouring calibration methods that are underestimating the amplitude of climate variability in the calibration period. Hence, reconstructions relying on these calibration measures are as well underestimating the amplitude of climate variability in the reconstruction period. Since one goal of climate reconstruction is to assess the 'real' climate variability the choice of the calibration method based on RE and CE will result in misleading conclusions.

Therefore, calibration measures proposed in this thesis (RMSEP/Amplitude, or correct representation of the climate amplitude in the calibration period) need further investigation. These two measures are neither perfect: the ratio RMSEP/Amplitude is favouring the calibration method producing the largest amplitude. In fact an amplitude larger than natural climate variability. When using the correct representation of the amplitude of the instrumental target as calibration measure a fundamental problem arises: if the probability density functions (PDF) of the instrumental target and the proxy are different (especially the skewness) parametric regression methods will give the correct amplitude but the reconstruction will be biased. To avoid this problem power transformations such as the box-cox transformation (Box and Cox, 1964) can be applied (i.e. variance is stabilised). Another problem is non-linearity in the relation between proxy and instrumental target. This problem may be approached by other power transformations such as the box-tidwell transformation (Box and Tidwell, 1962). More attention has to be given to these points when preparing a reconstruction. Since this has not been done so far many proxy data series and many reconstructions have to be reassessed. This might yield new estimates of past climate variability. However, applying all mentioned statistical techniques to proxy series might result in an over interpretation of proxy records and produce artefacts (e.g. Blass, 2006).

In paleoclimatology based on sedimentary records uncertainties in the chronology i.e. in the x-axis of a reconstruction exist. This problem can be approached in two ways: (i) reduce the chronology uncertainty (ii) produce reconstructions that include an uncertainty on the x-axis.

(i) to reduce the chronology uncertainty is absolutely fundamental because the lack of accurate chronologies is often the bottleneck for paleoclimate reconstructions based on sedimentary archives (e.g. Grosjean et al. 2009). In the past

considerable advances have been made in improving chronological techniques (e.g. Telford et al. 2004; Heegaard et al. 2005; Goslar et al. 2009; von Gunten et al. 2009).

(ii) An approach to make reconstructions that include an uncertainty on the x-axis is to take all possible age-depth models based on ^{14}C measurements (e.g. Goslar et al. 2009) and to calculate the calibration and reconstruction for all of these age-depth models (Christian Kamenik, personal communication 2009).

When combining proxy records from different archives with different chronologies the challenge of including chronology uncertainty in the reconstructions is even increased.

From the chronology issue a new problem arises: for records at non-annual resolution, we have to know how much time is integrated in one sample. Changing temporal resolution of samples has the same effect as applying filters with changing band-width resulting in changing amplitudes. This effect is visible in the study by Larocque et al. (in review) and highlights the need of high-precision chronologies for reconstructions using transfer functions. This problem can partly be avoided by filters with a band width of four times the lowest resolution of the proxy record (Koinig et al. 2002). In this context many existing records have to be reassessed as well.

To gain a more sound knowledge about global climate more proxy records are needed. Therefore advances are required in three areas: (i) new techniques have to be explored, (ii) proxies for other seasons and other climate state variables (mainly precipitation) should be developed (iii) the spatial coverage of proxy records has to be improved.

(i) In the most recent issue of *Pages-News* titled 'Advances in Paleolimnology' methods and techniques like ITRAX-XRF, TEX86 and analysis of isotopes on aquatic invertebrates are mentioned as methods with the potential for climate reconstruction (Pienitz and Lotter, 2009). The potential of these techniques for high-resolution quantitative climate reconstructions should be further explored. For example Francus et al. (2009) showed the potential of ITRAX-XRF scans to infer bSi concentration in sediments of Lake Malawi. The potential of this technique has to be tested in lakes with lower bSi concentrations (Lake Malawi 10-30%) in generally different environments and at higher temporal resolution (raw resolution of 30 years, applying a 21 point running mean results in a resolution of about 600 years).

(ii) Most natural climate archives are recording

summer temperatures. There is an absolute need for climate proxies sensitive to other seasons. In the past significant advances have been made in reconstructing cold season temperatures using chrysophyte stomatocysts. Information about other seasons than summer is as well provided by documentary data. Latest publications remain inconclusive about the ability of documentary data to retain low-frequency climate variability (Glaser and Riemann, 2009; Moberg et al. 2009).

New ways of producing proxies for precipitation should be explored. This is as important as producing temperature proxies because precipitation is more heterogeneously distributed over space than temperature (e.g. Stössel, 2008).

(iii) Currently, most paleoclimate records are spread over North America and Europe (e.g. Mann et al. 2008). To improve the knowledge about global climate variability new proxies from regions currently under represented in the global and hemispheric temperature reconstructions have to be produced. For example the knowledge about the eastern parts of Russia is poor (Mann et al. 2008). On the largely under represented southern hemisphere a large climate reconstruction campaign is under way (Villalba et al. 2009).

New high-quality proxy data will give further insight into past climate variability resulting in a reduction of the uncertainties about structure and amplitude of past climate variability. This will allow new detection and attribution studies (e.g. Hegerl et al. 2007) and further reduce the uncertainty about the importance of different climate forcings. Constraining the effects of different forcings will further improve climate models. A better spatial coverage of proxies and improved climate models will allow further advances in comparing proxy data and model output (Goosse et al. 2006; Graham et al. 2007; Yamazaki et al. 2009).

Hence there are many challenges remaining in paleoclimatology and large efforts are needed to solve these challenges.

References

Blass, A., 2006. Sediments of two high-altitude Swiss lakes as high-resolution late Holocene paleoclimate archives. PhD thesis. University of Bern, Bern.

Blass, A., Grosjean, M., Troxler, A., Sturm, M., 2007a. How stable are twentieth-century calibration models? A high-resolution summer temperature reconstruction for the eastern Swiss Alps back to AD 1580 derived from proglacial varved

sediments. *Holocene* 17, 51 - 63.

Blass, A., Bigler, C., Grosjean, M., Sturm, M., 2007b. Decadal-scale autumn temperature reconstruction back to AD 1580 inferred from the varved sediments of Lake Silvaplana (southeastern Swiss Alps). *Quaternary Research* 68, 184 - 195.

Box, G.E.P. and Cox, D.R., 1964. An Analysis of Transformations. *Journal of the Royal Statistical Society Series B-Statistical Methodology* 26, 211 - 252.

Box, G.E.P. and Tidwell, P.W., 1962. Transformation of Independent Variables. *Technometrics* 4, 531 - &.

Büntgen, U., Frank, D.C., Nievergelt, D., Esper, J., 2006. Summer temperature variations in the European Alps, AD 755-2004. *Journal of Climate* 19, 5606 - 5623.

Casty, C., Wanner, H., Luterbacher, J., Esper, J., Böhm, R., 2005. Temperature and precipitation variability in the European Alps since 1500. *International Journal of Climatology* 25, 1855 - 1880.

Caviezel, G., 2007. Hochwasser und ihre Bewältigung anhand des Beispiels Oberengadin 1750 - 1900. MSc thesis. University of Bern, Bern.

Cook, E.R., Briffa, K.R., Jones, P.D., 1994. Spatial Regression Methods in Dendroclimatology - A Review and Comparison of 2 Techniques. *International Journal of Climatology* 14, 379 - 402.

Della-Marta, P., Haylock, M., Luterbacher, J., Wanner, H., 2007. Doubled length of western European summer heat waves since 1880. *Journal of Geophysical Research* 112..

Esper, J., Niederer, R., Bebi, P., Frank, D., 2008. Climate signal age effects - Evidence from young and old trees in the Swiss Engadin. *Forest Ecology and Management* 255, 3783 - 3789.

Fischer, E.M., Seneviratne, S.I., Lüthi, D., Schär, C., 2007a. Contribution of land-atmosphere coupling to recent European summer heat waves. *Geophysical Research Letters* 34.

Fischer, E.M., Seneviratne, S.I., Vidale, P.L., Lüthi, D., Schär, C., 2007b. Soil moisture - Atmosphere interactions during the 2003 European summer heat wave. *Journal of Climate* 20, 5081 - 5099.

Francus, P., Lamb, H., Nakagawa, T., Marshall, M., Brown, E., 2009. The potential of high-resolution X-ray fluorescence core scanning: Applica-

- tions in paleolimnology. In: Pienitz, R., Lotter, A.F., Newman, L., Kiefer, T., (eds.) *Advances in Paleolimnology*. Pages News 17, 93 - 95.
- Glaser, R. and Riemann, D., 2009. A thousand-year record of temperature variations for Germany and Central Europe based on documentary data. *Journal of Quaternary Science* 24, 437 - 449.
- Gobet, E., Tinner, W., Hochuli, P.A., van Leeuwen, J.F.N., Ammann, B., 2003. Middle to Late Holocene vegetation history of the Upper Engadine (Swiss Alps): the role of man and fire. *Vegetation History and Archaeobotany* 12, 143 - 163.
- Goosse, H., Renssen, H., Timmermann, A., Bradley, R.S., Mann, M.E., 2006. Using paleoclimate proxy-data to select optimal realisations in an ensemble of simulations of the climate of the past millennium. *Climate Dynamics* 27, 165 - 184.
- Goslar, T., van der Knaap, W.O., Kamenik, C., van Leeuwen, J.F.N., 2009. Free-shape C-14 age-depth modelling of an intensively dated modern peat profile. *Journal of Quaternary Science* 24, 481 - 499.
- Graham, N.E., Hughes, M.K., Ammann, C.M., Cobb, K.M., Hoerling, M.P., Kennett, D.J., Kennett, J.P., Rein, B., Stott, L., Wigand, P.E., Xu, T.Y., 2007. Tropical Pacific - mid-latitude teleconnections in medieval times. *Climatic Change* 83, 241 - 285.
- Grosjean, M., von Gunten, L., Trachsel, M., Kamenik, C., 2009. Calibration-in-time: Transforming biogeochemical lake sediment proxies into quantitative climate variables. In: Pienitz, R., Lotter, A.F., Newman, L., Kiefer, T., (eds.) *Advances in Paleolimnology*. Pages News 17, 108 - 110.
- Heegaard, E., Birks, H.J.B., Telford, R.J., 2005. Relationships between calibrated ages and depth in stratigraphical sequences: an estimation procedure by mixed-effect regression. *Holocene* 15, 612 - 618.
- Hegerl, G.C., Crowley, T.J., Allen, M., Hyde, W.T., Pollack, H.N., Smerdon, J., Zorita, E., 2007. Detection of human influence on a new, validated 1500-year temperature reconstruction. *Journal of Climate* 20, 650 - 666.
- Kamenik, C., van der Knaap, W.O., van Leeuwen, J.F.N., Goslar, T., 2009. Pollen/climate calibration based on a near-annual peat sequence from the Swiss Alps. *Journal of Quaternary Science* 24, 529 - 546.
- Koinig, K.A., Kamenik, C., Schmidt, R., Agustí-Panareda, A., Appleby, P., Lami, A., Prazakova, M., Rose, N., Schnell, O.A., Tessadri, R., Thompson, R., Psenner, R., 2002. Environmental changes in an alpine lake (Gossenkollesee, Austria) over the last two centuries the influence of air temperature on biological parameters. *Journal of Paleolimnology* 28, 147 - 160.
- Küttel, M., 2009. European climate dynamics and long-term variations over the past centuries. PhD thesis. University of Bern, Bern.
- Lamoureux S., 2001. Varve chronology techniques. In: Last, W.M., and Smol, J.P., (eds.) *Tracking environmental change using lake sediments*. Kluwer, Dordrecht, pp. 247 - 259.
- Larocque, I., Grosjean, M., Heiri, O., Bigler, C., Blass, A., 2009a. Comparison between chironomid-inferred July temperatures and meteorological data AD 1850-2001 from varved Lake Silvaplana, Switzerland. *Journal of Paleolimnology* 41, 329 - 342.
- Larocque-Tobler I., Grosjean, M., Heiri, O., Trachsel, M., Kamenik, C., (in review) 1000 years of climate change reconstructed from chironomid subfossils preserved in varved-lake Silvaplana, Engadine, Switzerland. *Quaternary Science Reviews*.
- Leemann, A., and Niessen, F., 1994. Holocene glacial activity and climatic variations in the Swiss Alps: reconstructing a continuous record from proglacial lake sediments. *The Holocene* 4, 259-268.
- Mann, M.E., Zhang, Z.H., Hughes, M.K., Bradley, R.S., Miller, S.K., Rutherford, S., Ni, F.B., 2008. Proxy-based reconstructions of hemispheric and global surface temperature variations over the past two millennia. *Proceedings of the National Academy of Sciences of the United States of America* 105, 13252 - 13257.
- Mathieu, J., 1998. *Geschichte der Alpen 1500-1900*. Böhlau, Wien.
- Moberg A., Dobrovolny, P., Wilson, R., Brazdil, R., Pfister, C., Glaser, R., Leijonhufvud, L., Zorita E., 2009. Quantifying uncertainty in documentary-data based climate reconstructions? EGU general assembly, CL50, Uncertainties in climate estimates and their time-scales: past, present and future.
- Pienitz, R., and Lotter, A.F., 2009. *Advances in Paleolimnology*. In: Pienitz, R., Lotter, A.F., Newman, L., Kiefer, T., (eds.) *Advances in Paleolimnology*. Pages News 17, 93 - 95.

- Röthlisberger, G., 1991. Chronik der Unwetter-schäden in der Schweiz. WSL, Birmensdorf.
- Stössel, M., 2008. Reconstruction of precipitation in Europe: the challenge of an optimised proxy network. MSc thesis. University of Bern, Bern.
- Sturm, M., and Matter, A., 1978. Turbidites and varves in Lake Brienz (Switzerland): deposition of clastic detritus by density currents. In: Matter, A., Tucker, M. (Eds.), *Modern and ancient lake sediments*. Blackwell Scientific Publications, Bern, pp. 147 - 168.
- Telford, R.J., Heegaard, E., Birks, H.J.B., 2004. All age-depth models are wrong: but how badly? *Quaternary Science Reviews* 23, 1 - 5.
- Trachsel, M., Eggenberger, U., Grosjean, M., Blass, A., Sturm, M., 2008. Mineralogy-based quantitative precipitation and temperature reconstructions from annually laminated lake sediments (Swiss Alps) since AD 1580. *Geophysical Research Letters* 35.
- Trachsel, M., Grosjean, M., Larocque-Tobler, I., Schwikowski, M., Blass, A., Sturm, M., (in review). Quantitative summer temperature reconstruction derived from a combined biogenic Si and chironomid record from varved sediments of Lake Silvaplana (south-eastern Swiss Alps) back to AD 1177. *Quaternary Science Reviews*.
- Westover, K., and Bigler C., 2009. High-resolution diatom-inferred temperature reconstruction from the southeastern Swiss Alps, AD 1350 to present. *Millennium Abstract Volume*.
- Villalba, R., Grosjean, M., Kiefer, T., 2009. Long-term multi-proxy climate reconstructions and dynamics in South America (LOTRED-SA): State of the art and perspectives Preface. *Palaeogeography Palaeoclimatology Palaeoecology* 281, 175 - 179.
- von Gunten, L., Grosjean, M., Beer, J., Grob, P., Morales, A., Urrutia, R., 2009. Age modeling of young non-varved lake sediments: methods and limits. Examples from two lakes in Central Chile. *Journal of Paleolimnology* 42, 401 - 412.
- Yamazaki, Y.H., Allen, M.R., Huntingford, C., Frame, D.J., Frank, D.C., 2009. Refining future climate projections using uncertain climate data of the last millennium. EGU general assembly, CL50, *Uncertainties in climate estimates and their time-scales: past, present and future*.
- Yiou, P., Dacunha-Castelle, D., Parey, S., Hoang, T.T.H., 2009. Statistical representation of temperature mean and variability in Europe. *Geophysical Research Letters* 36.

Acknowledgments

This thesis would not have been possible without the support of numerous people. First of all I would like to acknowledge Prof. Martin Grosjean for giving me the opportunity to write this PhD study. I greatly benefited from his immense knowledge, his countless innovative ideas and his enthusiastic way of seeing things. Martin further gave me the opportunity to attend several conferences and workshops in the frame of the EU-FP 6 project 'Millennium'. Attending these meetings and conferences provided large scientific inspiration. In this context I may as well acknowledge Prof. Atle Nesje from the University of Bergen for his support as co-referee of this thesis.

My very special thanks are due to Dr. Christian Kamenik. I had the great pleasure and privilege to share the office with him during the last three years. I could benefit from his extensive knowledge about statistics, and from his intuitive approach to statistics. Without his advice my knowledge about statistics and R would be inexistent.

I may further acknowledge Pascal Hänggi. I really enjoyed writing a paper with him. He was a great help for me when making calculations and with any kind of problem occurring in R. I enjoyed the countless discussions we had about statistics and of course other topics :-).

This thesis would not have been possible without many persons making infrastructure and measurement devices available. Prof. Margit Schwikowski is acknowledged for making available ICP-OES at PSI in Villigen. I would like to thank Dr. Urs Eggemberger for giving me the opportunity to measure XRD in his lab. Jörg Leuenberger and Karl Schrott made available the freeze labs at ETH in Zürich.

I would like to acknowledge all persons who supported me (and carried out) during lab work: Dr. Daniela Fischer, Philipp Grob, Lea Moser, Silvia Köchli, Christine Lemp, Christoph Wanner and Fabian Mauchle.

Scientific work on the lakes in the Upper Engadine has been carried out for more than twenty years with Dr. Michael Sturm as advisor. Thank you Mike for coordinating and supervising all these efforts. In this study I greatly benefited from the three outstanding PhD studies about Lake Silvaplana that have been conducted until now. I would like to acknowledge Dr. Andreas Leeman, Dr. Christian Ohlendorf and Dr. Alex Blass for their work. Alex thank you very much for introducing me to work with sediment cores and for giving me the opportunity to play around with your data.

Dr. Marcel Küttel and Dr. Isabelle Larocque-Tobler are acknowledged for providing me with data. Further thanks go to Samuel Nussbaumer and Dr. Friedhelm Steinhilber. It was a pleasure to prepare a manuscript with you.

I enjoyed the stays in Vienna at EGU. Thank you Franz, Marco, Samuel, Marcel, Lucien, Pascal, Raphi, This and of course Heinz. Attending concerts will always have a special place in my memories of EGU.

Dr. Thomas Kulbe, Alois Zwysig, Richard Niederreiter and Dr. Lucien von Gunten are acknowledged for their essential help during field work in the Engadine and in the Bernese Oberland. In this context I may acknowledge all former and present members of the 'lake sediment and paleolimnology research group' for their help during field work.

I may further acknowledge Basilio Ferrante and Thomas Trüssel for the IT-support and Margret Möhl and Monika Wälti for administrative work.

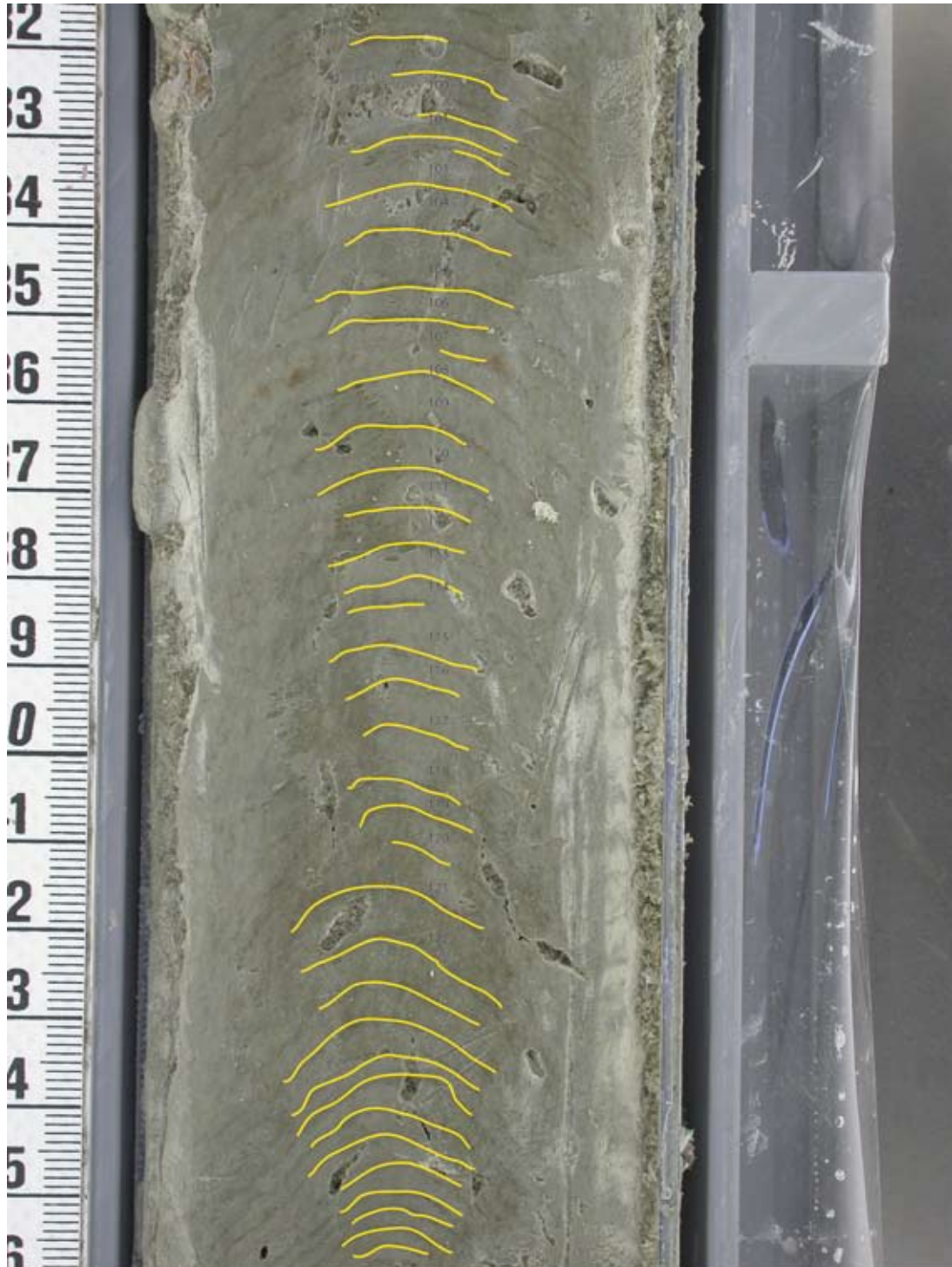
Last but not least I would like to thank my parents for their support which enabled me to follow my interests. I may further acknowledge my brother Samuel for proof reading of this thesis.

Appendix

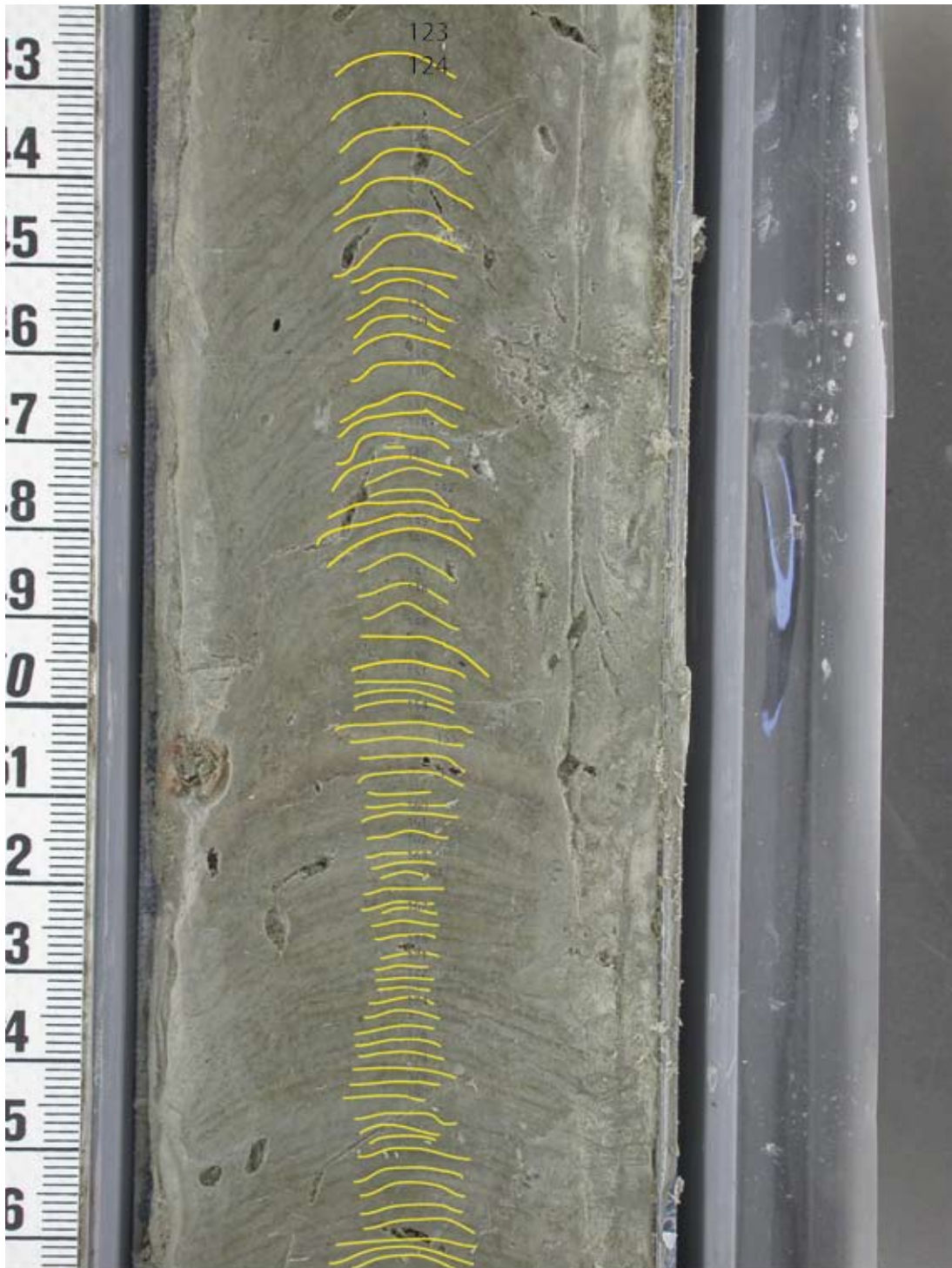


Appendix

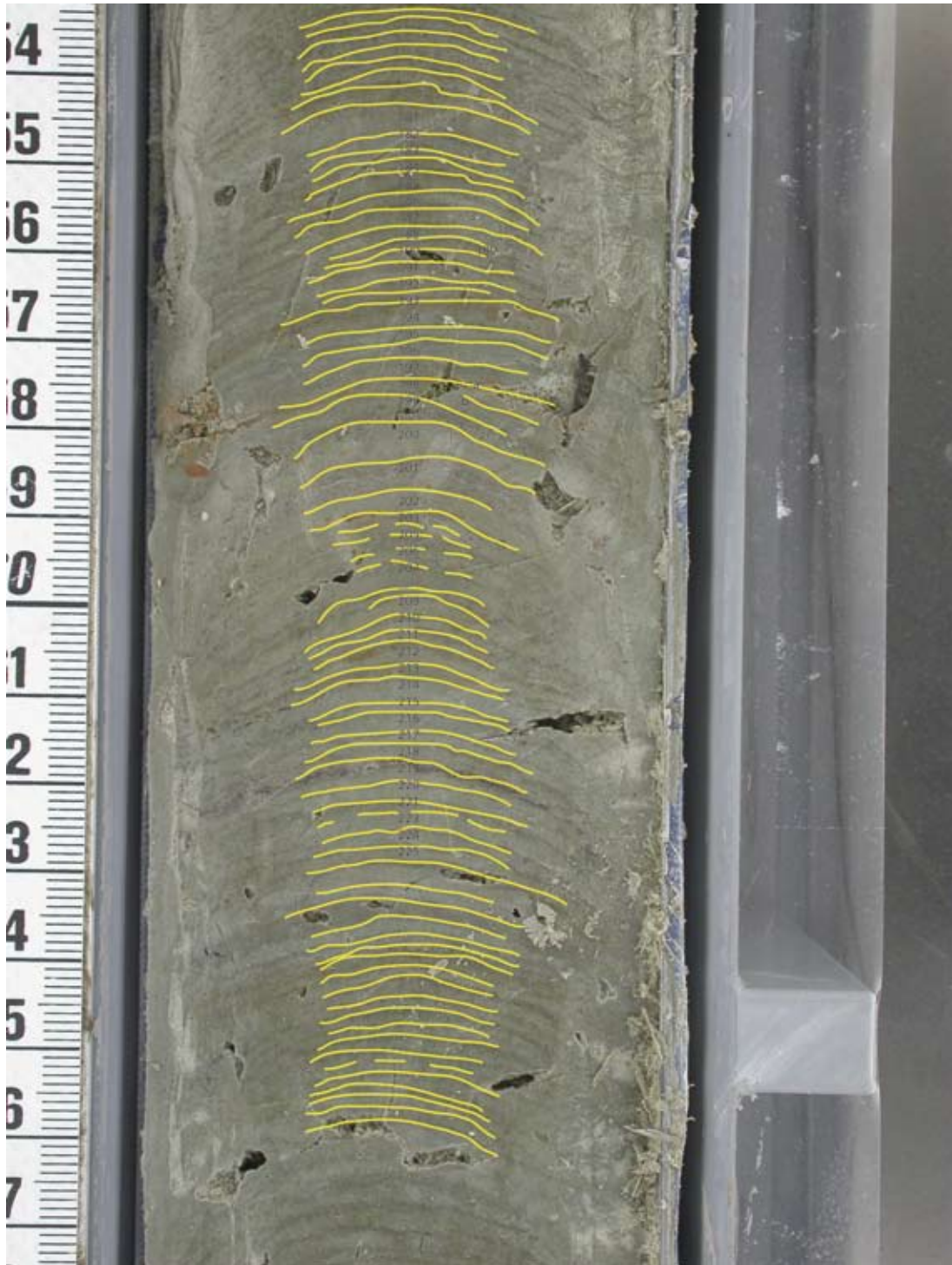
Core Picture SVP 06-3 I



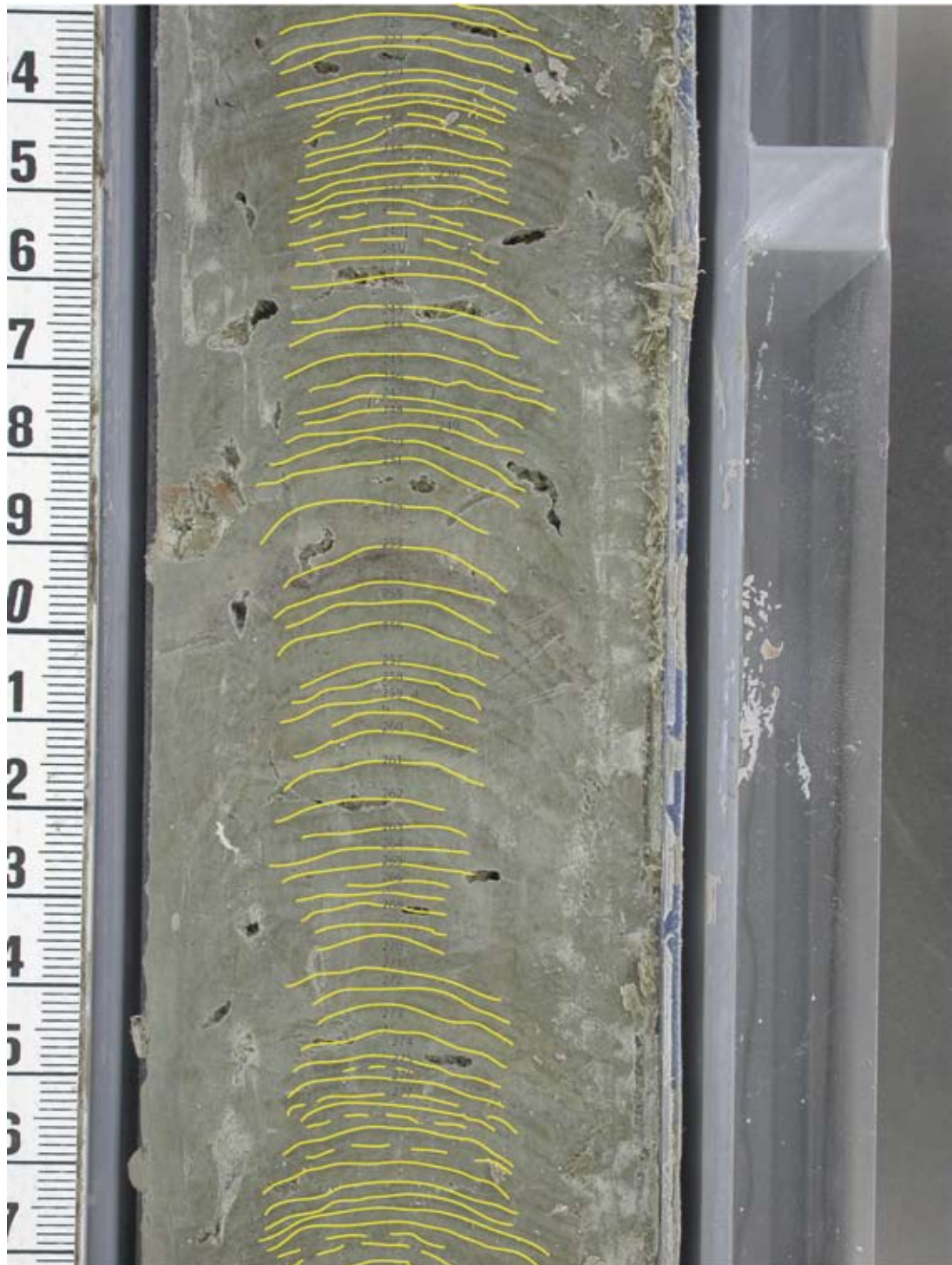
Core Picture SVP 06-3 I



Core Picture SVP 06-3 I



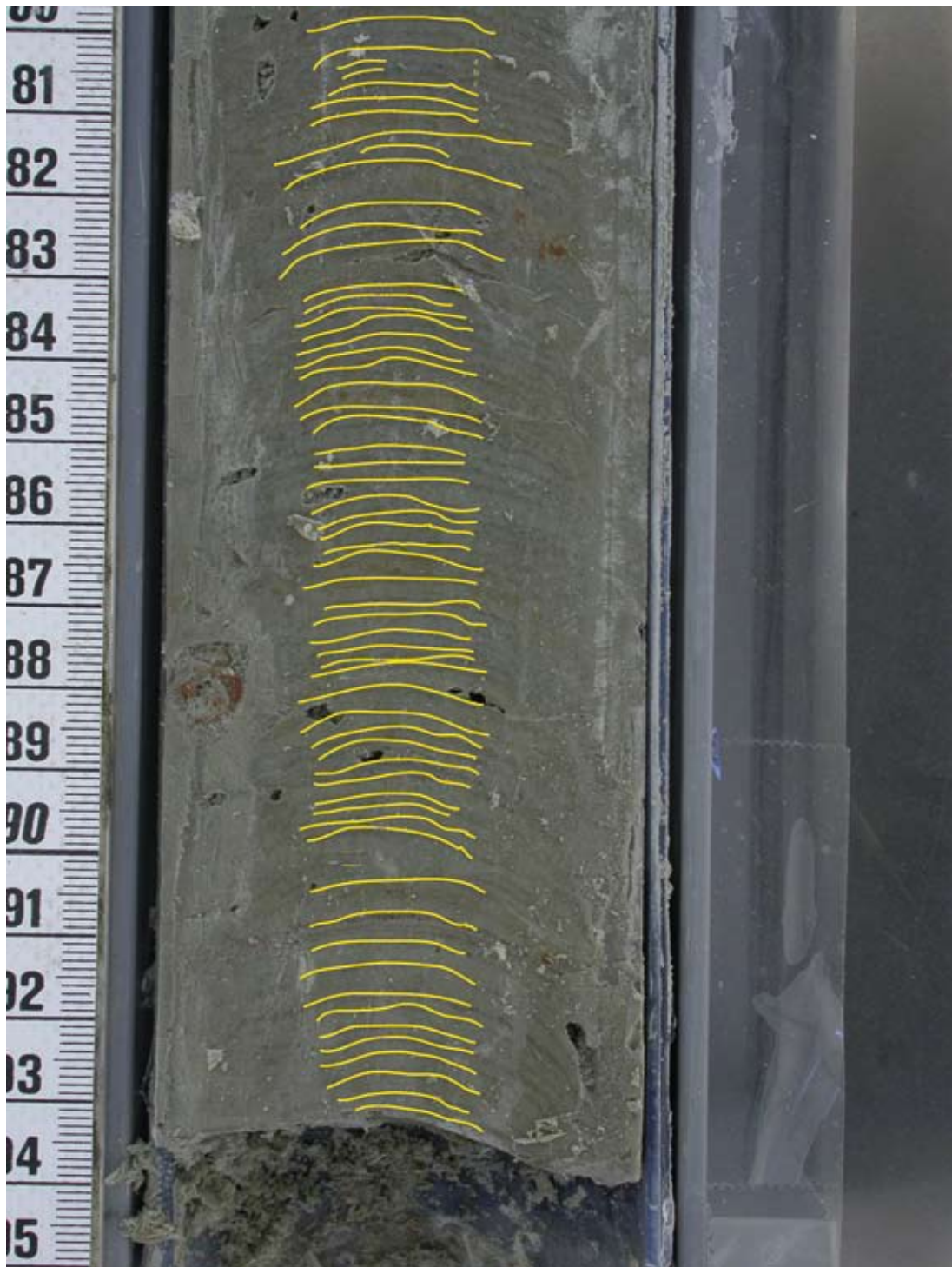
Core Picture SVP 06-3 I



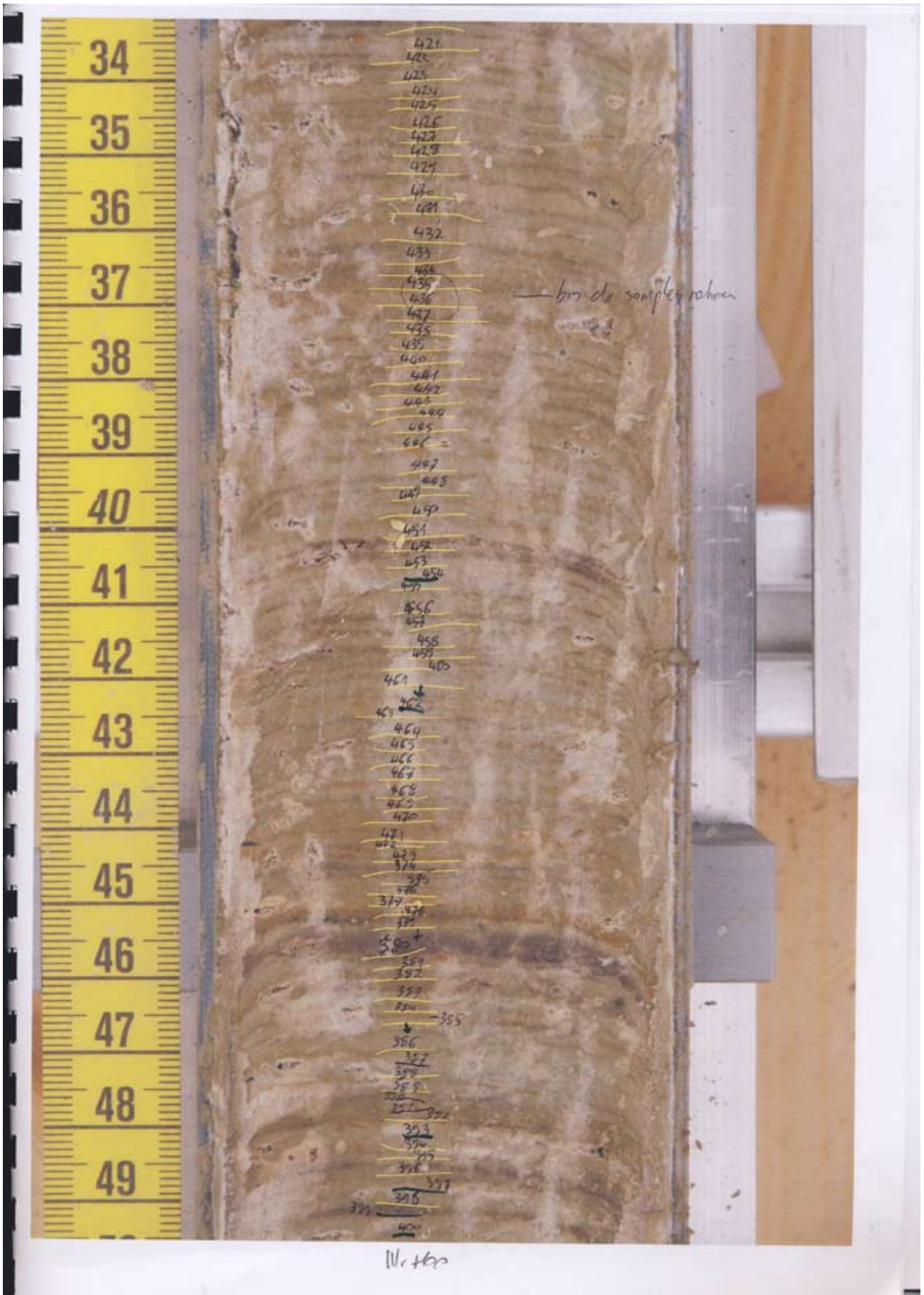
Core Picture SVP 06-3 I



Core Picture SVP 06-3 I



Core Picture SVP 06-2 II



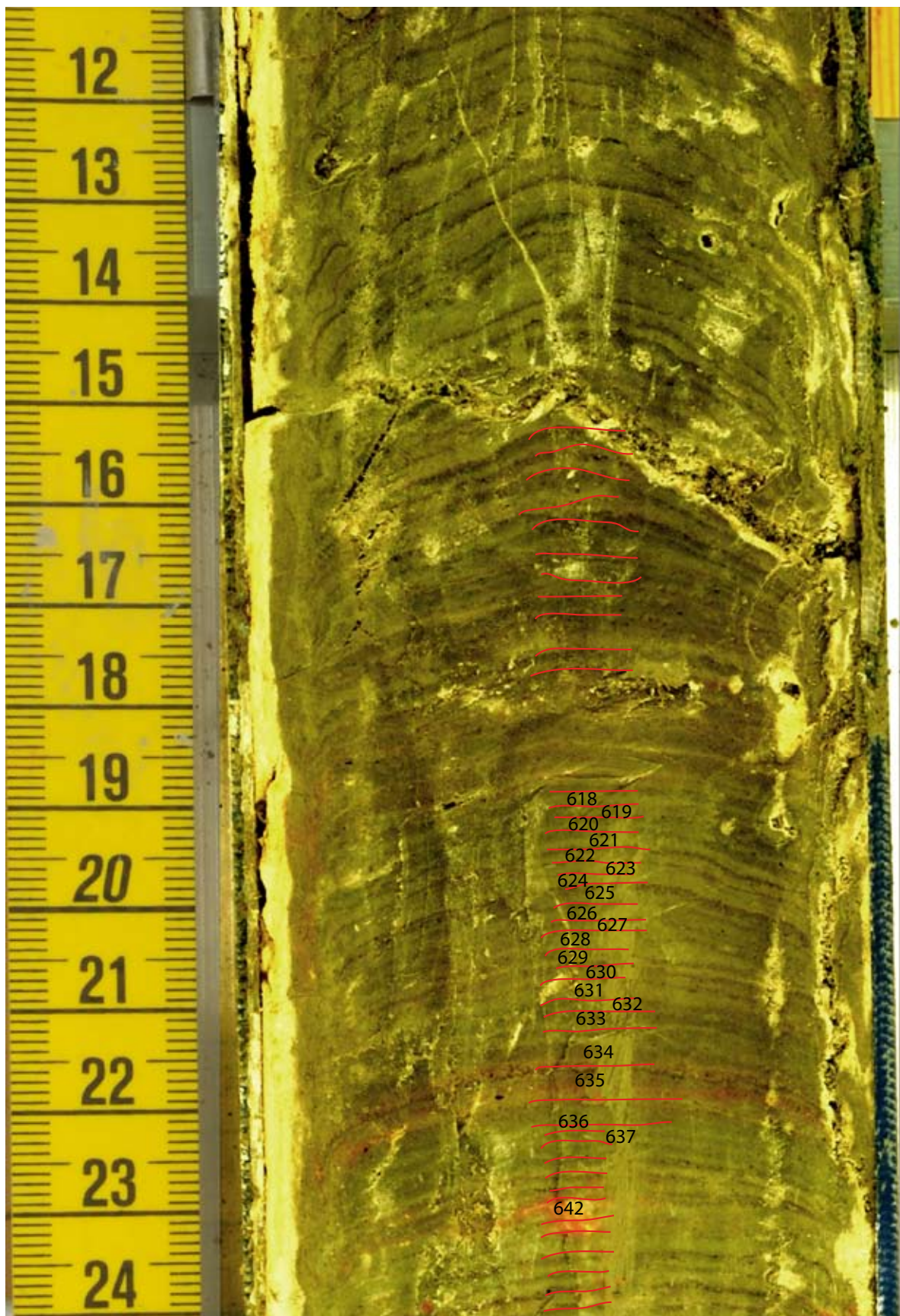
Core Picture SVP 06-3 II



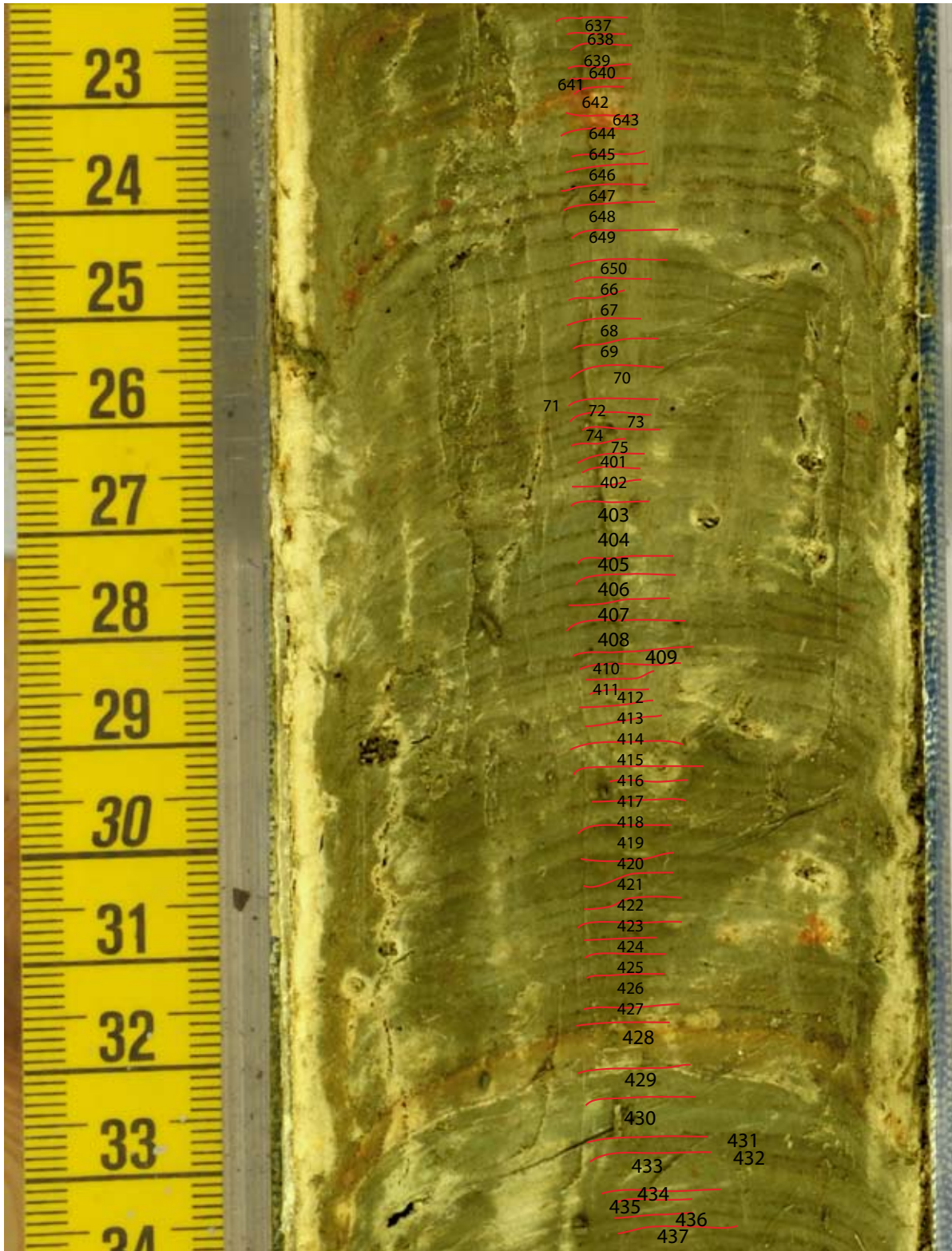
Core Picture SVP 06-3 II



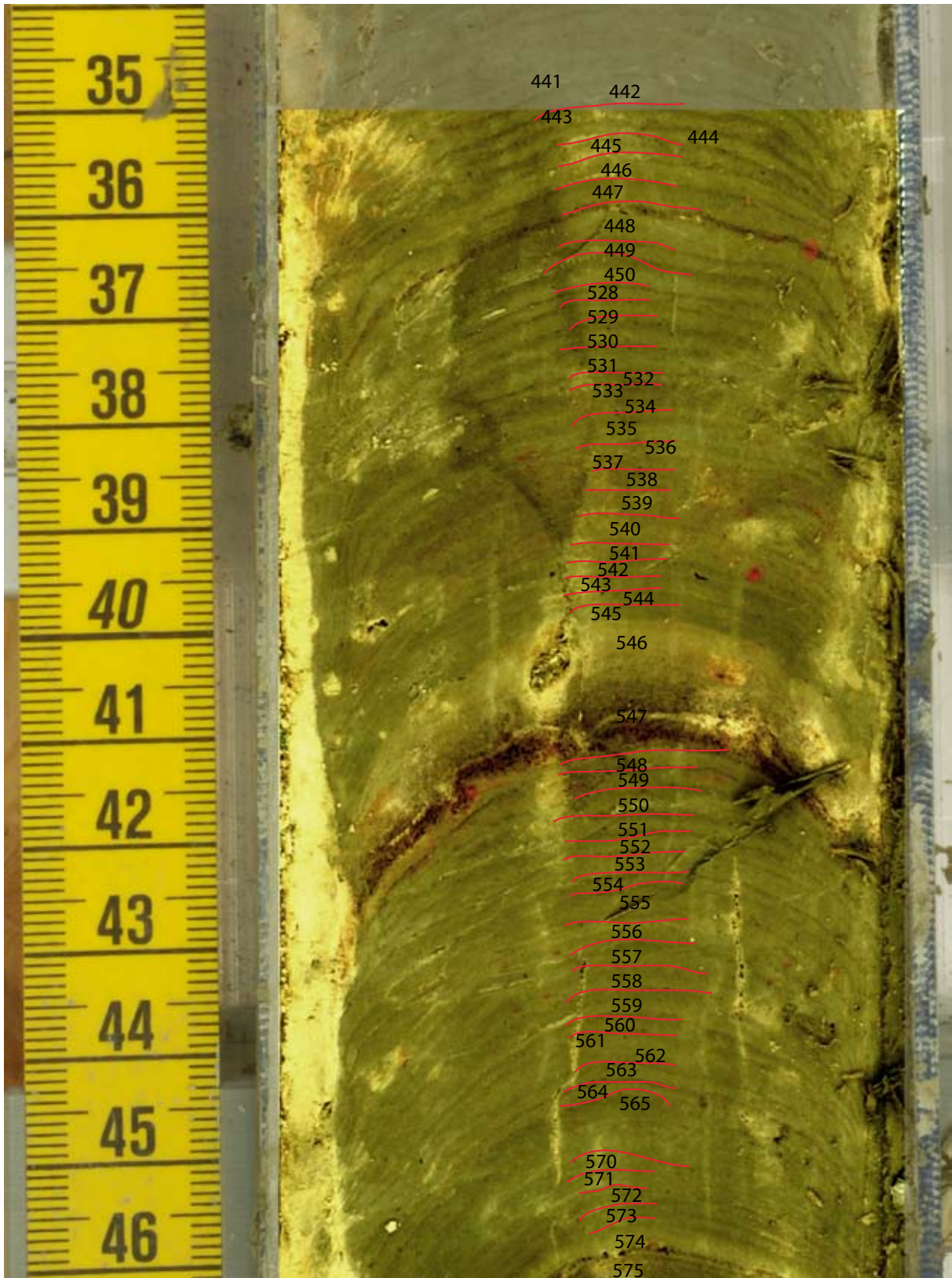
Core Picture SVP 06-3 II



Core Picture SVP 06-3 II



Core Picture SVP 06-3 II



Chronology SVP 06-3 I

Layer NR	Box Nr.	Year AD	Layer NR	Box Nr.	Year AD
99	99	1617	146	146	1574
100	100	1616	147	147	1573
100(b)	30	1616	148 und 149	148 und 149	1572
101	101	1615	150	150	1571
102	102	1614	151	151	1570
103	36	1614	152	152	1569
104	37	1613	153	153	1568
105	38	1612	154	154	1567
106	39	1611	155	155	1566
107	107	1611	156	156	1566
108	108	1611	157	157	1566
109	109	1610	158a	158	1566
110	110	1609	158b	215	1566
111	111	1608	158c	221	1566
112	112	1607	159	159	1566
113	113	1606	160	160	1566
114	114	1605	161	161	1566
114	114	1605	162	278	1565
115	115	1604	162	278	1565
116	116	1603	163	162	1564
117	117	1602	164	163	1563
118	118	1601	165	164	1562
119	119	1600	166	165	1561
120	120	1599	167	166 und 167	1560
121	121	1598	168	168	1559
122	122	1597	169	169	1558
123	123	1596	170	170	1557
124	124	1595	171	171	1556
125	125	1594	172	315	1555
126	126	1593	keine Nummer	172	1555
127	127	1592	173	173	1554
128	128	1591	174	174	1553
129	130	1591	175	175	1552
130	130	1590	176	176	1551
131	132	1589	177	177	1550
132	132	1588	178	178	1549
133	133	1587	179	179	1548
134	134	1586	180	180	1547
135	135	1585	181	181	1546
136	136	1584	182	182	1546
137	137	1583	183	183	1545
138	138	1582	184	184	1544
139	139	1581	185	185	1543
140	140	1580	186	186	1542
141	141	1579	187	187	1541
142	142	1578	188	188	1540
143	143	1577	189	189	1539
144	144	1576	190	190	1538
145	145	1575	191	191	1537

Chronology SVP 06-3 I

Layer NR	Box Nr.	Year AD		Layer NR	Box Nr.	Year AD
192	192	1536		240	240	1499
192	192	1536		241	241	1498
193	193	1535		242	242	1497
194	194	1535		243	243	1496
195	195	1534		244	244	1495
196	196	1533		245	245	1494
196		1532		246	246	1493
197	197	1531		247	247	1492
197		1531		248	248	1491
198a und 198b	198 und 198b	1530		249	249	1490
199	199	1529		250	250	1489
200	200	1529		251	251	1488
201	201	1529		252	252	1487
202	202	1529		253	253	1486
203 und 204	203	1529		254	254	1486
205	205	1529		254	254	1486
206	206	1528		255	255	1485
207	207	1527		256	256	1484
208	208	1526		257	257	1483
209	209	1525		258	258	1482
210	210	1524		259a	311	1481
211	211	1523		259b	259	1480
212	212	1522		260	260	1479
213	213	1522		261	261	1479
214	214	1521		262 u 262 b	262 und 312	1479
215		1520		263	263	1478
216	216	1519		264	264	1477
217	217	1518		265	265	1476
218	218	1517		266	266	1475
219	219	1516		267	267	1474
220 und 221	220 und 221	1516,1515		268	313	1474
223	223	1515		269	268	1474
224	224	1514		ohne Nummer	keine Layer Nr	1473
225	225	1513		270	270	1472
226	226	1512		270		1472
227	227	1511		271	271	1471
228	228	1510		272	272	1470
229	229	1510		272		1470
230	230	1509		273	273	1469
231	231	1508		274	274	1468
232	232	1507		275	275	1467
233	233	1507		276	276	1466
234	234	1506		277	279	1465
235	235	1505			280	1464
236	236	1504			281	1463.1442
237	237	1503			282	1461
keine Nummer	277	1502			283	1460.1439
238	238	1501			284	1458
239	239	1500			285	1458

Chronology SVP 06-3 I

Layer NR	Box Nr.	Year AD	Layer NR	Box Nr.	Year AD
3 gleichmässige samples	286	1457	320	321	1422
	287	1456	321	322	1422
	288	1455	322	322	1421
289	289	1455	323	323	1420
290a	290	1454	324	324	1419
290b	314	1454	325	325	1418
291	291	1153	326	326	1417
291		1453	327	327	1416
292	292	1452	328	328	1416
292		1451	329	329	1415
293	293	1450	330	330	1414
293		1449	331	331	1413
294	294	1448	332	332	1412
294		1447	333	333	1411
295	295	1446	334	334	1410
295		1446	335	335	1409
296		1446	336	336	1408
297	296	1445	337	337	1407
298a	297	1444	338	338	1406
298a		1444	339	339	1405
298b	298	1443	339	339	1405
298b		1443	340	340	1404
299	299	1442	341	341	1403
300	300	1441	342	342	1402
300		1440	343	343	1401
301a, 301b	301	1439.1428	344	344	1400
301c	375	1437	345a	369	1399
302	303	1436	345a	369	1399
302		1436	345b	368	1398
303	302	1435	345c	345	1398
304	304	1434	346	346	1397
305	305	1434	346	346	1397
306	306	1433	347a	347	1397
307	307	1432	347b	348	1397
307	364	1432	348	349	1397
307	362	1432	349	350	1397
308	363	1432	350	351	1396
309	309	1431	351	352	1395
310	310	1430	352	353	1394
	316	1430	353	354	1393
	317	1429	354	354	1392
	317	1429	355	355	1391
	318	1428	356	356	1390
	318	1427	357	357	1389
318	318	1426			
	319	1426			
	319	1425			
	320	1424			
	320	1423			

Chronology SVP 06-2 II

Layer Nr.	Box Nr	Year AD		Layer Nr.	Box Nr	Year AD
453	467	1389		386	498	1366
455/454	468	1388		387	499	1365
456	469	1387		388	500	1364
457	470	1386		389	501	1363
458	471	1385		390	502	1362
460/459	472	1384,1383		391	503	1362
461	473	1382		392	504	1362
462	474	1381		394	505	1362
463	475	1381		395	506	1361
464	476	1380		396	507	1360
465	477	1379		397	508	1360
466	478	1378		398	509	1359
467	479	1377		400/399	510	1358
468	480	1376			511	1358
469	481	1375			512	1357
470	482	1374			513	1356
471	483	1373		517	514	1356
472	484	1372		518	515	1355
473b	485	1372		519	516	1354
473a	486	1372		520	517	1353
374	487	1371		521	518	1352
375	488	1370		522	519	1351
376	489	1370		523	520	1350
377	490	1369		524	521	1350
378	491	1369		525	522	1349
379	492	1369		525	523	1348
380	493	1369		526	524	1347
381	494	1369		526	525	1346
382/383	495	1368		527	526	1345
384	496	1368		528	578	1344
385	497	1367				

Chronology SVP 06-3 II

Box NR	Year AD			Box NR	Year AD
47	1344			617	1303
48	1344			617	1302
49	1343			617	1301
50	1342			618	1299
51	1341			619	1298
52	1340			620	1297
53	1339			621	1296
54	1338			622	1295
55	1337			622	1294
56	1336			623	1293
57	1335			624	1292
58	1334			625	1291
59	1333			626	1290
60	1332			627	1289
61	1331			628	1288
62	1331			629	1287
63	1330			630	1286
64	1329			631	1285
65	1328			632	1284
601	1327			633	1283
602	1326			634	1282
603	1325			635	1281
604	1324			636	1281
605	1323			637	1280
606	1323			638	1279
607	1322			639	1278
608	1321			640	1277
609	1321			641	1276
610	1320			642	1275
611	1319			643	1274
612	1318			644	1273
613	1317			645	1272
613	1316			646	1271
613	1315			647	1270
613	1314			648	1269
614	1313			649	1268
614	1312			650	1267
614	1311			66+67	1266
614	1310			68	1265
615	1309			69	1264
615	1309			70	1263
615	1309			71	1262
616	1309			72	1261
616	1308			73	1260
616	1307			73	1259
616	1306			74	1258
616	1305			75	1257
617	1304			401	1256

Chronology SVP 06-3 II

Box NR	Year AD			Box NR	Year AD
402	1255			448/447	1210
402	1254			449	1210
403	1253			450	1209
404	1252			528	1208
405	1251			529	1207
406	1250			530	1206
407	1249			531	1205
408	1248			532	1204
409	1247			533	1203
410	1246			535	1203
411	1245			536	1202
411	1244			537	1201
412	1243			538	1200
413	1242			539	1199
414	1241			540	1198
415	1240			541	1197
416	1239			542	1196
417	1238			543	1195
418	1237			545+544	1194
419	1236			546	1193
420	1235			547	1193
421	1234			548	1193
422	1233			549	1193
423	1232			550	1192
424	1231			551	1191
425	1230			552	1190
426	1229			553	1189
427	1228			554	1188
428	1227			555	1187
429	1227			556	1186
430	1227			557	1185
431	1227			558	1184
432	1226			559	1183
433	1225			560	1182
434	1224			561	1181
435	1223			562	1180
436	1222			563	1179
437	1221			564	1178
438	1220			565	1177
439	1219			566	1176
439	1218			567	1175
440	1217			568	1174
441	1216			569	1173
442	1215			570	1172
443	1214			572	1171
444	1213			573	1170
445	1212			574	1169
446	1211			575	1169

Curriculum Vitae

Name	Mathias Trachsel
Date of Birth	14.08.1983
Place of Birth	Aarberg

Education

2006 – 2010	PhD student in climate sciences, Institute of Geography, University of Bern. Thesis title: 'Climate variability over the last millennium as recorded in the sediments of high-altitude Lake Silvaplana, Switzerland: data, methods and limitations.' Advisor: Prof. Dr. Martin Grosjean. External referee: Prof. Dr. Atle Nesje, University of Bergen. Faculty member: Prof. Dr. Heinz Wanner.
2001 – 2006	Student of Geography, History and Physics, University of Bern. Thesis title: 'Mineralogie der Warven des Silvaplanersees (Engadin) als quantitativer Proxy für eine hochaufgelöste Klimarekonstruktion 1580-1950 AD.' Advisor: Prof. Dr. Martin Grosjean.
1997 – 2001	Mathematisch-Naturwissenschaftliches Gymnasium Bern-Neufeld